Applied Catalysis B: Environmental 87 (2009) 105–145

Contents lists available at ScienceDirect

Applied Catalysis B: Environmental

journal homepage: www.elsevier.com/locate/apcatb

Review

Decontamination of wastewaters containing synthetic organic dyes by electrochemical methods: A general review

Carlos A. Martínez-Huitle [a], Enric Brillas [b,*]

[a] DiSTAM, University of Milan, via Celoria 2, CAP-20133 Milan, Italy
[b] Laboratori d'Electroquímica dels Materials i del Medi Ambient, Departament de Química Física, Facultat de Química, Universitat de Barcelona, Martí i Franquès 1-11, 08028 Barcelona, Spain

ARTICLE INFO

Article history:
Received 21 June 2008
Received in revised form 14 September 2008
Accepted 19 September 2008
Available online 27 September 2008

Keywords:
Dyes removal
Electrocoagulation
Electrocatalysis
Hydroxyl radical
Active chlorine
Electro-Fenton
Photoelectro-Fenton
Photoelectrocatalysis

ABSTRACT

Effluents of a large variety of industries usually contain important quantities of synthetic organic dyes. The discharge of these colored compounds in the environment causes considerable non-aesthetic pollution and serious health-risk factors. Since conventional wastewater treatment plants cannot degrade the majority of these pollutants, powerful methods for the decontamination of dyes wastewaters have received increasing attention over the past decade. This paper presents a general review of efficient electrochemical technologies developed to decolorize and/or degrade dyeing effluents for environmental protection. Fundamentals and main applications of typical methods such as electrocoagulation, electrochemical reduction, electrochemical oxidation and indirect electro-oxidation with active chlorine species are reported. The influence of iron or aluminium anode on decolorization efficiency of synthetic dyes in electrocoagulation is explained. The advantages of electrocatalysis with metal oxides anodes and the great ability of boron-doped diamond electrodes to generate heterogeneous hydroxyl radical as mediated oxidant of these compounds in electrochemical oxidation are extensively discussed. The effect of electrode material, chloride concentration, pH and temperature on the destruction of dyestuffs mediated with electrogenerated active chlorine is analyzed. The degradation power of these pollutants with an emerging electrochemical advanced oxidation process such as electro-Fenton, based on the mediated oxidation by homogeneous hydroxyl radical formed from Fenton's reaction between cathodically produced hydrogen peroxide and catalytic Fe^{2+}, is examined. Recent progress of emerging photoassisted electrochemical treatments with UV irradiation such as photoelectro-Fenton and photoelectrocatalysis is also described.

Contents

* Corresponding author. Tel.: +34 93 4021223; fax: +34 93 4021231.
E-mail address: brillas@ub.edu (E. Brillas).

Abbreviations: ACF, activated carbon fiber; AOP, advanced oxidation process; ABS^M, average absorbance; BDD, boron-doped diamond; DSA, dimensionally stable anode; EAOP, electrochemical advanced oxidation process; EO, electrochemical oxidation; EC, electrocoagulation; EF, electro-Fenton; EBT, Eriochrome Black T; GC–MS, gas chromatography–mass spectrometry; HPLC, high-performance liquid chromatography; PEF, photoelectro-Fenton; PTFE, polytetrafluoroethylene; ROS, reactive oxygen species; RVC, reticulated vitreous carbon; SCE, saturated calomel electrode; SHE, standard hydrogen electrode; UV, ultraviolet; UVA, ultraviolet A; UVB, ultraviolet B; UVC, ultraviolet C; UV-Vis, ultraviolet-visible.

0926-3373/$ – see front matter © 2008 Elsevier B.V. All rights reserved.
doi:10.1016/j.apcatb.2008.09.017

List of symbols

C_0	initial dye concentration (mg dm^{-3}, mM)
COD	chemical oxygen demand (mg of O_2 dm^{-3})
E_{anod}	anodic potential (V)
E_{cat}	cathodic potential (V)
E^0	standard potential (V vs. SHE)
F	Faraday constant (96,487 C mol^{-1})
I	current (A)
j	current density (mA cm^{-2})
k_1	pseudo-first-order rate constant (s^{-1})
k_2	second-order rate constant (M^{-1} s^{-1})
Q	specific charge (Ah dm^{-3})
t	electrolysis time (s, min, h)
t_r	retention time (min)
TOC	total organic carbon (mg of C dm^{-3})
TSS	total suspended solids (mg dm^{-3})
V	cell voltage (V)
V_s	solution volume (dm^3)

Greek symbols

λ	wavelength (nm)
λ_{max}	maximum wavelength (nm)

1. Introduction

The exact amount of synthetic organic dyes produced in the world is unknown, although financial reports estimate their continuous increase in the worldwide market up to about US$11 billion in 2008 with a production of dyestuffs over 7×10^5 tons [1]. A large variety of these compounds are extensively used in many fields of up-to-date technology involving various branches of the textile industry [2,3], leather tanning industry [4,5], paper production [6], food technology [7,8], agricultural research [9,10], light-harvesting arrays [11], photoelectrochemical cells [12] and in hair colorings [13]. Synthetic dyes are also employed for the control of the efficacy of sewage and wastewater treatment [14–16], for the determination of specific surface area of activated sludge for ground water tracing [17,18] and so on.

Dyes are commonly classified from their chromophore group. The majority of these compounds consumed at industrial scale are azo (–N=N–) derivatives, although antraquinone, indigoide, triphenylmethyl, xanthene, sulphur and phtalocyanine derivatives are frequently utilized [19]. Fig. 1 illustrates this classification for several typical dyes, showing their chemical structure along with their common and/or color index name. The latter nomenclature is commonly utilized and consists of the name of a general characteristic property of the product, followed by the name of its color and an order number. The first name can be Acid (it is negatively charged), Basic (it is positively charged), Reactive (an anionic dye used in the textile industry), Mordant (a metallic ion is required for showing their color or staining selectivity), Vat (it derives of natural indigo), Disperse (a non-ionic dye used in aqueous dispersion) and so on.

Important quantities of synthetic dyes are discharged in the environment from industrial effluents [20]. A loss of 1–2% in production and 1–10% in use are a fair estimate. For reactive dyes in the textile industry, their loss can be about 4%. The presence of these pollutants in waters can change their appearance, e.g. 1 mg dm^{-3} of a dye is likely to cause visible colorization of the water or alter the clarity. Due to their large-scale production and extensive application, synthetic dyes can cause considerable non-aesthetic pollution and are serious health-risk factors. Although the growing impact of environmental protection on industrial development promotes eco-friendly technologies [21], reduced consumption of water and lower output of wastewater [22,23], the

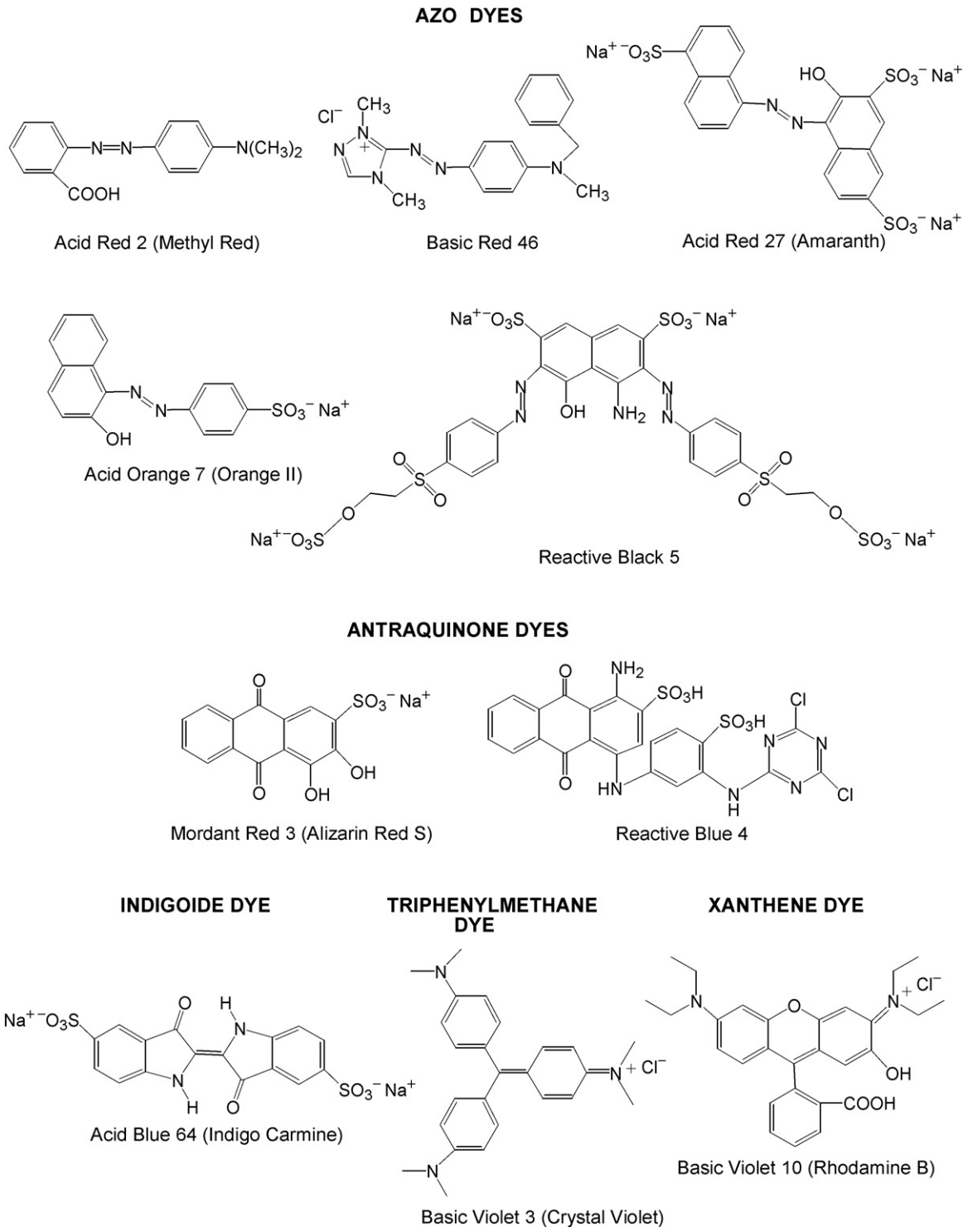

Fig. 1. Chemical structure of typical synthetic organic dyes classified by their chromophore group. The color index and/or common (between parentheses) name of each dye are given.

release of important amounts of synthetic dyes to the environment causes public concern and legislation problems are a serious challenge to environmental scientists [19,20]. The impact and toxicity of these pollutants in the environment have been extensively studied [24–30]. However, the knowledge concerning their carcinogenic, mutagenic and bactericide properties is still incomplete owing to the large variety of dyes produced.

Since dyes usually present high stability under sunlight and resistance to microbial attack and temperature, the large majority of these compounds are not degradable in conventional wastewater treatment plants. The research of powerful and practical treatments to decolorize and degrade dyeing wastewaters to decrease their environmental impact has then attracted increasing interest over the past two decades. Fig. 2 summarizes the main technologies utilized for the removal of these pollutants. An

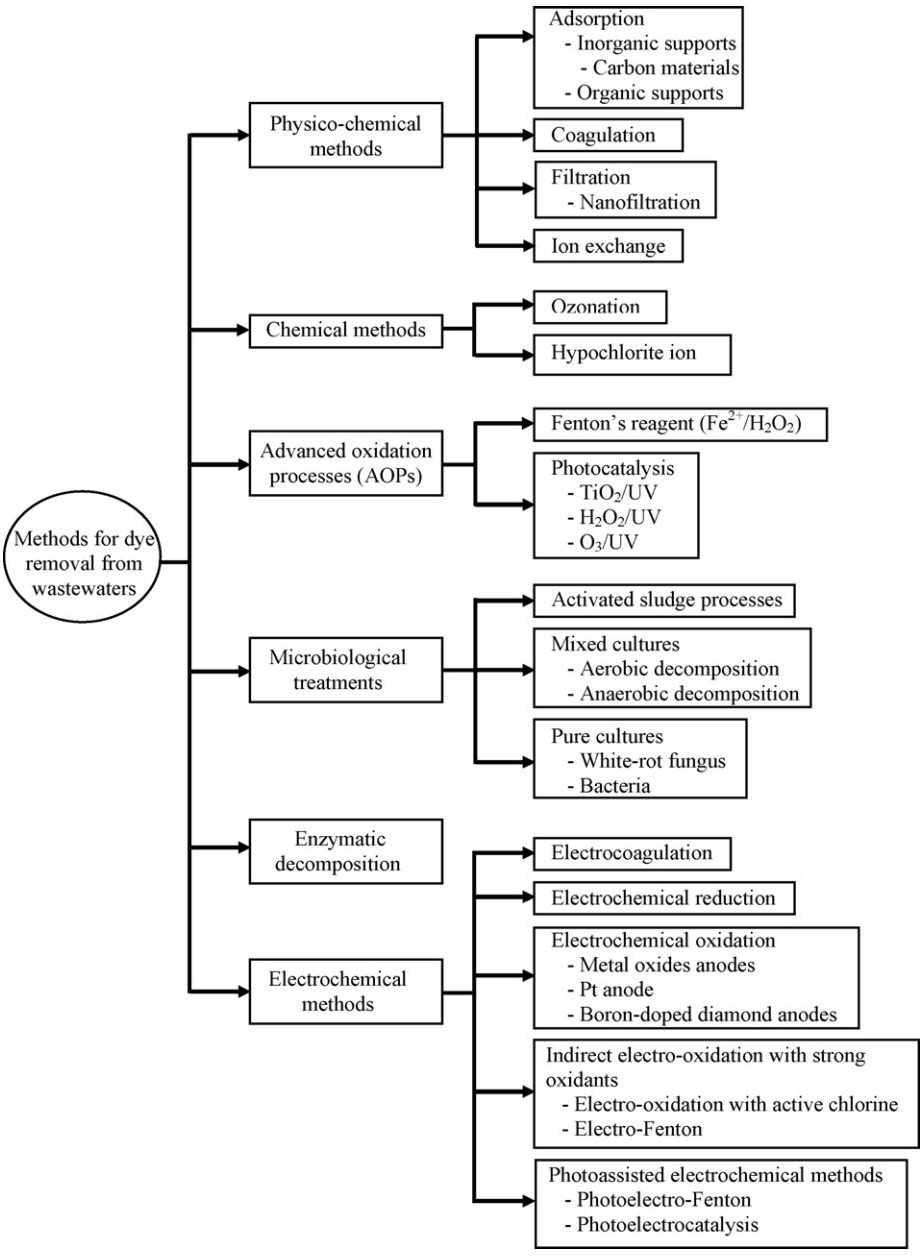

Fig. 2. Main methods used for the removal of organic dyes from wastewaters.

extensive literature reporting the characteristics and applications of most important conventional technologies developed for this purpose including physico-chemical and chemical methods, advanced oxidation processes (AOPs), microbiological treatments and enzymatic decomposition, has been collected in several critical reviews [19,20,31–34]. In contrast, only little information on the interest of electrochemical technologies for destroying dyes from wastewaters has been shown in some previous reviews [20,31,33,34], without considering the recent advances of these promising methods, mainly developed since 2002.

Traditional physico-chemical treatments applied to the purification of dyeing wastewaters include adsorption with inorganic (mainly, activated carbon materials) and organic supports, coagulation by lime, aluminium or iron salts, filtration and ion exchange (see Fig. 2). These procedures lead to effective decolorization, but their application is restricted by the formation of sludge to be disposed or by the need to regularly regenerate the adsorbent materials [19,20,34]. More powerful chemical methods such as ozonation and oxidation with hypochlorite ion, as well as AOPs such as Fenton's reagent and photocatalytic systems involving TiO_2/UV, H_2O_2/UV and O_3/UV, collected in Fig. 2, also provide fast decolorization, along with degradation of dyes. However, the use of these methods is not completely accepted at present because they are quite expensive and have operational problems [19,20,31,33]. On the other hand, the application of microorganisms to the biodegradation of synthetic dyes is an attractive and simple method by operation. A large number of activated sludge processes, mixed cultures with aerobic and anaerobic decomposition and pure cultures with white-rot fungus and bacteria (see Fig. 2) have been tested for decolorization and destruction of dyes. Unfortunately, these treatments are very inefficient because the majority of these compounds are chemically stable and resistant to microbiological attack [19,20,34]. The characteristics of enzymes in microorganisms that are suitable for the decomposition of dyes have also been extensively investigated, requiring a greater knowledge of the enzymatic processes involved in them for application to environmental protection [19].

Over the past 10 years, the electrochemical technology has been largely developed for its alternative use for wastewater remediation. It currently offers promising approaches for the prevention of pollution problems from industrial effluents. The application of electrochemistry to environmental pollution abatement has been the topic of several books and reviews [31,35–43]. The main advantage of this technology is its environmental compatibility, due to the fact that its main reagent, the electron, is a clean reagent [35]. Other advantages are related to its versatility, high energy efficiency, amenability of automation and safety because it operates at mild conditions [35,39,42]. The strategies of electrochemistry include both the treatment of effluents and waste and the development of new processes or products with less harmful effects, often denoted as process-integrated environmental protection.

The main electrochemical procedures utilized for the remediation of dyestuffs wastewaters are also given in Fig. 2. Electrocoagulation (EC), electrochemical oxidation (EO) with different anodes and indirect electro-oxidation with active chlorine are typical methods for the removal of these pollutants. The treatment by emerging technologies such as electro-Fenton (EF) and photoassisted systems like photoelectro-Fenton (PEF) and photoelectrocatalysis has recently received great attention, but the possible role of electrochemical reduction has been clarified in much lesser extent. Note that electrochemical oxidation, electro-Fenton and photoassisted electrochemical systems have been classified as electrochemical advanced oxidation processes (EAOPs). In this paper we present a general review of lab and pilot plant experiments related to the most relevant applications of all these electrochemical methods to synthetic and real effluents. Fundamentals of each technology are also briefly discussed to better understand its advantages and limitations for the environmental prevention of pollution from synthetic organic dyes.

2. Electrocoagulation

A traditional physico-chemical treatment of phase separation for the decontamination of dyes wastewaters before discharge to the environment is coagulation. It consists in the addition of coagulating agents such as Fe^{3+} or Al^{3+} ions, usually in the form of chlorides, for dyes precipitation. The electrochemical technology can produce similar effects by means of the EC method [35,39,40]. This technique uses a current to dissolve Fe (or steel) or Al sacrificial anodes immersed in the polluted water, giving rise to the corresponding metal ions that yield different Fe(II) (and/or Fe(III)) or Al(III) species with hydroxide ion depending on the medium pH, as can be seen in Fig. 3 [44,45]. These species act as coagulants or destabilization agents that bring about charge neutralization for dyes separation from the wastewater. The coagulated particles can also be separated by electroflotation when they are attached to the bubbles of H_2 gas evolved at the cathode and transported to the top of the solution where they can be separated. In general, the following main processes take place during an EC treatment [46–49]:

(i) electrode reactions to produce metal ions from Fe or Al anodes and H_2 gas at the cathode;
(ii) formation of coagulants in the wastewater;
(iii) removal of dyes with coagulants by sedimentation or by electroflotation with evolved H_2;
(iv) other electrochemical and chemical reactions involving reduction of organic impurities and metal ions at the cathode and coagulation of colloidal particles.

Many advantages for EC have been reported [39,40,50]:

(i) more effective and rapid organic matter separation than in coagulation;
(ii) pH control is not necessary, except for extreme values;
(iii) the amount of chemicals required is small;
(iv) the amount of sludge produced is smaller when compared with coagulation. For example, the sludge formed in the EC method with Fe contains higher content of dry and hydrophobic solids than that produced in coagulation by the action of $FeCl_3$ followed by the addition of NaOH or lime;
(v) the operating costs are much lower than in most conventional technologies.

However, this method presents as major disadvantages [39]:

(i) anode passivation and sludge deposition on the electrodes that can inhibit the electrolytic process in continuous operation mode;
(ii) high concentrations of iron and aluminium ions in the effluent that have to be removed.

In subsections below the characteristics of EC and its relevant applications to dyes removal will be discussed on the basis of the sacrificial anode used.

2.1. Fe or steel anode

When an iron or steel anode is utilized in EC, Fe^{2+} is dissolved in the wastewater from Fe oxidation at the anode (standard potential $E^0 = -0.44$ V vs. SHE) as follows [46,51,52]:

$$Fe \rightarrow Fe^{2+} + 2e^- \quad (1)$$

whereas hydroxide ion and H_2 gas are generated at the cathode from the reaction ($E^0 = -0.83$ V vs. SHE):

$$2H_2O + 2e^- \rightarrow 2OH^- + H_{2(g)} \quad (2)$$

OH^- production from reaction (2) causes an increase in pH during electrolysis. As can be seen in Fig. 3a, insoluble $Fe(OH)_2$ precipitates at pH > 5.5 and remains in equilibrium with Fe^{2+} up to pH 9.5 or with monomeric species such as $Fe(OH)^+$, $Fe(OH)_2$ and $Fe(OH)_3^-$ at higher pH values. The formation of insoluble $Fe(OH)_2$ can be written as

$$Fe^{2+} + 2OH^- \rightarrow Fe(OH)_{2(s)} \quad (3)$$

and the overall reaction for the electrolytic process from the sequence of reactions (1)–(3) is:

$$Fe + 2H_2O \rightarrow Fe(OH)_{2(s)} + H_{2(g)} \quad (4)$$

In the presence of O_2, dissolved Fe^{2+} is oxidized to insoluble $Fe(OH)_3$ [46,51,52]:

$$4Fe^{2+} + 10H_2O + O_{2(g)} \rightarrow 4Fe(OH)_{3(s)} + 8H^+ \quad (5)$$

and protons can be directly reduced to H_2 gas at the cathode:

$$8H^+ + 8e^- \rightarrow 4H_{2(g)} \quad (6)$$

The corresponding overall reaction obtained by combining reactions (1), (5) and (6) is:

$$4Fe + 10H_2O + O_{2(g)} \rightarrow 4Fe(OH)_{3(s)} + 4H_{2(g)} \quad (7)$$

In acidic media of pH < 5.0, however, a greater quantity of Fe anode than that expected from Faraday law following reaction (1) is dissolved owing to the chemical attack of protons [53].

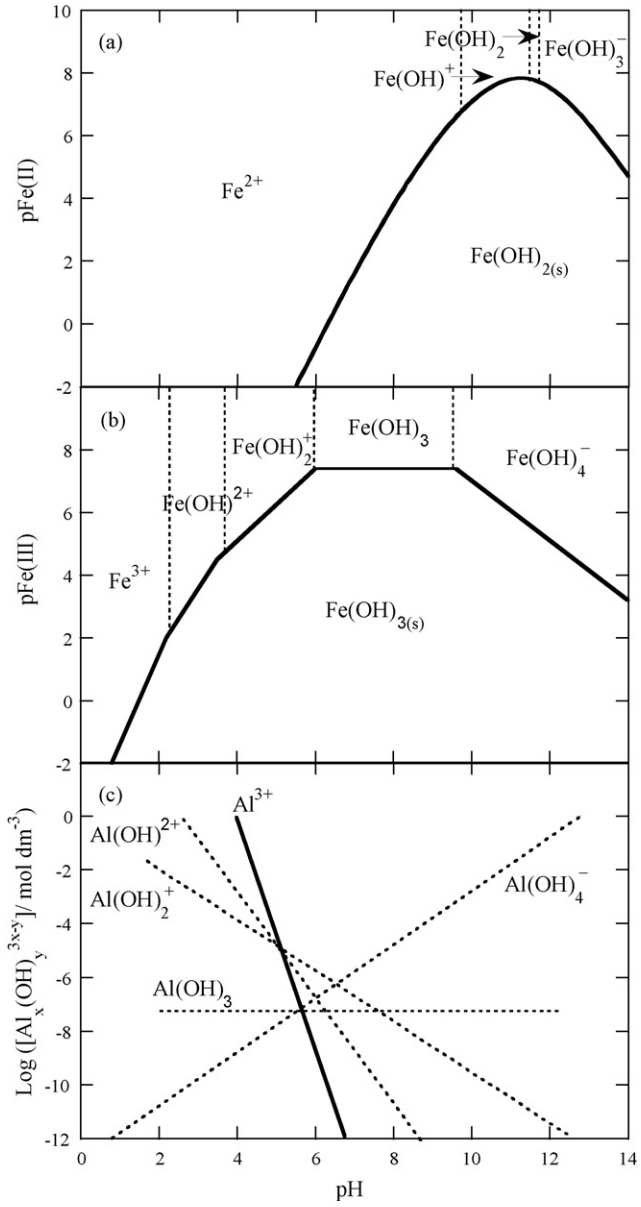

Fig. 3. Predominance-zone diagrams for (a) Fe(II) and (b) Fe(III) chemical species in aqueous solution. The straight lines represent the solubility equilibrium for insoluble $Fe(OH)_2$ and $Fe(OH)_3$, respectively, and the dotted lines represent the predominance limits between soluble chemical species. Adapted from Ref. [44]. (c) Diagram of solubility of Al(III) species as a function of pH. Adapted from Ref. [45].

Fig. 3b shows that $Fe(OH)_3$ coagulates from pH > 1.0, i.e., it is present in much stronger acidic media than $Fe(OH)_2$ (see Fig. 3a). Then, this precipitate can be in equilibrium with soluble monomeric species like Fe^{3+}, $Fe(OH)^{2+}$, $Fe(OH)_2^+$, $Fe(OH)_3$ and $Fe(OH)_4^-$ as a function of the pH range [44]. Among them, hydroxo iron cations have a pronounced tendency to polymerize at pH 3.5–7.0 to give polymeric cations such as $Fe_2(OH)_2^{4+}$ and $Fe_2(OH)_4^{2+}$ [54].

Once the insoluble flocs of $Fe(OH)_3$ are produced, they can remove dissolved dyes by surface complexation or electrostatic attraction [3,51]. The first mechanism considers that the dye can act as a ligand to bind a hydrous iron moiety of the floc yielding a surface complex:

$$\text{Dye}{-}\text{H} + (\text{HO})\text{OFe}_{(s)} \rightarrow \text{Dye}{-}\text{OFe}_{(s)} + \text{H}_2\text{O} \quad (8)$$

and the second one supposes that $Fe(OH)_3$ flocs with surface complexes contain areas of apparent positive or negative charge that attract the opposite regions of the dyestuff. Coagulation of these flocs forms particles that are separated from the wastewater by sedimentation or electroflotation.

From these fundamentals, many systems and reactors have been built up to apply this procedure, being even operative for industrial wastewaters [3,54–58]. Examples of several bench-scaled stirred tank reactors [59,60] and filter-press flow plants [61] operating in batch or continuous mode are illustrated in Figs. 4 and 5, respectively. They contain parallel plate electrodes with monopolar or bipolar connection. Monopolar electrodes need an external electrical contact to the power supply and their two faces are active with the same polarity. In contrast, bipolar electrodes do not possess electrical connections and are located between two end monopolar electrodes. The voltage applied between the latter electrodes by the power supply causes the polarization of the intermediate bipolar electrodes, which then present different polarities in the opposite faces [37].

Experimentally, the decolorization efficiency or percentage of color removal during the treatment of dyes wastewaters is determined by the expression [3]:

$$\text{color removal}\ (\%) = \frac{\text{ABS}_0^{\text{M}} - \text{ABS}_t^{\text{M}}}{\text{ABS}_0^{\text{M}}} \times 100 \quad (9)$$

where ABS_0^{M} and ABS_t^{M} are the average absorbances before electrolysis and after an electrolysis time t, respectively, at the maximum visible wavelength (λ_{max}) of the wastewater. The decontamination process of the dyes wastewater is monitored from the abatement of its chemical oxygen demand (COD) and/or total organic carbon (TOC). From these data, the percentages of COD and TOC decays are calculated from the following equations:

$$\text{COD decay}\ (\%) = \frac{\Delta\text{COD}}{\text{COD}_0} \times 100 \quad (10)$$

$$\text{TOC decay}\ (\%) = \frac{\Delta\text{TOC}}{\text{TOC}_0} \times 100 \quad (11)$$

where ΔCOD and ΔTOC are the corresponding removals in COD (mg of O_2 dm^{-3}) and TOC (mg of C dm^{-3}) at electrolysis time t, and COD_0 and TOC_0 are their initial values before treatment. Important specific energetic parameters such as energy consumption per volume of treated effluent (kWh m^{-3}), dye mass (kWh (kg dye)$^{-1}$), anode mass (kWh (kg Fe)$^{-1}$) or amount of COD (kWh (kg COD)$^{-1}$) destroyed can be obtained as follows:

$$\text{energy consumption}\ (\text{kWh m}^{-3}) = \frac{IVt}{V_s} \quad (12)$$

$$\text{energy consumption}\ (\text{kWh (kg dye)}^{-1}) = \frac{IVt}{\Delta m_{\text{dye}}} \quad (13)$$

$$\text{energy consumption}\ (\text{kWh (kg Fe)}^{-1}) = \frac{IVt}{\Delta m_{\text{anode}}} \quad (14)$$

$$\text{energy consumption}\ (\text{kWh (kg COD)}^{-1}) = \frac{IVt}{(\Delta\text{COD})V_s} \quad (15)$$

where I is the average applied current (A), V is the average cell voltage (V), t is the electrolysis time (h), V_s is the solution volume (dm^3), Δm_{dye} is the dye mass removed (g), Δm_{anode} is the anode mass dissolved (g) and ΔCOD is the decay in COD (g dm^{-3}). Similar expressions to Eqs. (9)–(15) are also utilized to analyze the performance of EC with Al.

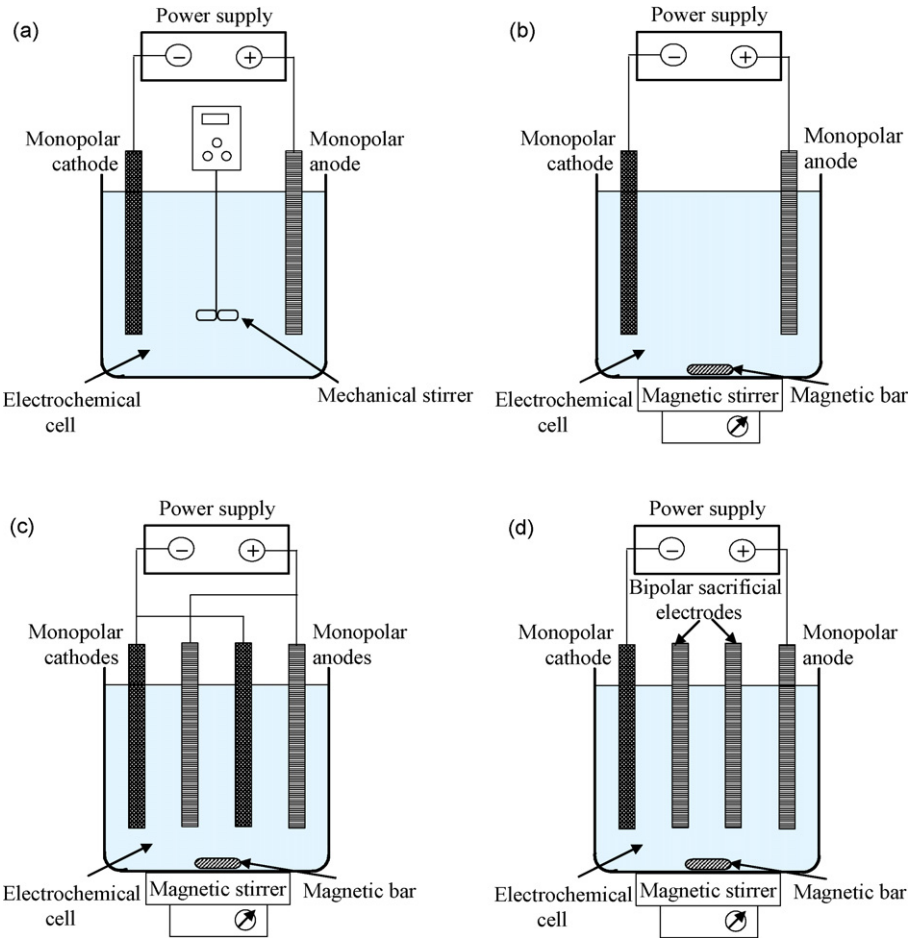

Fig. 4. Schemes of bench-scaled electrochemical cells with stirred tank reactors for treating dyes by electrocoagulation in batch operation mode. Two-electrode cell with (a) mechanical stirrer and (b) magnetic bar stirrer. Electrochemical cell with (c) monopolar electrodes in parallel connection and (d) bipolar sacrificial electrodes. Adapted from Refs. [59,60].

Table 1 summarizes the percentage of color removal and COD decay for selected synthetic dyes wastewaters under optimized EC conditions with monopolar and bipolar Fe or steel electrodes. Apart from the electrolytic system, dyes removal mainly depends on solution pH, retention time (t_r), stirring or flow rate and applied current density (or cell voltage) [51,52,59,62–69]. Fig. 6 illustrates the effect of initial pH, retention time and current density as function of decolorization efficiency for 250 cm^3 of 50 mg dm^{-3} solutions of the azo dye Basic Red 46 in NaCl (conductivity 8 mS cm^{-1}) using an unstirred Fe/steel tank reactor, similar to those shown in Fig. 4, with electrodes of 50 mm × 50 mm × 3 mm in dimension operating in batch mode [51]. As can be seen in Fig. 6a, the maximum color removal of about 95% is achieved at pH 5.5–8.5. A similar optimum pH range is also found for most dyes given in Table 1 [52,59,62–65]. Under these conditions, the majority of electrogenerated Fe^{3+} forms $Fe(OH)_3$ flocs that can remove rapidly the dye molecules by complexation or electrostatic attraction, followed by coagulation. In contrast, at pH < 3.0 soluble Fe^{3+} is the dominant species and $Fe(OH)_3$ flocs are quite poorly produced, whereas at pH > 9.0 a part of $Fe(OH)_3$ is solubilized as $Fe(OH)_4^-$ and lower amount of dye can be separated.

Other important parameter is the retention time or total electrolysis time of the dye wastewater in the reactor. Fig. 6b evidences that a minimum retention time of 5 min is needed to reach the highest decolorization efficiency of a 50 mg dm^{-3} Basic Red 46 solution at pH 5.8 and 6 mA cm^{-2}. At this t_r sufficient $Fe(OH)_3$ flocs are produced to remove efficiently the dyestuff [51]. Although the retention time is a function of operating parameters such as current density and dye concentration, the use of stirred tank reactors with stirring rates between 150 and 250 rpm is preferred to operate in batch mode [52,59,64–66]. Daneshvar et al. [66] described an enhancement of color removal with increasing stirring rate up to 200 rpm during the EC treatment of 250 cm^3 of 50 mg dm^{-3} of the azo dye Acid Orange 7 in a Fe/Fe cell like Fig. 4b, because aggregation of flocs is gradually favored and coagulation becomes easier. Higher stirring rates, however, cause a progressive degradation of flocs and a fall in the dye removal efficiency. In flow cells the retention time is regulated by the effluent flow rate. Mollah et al. [63] used a flow-through cell of 450 cm^3 volume with two monopolar and three intermediate bipolar steel plate electrodes (11.0 cm × 11.4 cm in dimension) to find that the color removal of a 30 mg dm^{-3} Acid Orange 7 solution containing 0.034 M NaCl of pH 8.4 decays from 99 to 93% at 16 mA cm^{-2} and 25 °C when the flow rate varies from 21 to 36 dm^3 h^{-1}. Low flow rates with enough long retention times are then required to yield good decolorization efficiencies.

Current density (j) controls the generation rate of iron ions, the growth of $Fe(OH)_3$ flocs and the rate and size of H_2 bubbles evolved [40] and hence, it determines the retention time and energy cost of the EC process of a dyestuff effluent. In general, the highest decolorization rate with the smallest energy cost for a given t_r is attained at an optimum j. This behaviour is exemplified in Fig. 6c for the treatment of a 50 mg dm^{-3} Basic Red 46 solution at pH 5.8 and t_r = 5 min, where an optimum current density of 6 mA cm^{-2}

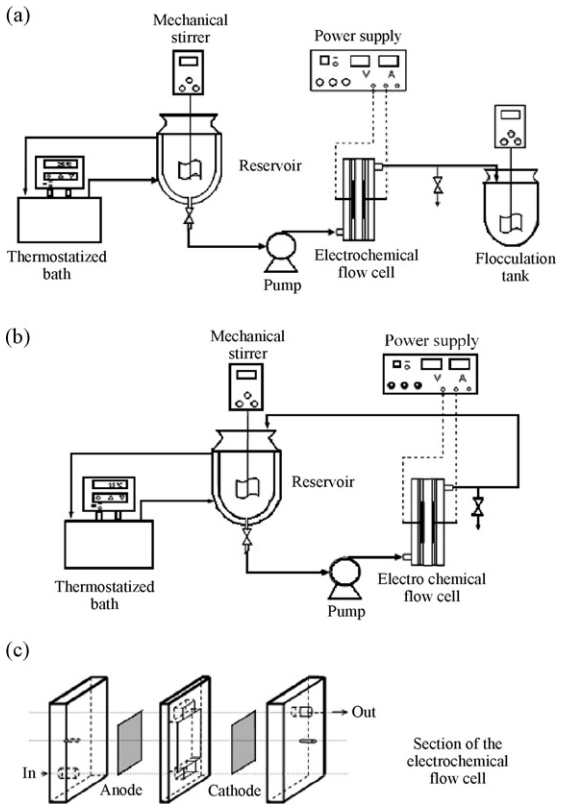

Fig. 5. Sketches of bench-scaled flow plants used for the electrocoagulation of dyes: (a) continuous operation mode; (b) batch operation mode; (c) section of the filter-press electrochemical cell. Adapted from Ref. [61].

related to 95% color removal with 4.7 kWh (kg dye)$^{-1}$ energy cost can be observed [51]. Higher j values allow a slightly greater decolorization efficiency, but the cost undergoes a dramatic rise to ca. 20 kWh (kg dye)$^{-1}$ at 14 mA cm^{-2}. Data collected in Table 1 evidence a change in the optimized current density for a given t_r in tank reactors with the dye tested. Thus, under similar conditions to those of Fig. 6c, the optimum treatment for Basic Blue 3 occurs at 8 mA cm^{-2} with 90% color removal and 7.5 kWh (kg dye)$^{-1}$ energy cost [51] and for Acid Yellow 23, at 11.2 mA cm^{-2} with 98% color removal and ca. 4 kWh (kg Fe)$^{-1}$ energy consumption [52]. At an optimized performance a rise in dye content causes a drop in decolorization efficiency because flocs formed cannot remove all the dye added [51,52,65]. The electrolyte concentration determines the wastewater conductivity and its increase mainly reduces the cell voltage at constant j and hence, the energy cost of the process [51,64]. When NaCl is employed at high current density, the anodic oxidation of Cl^- produces Cl_2 and ClO^-, which are strong oxidants that can also attack the dyes [68].

An inspection of Table 1 reveals the existence of a poor TOC or COD decay for most dyes treatments, very far from the large decolorization efficiency found under optimized conditions. Unfortunately, limited information is known in EC about by-products formed in the decolorization and decontamination processes. In the case of Acid Orange 7, for example, it has been demonstrated that its azo bond is reduced and broken, probably by oxidation with electrogenerated Fe^{2+} [35] and/or hypochlorite ion, to give 1-amino-2-naphtol and sulphanilic acid salt, being desorbed the former from the sludge formed [66].

The influence of different tank reactors on the comparative EC treatment in batch mode of 250 cm^3 of a solution containing until 150 mg dm^{-3} of the azo dye Acid Red 14 in the presence of 10 g dm^{-3} NaCl at pH 6–9 has also been investigated [59]. All monopolar and bipolar sacrificial electrodes were 25 cm^2 Fe plates and the monopolar cathode was a 25 cm^2 steel plate. Experimental results showed that the simple cell with two monopolar electrodes (see Fig. 4b, without stirring) is less effective, while the stirred cell with four monopolar electrodes (see Fig. 4c) gives slightly higher decolorization efficiency than that with two monopolar and two bipolar electrodes (see Fig. 4d). For t_r = 4 min, however, an optimized j of 8 mA cm^{-2} with color removal > 93% and COD decay > 85% at ca. 25 °C is found in all cases, indicating that the EC process is practically unaffected by the cell configuration.

An interesting study on the EC treatment of a sulphur dye wastewater from a textile industry has been recently reported [70]. The initial wastewater contained 1487 mg dm^{-3} of COD, 594 mg dm^{-3} of total suspended solids (TSS) and 9458 units of color in accordance with the American Dye Manufactures Institute. A tank reactor of 4 dm^3 volume containing two monopolar end steel plates and three intermediate bipolar steel plates as electrodes with a total contact surface area of 0.37 m^2 was used as electrochemical cell. Electrolyses were carried in batch operation mode and without stirring, using a 3^3 factorial design to optimize the initial pH, applied current and retention time. The optimum performance was obtained starting from pH 5.0 after consumption of 900 C (final pH 6.3) giving rise to decays of 76, 93 and 99% for COD, TSS and color, respectively.

The removal of some azo dyes has been comparatively studied by EC and electrochemical oxidation. Lopes et al. [67] treated 100–300 cm^3 of 350 mg dm^{-3} Direct Red 80 solutions in 5 g dm^{-3} Na_2SO_4 or NH_4NO_3 with conventional Fe/Fe, polypyrrole/steel and boron-doped diamond (BDD)/Cu cells in batch mode. Although 99–100% of color removal was attained in all cases, the COD decay was as low as 46–49% with Fe and polypyrrole anodes, but increased strongly to 87% with a BDD anode. In contrast, the smallest energy cost of 1.34 kWh m^{-3} at 5 mA cm^{-2} was found for EC, whereas much higher values of 5.46 kWh m^{-3} at 2 mA cm^{-2} and 6.65 kWh m^{-3} at 1.5 mA cm^{-2} were obtained for the electrochemical oxidation with polypyrrole and BDD, respectively. A similar behaviour has been reported by Muthukumar et al. [71] for the treatment of 2 dm^3 of 100 mg dm^{-3} Acid Orange 10 solutions in 0.017 M NaCl at pH 6–9 in a stirred tank reactor with various monopolar Fe, graphite and IrO_2–TaO_2–RuO_2 coated titanium rod electrodes in batch mode. The corresponding color and COD decays were 98 and 60% with the iron anode, whereas the solution was totally decontaminated with the graphite anode. Iron electrodes facilitated the reductive cleavage of azo linkage giving rise to the formation of aniline and 1-amino-2-naphthol-6,8-disulphonic acid, remaining the former in aqueous phase and co-precipitating the latter with $Fe(OH)_3$. The removal rate of Acid Orange 6 by O_3, AOPs such as O_3/UV, O_3/TiO_2/UV and Fenton's reagent, and EC using a flow-through cell with two monopolar and three bipolar iron plate electrodes in continuous mode, has also been compared by Hsing et al. [72]. They showed that EC provides a very rapid decolorization of the Acid Orange 6 solution, but it possesses a much smaller ability to destroy its TOC (<35%) than photocatalytic UV methods.

Several authors have described the acceleration of dyes removal by the combination of EC with other chemical or electrochemical procedures. For example, electrocoagulation combined with electro-oxidation for Acid Orange 7 using a cell with three-phase three-dimensional electrodes [73], electrocoagulation assisted by O_3 for Reactive Black 5 [74], electrocoagulation assisted by cobalt phosphomolybdate modified kaolin for Acid Red 18 [75] and electrocoagulation combined with AOPs like TiO_2/UV and O_3/UV for Reactive Red 2 [76] have been reported.

Table 1
Percentage of color removal and COD decay obtained for the electrocoagulation treatment with Fe or Al anodes of selected synthetic dyes solutions under optimized conditions at ambient temperature or 25 °C.

Dye[a]	Solution	Electrolytic system[b]	j[c]/mA cm^{-2}	Color removal/%	COD decay/%	Ref.
Fe or steel anode						
Acid Orange 6	200 mg dm^{-3} of dye with NaCl at pH 4	Flow-though cell with six monopolar anodes in continuous at 18–30 dm^3 h^{-1}	6.83	98	40[d]	[62]
Acid Orange 7 (Orange II)	10 mg dm^{-3} of dye with 0.034 M NaCl at pH 7.3	Flow-though cell with three bipolar electrodes in continuous at 21 dm^3 h^{-1}	32	99	–[e]	[63]
Acid Red 14	250 cm^3 of 150 mg dm^{-3} dye and 10 g dm^{-3} NaCl at pH 6–9	Stirred tank reactors with monopolar or bipolar electrodes in batch, t_r = 4 min	8	>93	>85	[59]
Acid Yellow 23	250 cm^3 of 50 mg dm^{-3} dye and 0.4 g dm^{-3} NaCl at pH 6	Stirred tank reactor with two monopolar electrodes in batch, t_r = 5 min	11.2	98	69	[52]
Acid Yellow 36	200 cm^3 of 50 mg dm^{-3} dye and 8 g dm^{-3} NaCl at pH 7–9	Tank reactor with two monopolar electrodes in batch without stirring, t_r = 6 min	12.8	85	–[e]	[64]
Basic Blue 3	250 cm^3 of 50 mg dm^{-3} dye	Tank reactor with two monopolar electrodes	8	90	75	[51]
Basic Red 46	and NaCl at pH 5.8	in batch without stirring, t_r = 5 min	6	95	99	
Mordant Black 11 (Eriochrome Black T)	1.5 dm^3 of 1 g dm^{-3} dye and 3 g dm^{-3} NaCl at pH 4	Filter-press flow cell with two monopolar electrodes in batch at 50 dm^3 h^{-1}	1.4	96	–[e]	[53]
Reactive Red 124	650 cm^3 of 100 mg dm^{-3} dye and 3 g dm^{-3} NaCl at pH 8	Stirred tank reactor with two bipolar electrodes in batch, t_r = 5 min	1.35	100	100	[65]
Al anode						
Disperse Blue 139, Disperse Red 74, Disperse Yellow 126	700 cm^3 of 370 mg dm^{-3} mixed dyes and 0.1 M NaCl at pH 9.0	Stirred tank reactor with two monopolar electrodes in batch, t_r > 5.1 min	30	99	–[e]	[60]
Mordant Black 11 (Eriochrome Black T)	1.5 dm^3 of 100 mg dm^{-3} dye and 3 g dm^{-3} Na_2SO_4 at pH 4	Filter-press flow cell with two monopolar electrodes in batch at 19 dm^3 h^{-1} for 18 min	1.4	94	–[e]	[61]
Reactive Orange 64 (Levafix Orange E3 GA)	250 cm^3 of 100 mg dm^{-3} dye and NaCl at pH 6.4	Stirred tank reactor with four monopolar electrodes in batch, t_r = 12 min	10	98	–[e]	[78]
Reactive Red 198 (Remazol Red RB 133)	250 cm^3 of 100 mg dm^{-3} dye and NaCl at pH 6	Stirred tank reactor with four monopolar electrodes in batch, t_r = 10 min	10	99	–[e]	[47]

[a] Color index (common) name.
[b] t_r is the retention time in batch operation mode.
[c] Applied current density.
[d] Percentage of TOC decay.
[e] Not determined.

2.2. Al anode

In the case of EC with Al, the anodic reaction leads to soluble Al^{3+} (E^0 = 1.66 V vs. SHE) [47,48,52,77]:

$$Al \rightarrow Al^{3+} + 3e^- \quad (16)$$

and the cathodic reaction produces hydroxide ion and H_2 gas:

$$3H_2O + 3e^- \rightarrow 3OH^- + (3/2)H_{2(g)} \quad (17)$$

Fig. 3c evidences that Al^{3+} is transformed into soluble monomeric species such as $Al(OH)^{2+}$, $Al(OH)_2^+$, $Al(OH)_3$ and $Al(OH)_4^-$ depending on the pH range. Monomeric cations predominate in acid medium and $Al(OH)_4^-$ in alkaline medium. The former can evolve to polymeric species such as $Al_2(OH)_2^{4+}$, $Al_6(OH)_{15}^{3+}$, $Al_7(OH)_{17}^{4+}$, $Al_8(OH)_{20}^{4+}$, $Al_{13}O_4(OH)_{24}^{7+}$ and $Al_{13}(OH)_{34}^{5+}$ [47,52,78]. Soluble monomeric and polymeric cations are also converted into insoluble $Al(OH)_3$ flocs by a complex precipitation kinetics. The overall reaction to give the latter product is:

$$Al + 3H_2O \rightarrow Al(OH)_{3(s)} + (3/2)H_{2(g)} \quad (18)$$

However, when an Al cathode is also utilized, it can be chemically attacked by OH^- generated during H_2 evolution at high pH values as follows [53,79]:

$$Al + 3H_2O + OH^- \rightarrow Al(OH)_4^- + (3/2)H_{2(g)} \quad (19)$$

and treated wastewater contains higher amount of aluminium ions than those expected from reaction (16). Note that a Fe or steel anode is not attacked by OH^- in alkaline medium, thus avoiding the formation of an excess of $Fe(OH)_4^-$ species.

Similarly to EC with Fe, the removal of dyes from wastewaters using Al can be explained by surface complexation and electrostatic attraction [3,47,77]. The surface complexes between dyes and hydrous aluminium moieties are formed in the following manner:

$$Dye{-}H + (HO)OAl_{(s)} \rightarrow Dye{-}OAl_{(s)} + H_2O \quad (20)$$

In this case interaction attractions between dye molecules and monomeric and polymeric aluminium cations via precipitation and/or adsorption mechanisms become more important in the EC process. Precipitation by neutralization of opposite charges predominates in acidic medium, taking place the reaction of dyes with monomeric species at pH < 5.0:

$$Dye + \text{monomeric Al} \rightarrow [Dye{-}\text{monomeric Al}]_{(s)} \quad (21)$$

and with polymeric species at pH 5–6

$$Dye + \text{polymeric Al} \rightarrow [Dye{-}\text{polymeric Al}]_{(s)} \quad (22)$$

Adsorption on $Al(OH)_3$ flocs, followed by coagulation to form particles, mainly occurs at pH > 6.5:

$$Dye + Al(OH)_{3(s)} \rightarrow [\text{particle}] \quad (23)$$

$$[Dye{-}\text{polymeric Al}]_{(s)} + Al(OH)_{3(s)} \rightarrow [\text{particle}] \quad (24)$$

The large surface areas of freshly formed amorphous $Al(OH)_3$ flocs can also adsorb soluble organic compounds and/or trap colloidal particles, which are thus separated from the aqueous solution [47].

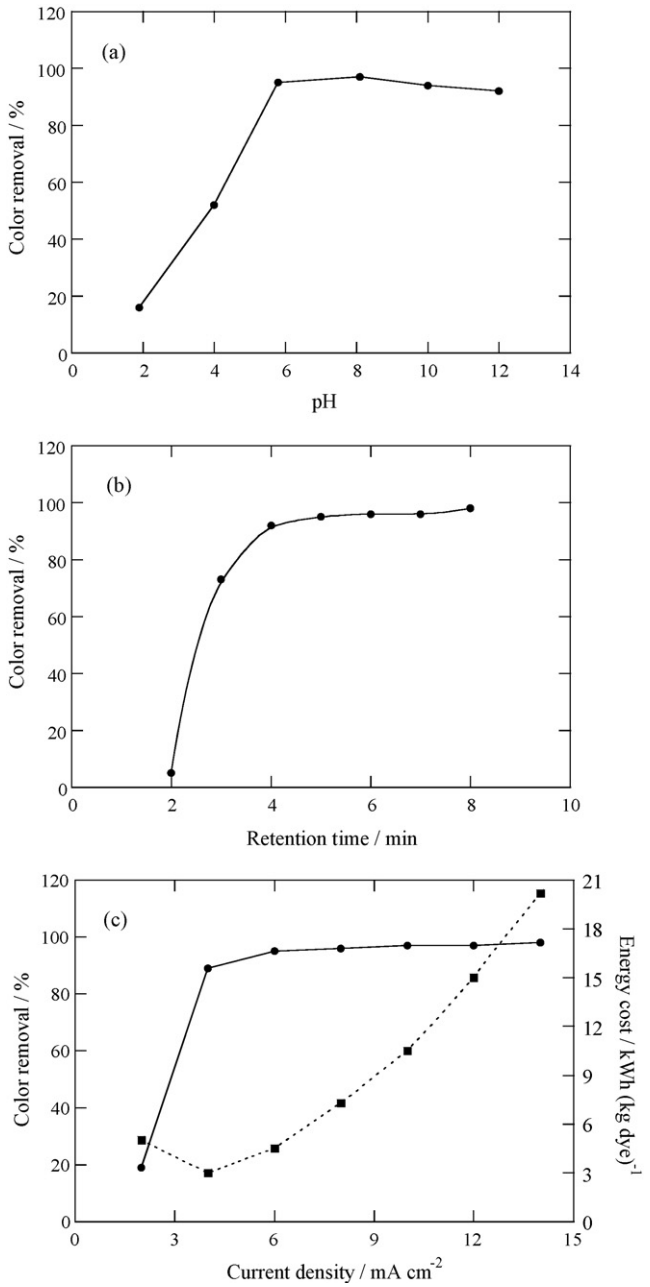

Fig. 6. Influence of (a) initial pH, (b) retention time and (c) current density on color removal efficiency for the electrocoagulation of 250 cm^3 of 50 mg dm^{-3} Basic Red 46 solutions with NaCl as background electrolyte (conductivity 8 mS cm^{-1}) in a tank reactor without stirring containing an iron plate as anode and a steel plate as cathode, both of 25 cm^2 area, at room temperature. Current density: (a and b) 6.0 mA cm^{-2}; retention time: (a and c) 5 min; initial pH: (b and c) 5.8. In plot (c), the energy cost per kg of dye removed is also given. Adapted from Ref. [51].

The existence of the above mechanisms has been tested by Cañizares et al. [61,80] for the EC process of 100 mg dm^{-3} of the azo dye Eriochrome Black T (EBT) in 3 g dm^{-3} Na_2SO_4 solutions within the pH range 2–12 using the filter-press flow cell of Fig. 5a with 100 cm^2 Al plates as electrodes at 1.4 mA cm^{-2} and flow rate of 19 dm^3 h^{-1}. Two maxima of 82 and 94% for color removal (associated with EBT decay) can be observed in Fig. 7a at steady pH values near 2.0 and 6.0, respectively, whereas it drops strongly at pH > 6.5. The maximum color removal at pH ca. 2 was ascribed to the binding of monomeric aluminium cations to the negative groups of EBT ($-SO_3^-$) via reaction (21) and the subsequent formation of insoluble compounds. The highest decolorization efficiency at pH near 6 was explained by the binding of the EBT anionic groups ($-SO_3^-$, $-O^-$) either to polymeric aluminium cations from reaction (22) or positively charged sites of $Al(OH)_3$ flocs via chemisorption from reaction (23), along with the enmeshment of EBT molecules into growing particles of $Al(OH)_3$ precipitate. At pH > 6.5, the formation of $Al(OH)_4^-$ and precipitation of negatively charged $Al(OH)_3$ are favoured, inhibiting the adsorption mechanisms of EBT anions via reactions (23) and (24) due to repulsion forces and reducing the decolorization efficiency.

Dye concentration, electrolyte composition, current density and operation mode also affect the coagulation mechanisms of EBT at the optimum steady pH of about 6 (initial pH 4.0). As can be seen in Fig. 7b, the color removal undergoes a continuous drop for increasing concentration from 100 mg dm^{-3} because polymeric aluminium cations and $Al(OH)_3$ flocs can only retain a stoichiometric amount of EBT as maximum and the dye in excess remains in the solution. This phenomenon is much more significant with NaCl than with Na_2SO_4 as background electrolyte, probably due to the existence of a much larger adsorption of Cl^- on $Al(OH)_3$ that strongly inhibits EBT removal. Fig. 7c shows that a steady decolorization efficiency of 94% is reached for a 100 mg dm^{-3} EBT solution with 3 g dm^{-3} Na_2SO_4 treated in continuous mode after passing a specific charge (Q) between 0.008 and 0.16 Ah dm^{-3}. This evidences that the stoichiometric ratio of coagulants to retain the maximum amount of EBT is produced with a minimum consumption of 0.008 Ah dm^{-3} and hence, the formation of an excess of coagulants at higher Q has little influence on the precipitation and adsorption mechanisms. On the other hand, the batch plant of Fig. 5b yields the same decolorization efficiency and similar pH evolution than the continuous plant of Fig. 5a, but with the generation of lower concentration of aluminium ions, as shown in Fig. 7d. The fact that the concentration of such ions increases gradually in batch mode after recirculation through the cell suggests a higher efficiency of EBT removal via precipitation with polymeric aluminium cations, present in larger extent in the solution under these conditions.

The effect of operating parameters on the decolorization efficiency of other dyes by EC with Al has been extensively studied [47,60,77,78,81,82]. Optimized conditions for selected compounds leading to about 98% of color removal are also collected in Table 1. Szpyrkowicz [60,81] utilized the stirred tank reactor of Fig. 4a equipped with a 100 cm^2 Al plate anode and a 100 cm^2 stainless-steel cathode to treat 700 dm^3 of a mixture of 370 mg dm^{-3} of three dispersed dyes in 0.1 M NaCl at pH 9.0. This author showed that the decolorization process occurred in two phases involving electrocoagulation of dyes with species formed *in situ* during Al dissolution and subsequent electroflotation of particle agglomerates, which are dependent on the hydrodynamic conditions in the reactor and current density. For a rotation speed of the mechanical stirrer of 9 Hz and j = 30 mA cm^{-2}, times as short as 1.1 min for electrocoagulation and 0.9 min for electroflotation were needed for achieving 99% color removal. The large influence of pH on decolorization efficiency has been corroborated by Kobya et al. when electrolyzing 250 cm^3 of Reactive Red 198 [47] and Reactive Orange 64 [78] solutions with different NaCl concentrations between pH 3 and 11 at 25 °C using the stirred tank reactor of Fig. 4c with Al plates of 46 mm × 53 mm × 3 mm in dimension as electrodes and a stirring rate of 200 rpm. These authors found higher color removal for pH < 6.5 than neutral and alkaline media owing to the predominance of precipitation mechanisms via monomeric and polymeric aluminium cations, along with decay in color removal and energy consumption with increasing dye and NaCl concentrations and j. For example, reductions from 98 to 88% for color removal and from 98 to 26 kWh (kg dye)$^{-1}$ for energy

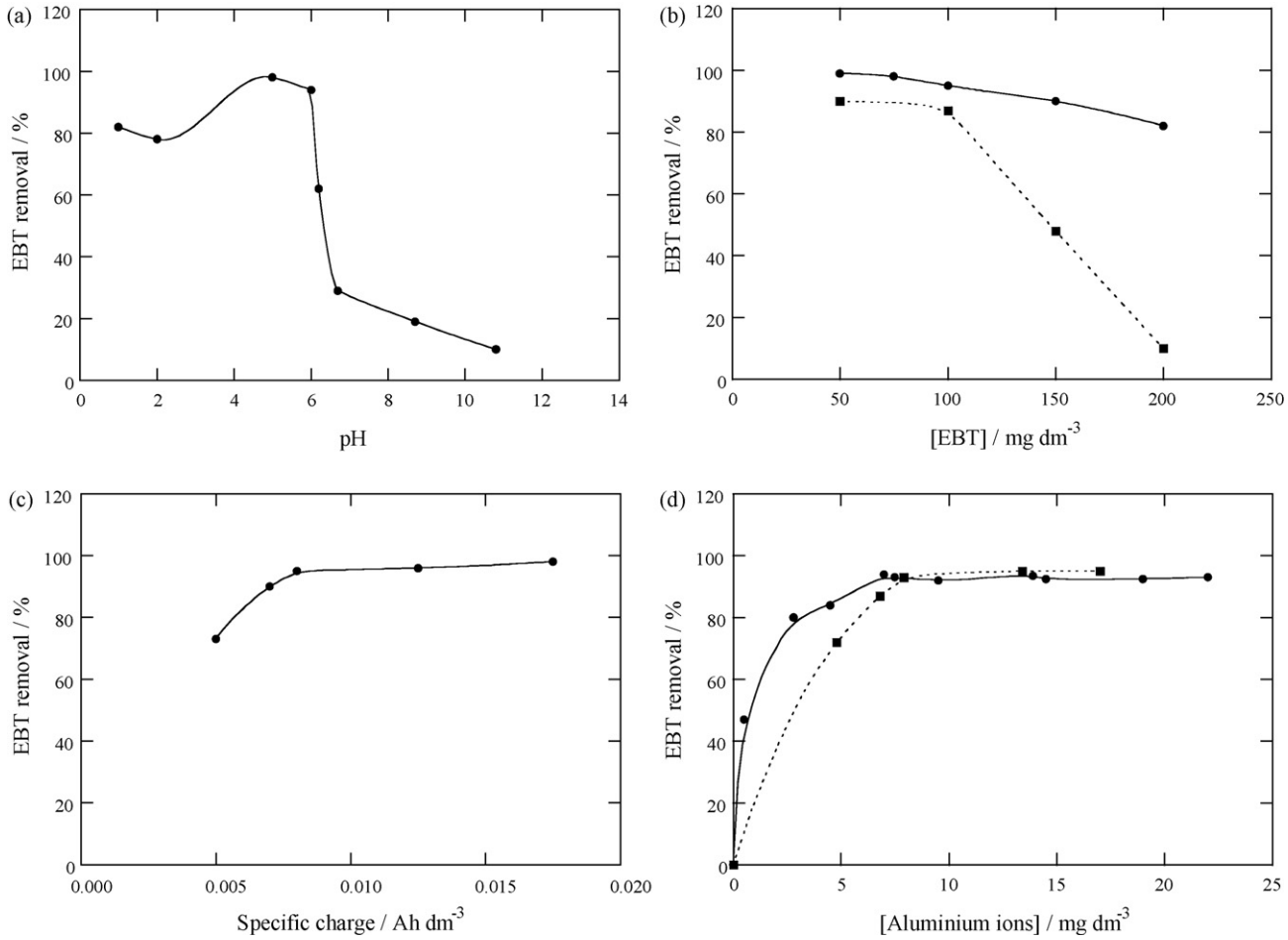

Fig. 7. Effect of (a) steady pH, (b) dye content, (c) specific charge and (d) aluminium concentration on Eriochrome Black T removal by electrocoagulation at 25 °C using the filter-press flow plants of Fig. 5 with a cell containing 100 cm^2 Al electrodes at flow rate of 19 dm^3 h^{-1}. Conditions: (a) 100 mg dm^{-3} dye solution in 3 g dm^{-3} Na_2SO_4 in continuous at 1.4 mA cm^{-2}; (b) effluents with (●) 3 g dm^{-3} Na_2SO_4 and (■) 3 g dm^{-3} NaCl of initial pH 4.0 in continuous at 1.4 mA cm^{-2}; (c) 100 mg dm^{-3} dye effluent with 3 g dm^{-3} Na_2SO_4 of initial pH 4.0 in continuous at different current density; (d) 100 mg dm^{-3} dye solution in 3 g dm^{-3} Na_2SO_4 at initial pH 4.0 in (●) batch (1.5 dm^3 treated for 18 min) and (■) continuous modes at 1.4 mA cm^{-2}. Adapted from Ref. [61].

consumption were obtained when Reactive Orange 64 concentration varies from 100 to 500 mg dm^{-3} at pH 6.4, 10 mA cm^{-2} and 0.75 mS cm^{-1} of conductivity for 15 min, whereas these parameters dropped from 97 to 87% and from 45 to 13 kWh (kg dye)$^{-1}$ with rising conductivity from 0.75 to 4.00 mS cm^{-1} after the same time of electrolysis of 500 mg dm^{-3} dye solutions at pH 6.4 and 10 mA cm^{-2}.

2.3. Comparative behaviour of anodes

Electrocoagulation appears to be an easy, fast, effective and economical method for almost total decolorization of chloride dyes wastewaters either using Fe (or steel) or Al anode, although poor decontamination is achieved in most cases due to the partial oxidation of dyes with Fe^{2+} and/or active chlorine species and desorption of by-products from the sludge formed. The comparative treatment of several synthetic dyes and industrial effluents with such sacrificial anodes has also been described to ascertain the best material for EC [3,48,52–54,83–89]. However, more research efforts are needed to better know what anode is preferable as a function of the chemical structure and/or applicability of the dye.

Most comparative studies with pure synthetic dyes have been performed with reactive, disperse and acid products utilized in the textile industry. Do and Chen [83] reported the superiority of Fe for decolorization efficiency when treating the reactive Drimarene Discharge X-3LG in front of the disperse Samaron Yellow 4, whereas the opposite tendency was preferred using Al. The same behaviour has been described when comparing the EC processes for Reactive Blue 49 and Reactive Yellow 84 with those of Disperse Blue 106 and Disperse Yellow 54 [84]. The best performances achieved with Fe than with Al for reactive dyes have also been confirmed for reactive dyebath effluents [89] and Procion Black 5B [3]. In the latter case, for example, the treatment of 400 cm^3 of 300 g dm^{-3} solutions of the dye in NaCl as electrolyte with stirred steel/steel and Al/steel cells like Fig. 4b at 10 mA cm^{-2} yielded 100% color and COD reductions with a cost of 78.5 kWh (kg COD)$^{-1}$ in the first cell and 89% color removal, 80% COD decay and 130.1 kWh (kg COD)$^{-1}$ energy consumption in the second one. On the other hand, Yang and McGarrahan [86] compared the decolorization rate of the antraquinone dye Reactive Blue 19 and the azo dyes Acid Red 226 and Disperse Yellow 218 to attain 98% color removal. For a steel anode, it decayed in the order: reactive > acid > disperse, and for Al, in the sequence: acid > reactive > disperse. For 250 cm^3 of 50 g dm^{-3} of the azo dye Acid Yellow 23 in NaCl (conductivity 16.5 mS cm^{-1}) at pH 6.0 treated with stirred Fe/steel and Al/steel cells like Fig. 4b containing plates of 40 mm × 50 mm × 1 mm as electrodes at a stirring rate of 200 rpm, a better performance was found for Al with almost 98% of color removal and 69% of COD decay at the

optimized j of 11.25 mA cm^{-2} for t_r = 5 min, since a quite poor color reduction < 25% was obtained for Fe [52]. A positive effect on the decolorization efficiency of Acid Yellow 23 has also been reported by Modirshahla et al. [48] when Fe and Al electrodes are combined in stirred tank reactors with monopolar (see Fig. 4c) and bipolar (see Fig. 4d) electrodes in comparison to the same electrochemical cells only containing one electrode material. Al was also found superior to Fe for the decolorization of 1.5 dm^3 of a 1 g dm^{-3} Eriochrome Black T solution in 3 g dm^{-3} NaCl of pH 4.0 using the system of Fig. 5b [53].

Bayramoglu et al. [85] analyzed the operating costs for the EC treatment of textile dye wastewaters with 3422 mg dm^{-3} COD, 1112 mg dm^{-3} TSS and 3990 mS cm^{-1} conductivity using the stirred tank reactor of Fig. 4c with two iron or two aluminium electrodes of 78 cm^2 area. In acidic medium higher COD removal close to 100% was obtained for Al, whereas in neutral and weakly alkaline medium only Fe allowed to attain a maximum decontamination of ca. 96%. Total operating (energy + electrode) cost at 10 mA was approximately of 0.1 US$ (kg COD)$^{-1}$ with Fe, much lower than ca. 0.3 US$ (kg COD)$^{-1}$ determined for Al. Electrode consumption accounted for nearly 50 and 80% of the total cost for Fe and Al, respectively.

3. Electrochemical reduction

A limited number of papers have been published dealing with the direct electroreduction of dyes in aqueous solution on suitable cathodes. The reason of the low interest for this conventional electrochemical technique is that it offers poor decontamination of wastewaters in comparison to more potent direct and indirect electro-oxidation methods, as will be detailed below.

Fig. 8a shows a conventional three-electrode two-compartment cell utilized for the electrochemical treatment of the azo dye Amaranth at room temperature [90]. The working compartment contains an activated carbon fiber (ACF) electrode and the contaminated solution is continuously stirred with a magnetic bar stirrer, whereas the counter electrode compartment contains a Pt wire and the same electrolyte solution (anolyte). Both compartments are separated by a cation selective membrane as ionic contact. The reference electrode is a saturated calomel electrode (SCE), which is connected to the working compartment through a salt bridge. This system was used to contrast the electroreduction process of 80 mg dm^{-3} Amaranth solutions in 0.1 M Na_2SO_4 with a phosphate buffer of pH 6.6 on ACF under galvanostatic [90] and potentiostatic [91] conditions. Fig. 8b presents the relationship of color, COD and TOC removals with applied electrode potential after 500 min of potentiostatic electrolyses [91]. For the electrochemical reduction, overall decolorization can be observed for cathodic potential (E_{cat}) > −0.500 V vs. SCE, with COD and TOC reductions of ca. 60%. Spectra analysis confirmed the destruction of the azo bond for E_{cat} from −0.200 to −0.800 V. Similar results of 95% color removal and 62% COD decay were obtained operating at constant j of −1.0 mA cm^{-2} for 8 h [90]. The low COD and TOC removals for Amaranth solutions were ascribed to the adsorption on ACF of by-products formed during the electroreduction process [90,91].

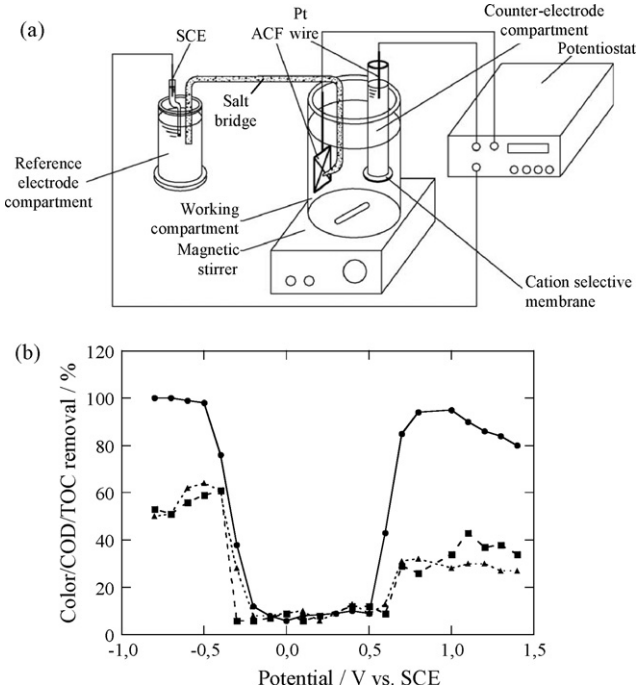

Fig. 8. (a) Experimental set-up for the electrochemical treatment of Amaranth with an activated carbon fiber (ACF) electrode using a three-electrode two-compartment cell. Adapted from Ref. [90]. (b) Change of (●) color, (■) COD and (▲) TOC removal with electrode potential for 80 mg dm^{-3} dye solution with 0.1 M Na_2SO_4 and a phosphate buffer of pH 6.6 for 500 min under potentiostatic treatment. Adapted from Ref. [91].

Jain et al. [92] studied the electrochemical reduction of 10 cm^3 of 0.2 mM of the azo dye Acid Yellow 23 solutions in 0.1 M KCl and Britton–Robinson buffers of pH 2.5, 5.6, 8.8 or 10.5 at room temperature using a three-electrode cell equipped with a 9 cm^2 Pt or 15 cm^2 steel foil as cathode, a Pt wire as anode and an Ag/AgCl (KCl saturated) electrode as reference electrode under N_2 atmosphere. Controlled-potential electrolyses at E_{cat} = −1.20 V vs. Ag/AgCl led to overall decolorization at 4 h with the Pt cathode and at much shorter time of approximately 2 h with the steel cathode, but with a COD removal as low as 48%. Coulometric measurements revealed the consumption of 2 electrons per molecule owing to the formation of the corresponding hydrazono derivative as the main by-product from electroreduction of the chromophoric –N=N– group to give a –NH–NH– bond. A similar behaviour has been recently reported by the same research group for the electroreduction of the azo dye Reactofix Golden Yellow 3 under the same experimental conditions [93]. In this case controlled-potential electrolyses were performed with 10 dm^3 of 0.5 mM dye solutions of pH 2.0, 7.0 and 10.2 using the above Pt cathode at E_{cat} = −0.80 V vs. Ag/AgCl and about 75% COD was removed.

Low decolorization efficiency and TOC removal were found by Carneiro et al. [94,95] for the electrochemical reduction of the antraquinone dye Reactive Blue 4 by means of a three-electrode two-compartment cell equipped with a 2.5 cm^2 reticulated vitreous carbon (RVC) cathode and a 4.0 cm^2 Pt gauze anode. The two compartments were separated by a fine glass sinter and an Ag/AgCl electrode was used as reference electrode. Electrolyses were carried out with 50 cm^3 of 40 mM dye solutions with HCl/KCl of pH 2.2 and Britton–Robinson buffers of pH 7.0 and 10.0 by applying E_{cat} values of −0.600, −0.850 and −0.900 V vs. Ag/AgCl for 2, 3 and 4 h, respectively. Color removal of 61, 62 and 37% was obtained for these treatments, although the highest TOC decay of 64% was achieved in the former electrolysis at pH 2.2. Analysis of the remaining intermediates allowed discriminating between two initial reaction paths on RVC depending on pH [95]. Fig. 9 illustrates that at pH < 8.0 the two carbonyl groups are protonated and the resulting diprotonated form undergoes further reduction with two electrons giving rise to the hydroquinone derivative, which is subsequently broken with the loss of a HSO_3^- ion and two Cl^- ions. In contrast, at pH > 8.0 the hydroquinone derivative with the release of a HSO_3^- ion is formed from two parallel ways involving the two-electron reduction of the dye and of its monoprotonated form.

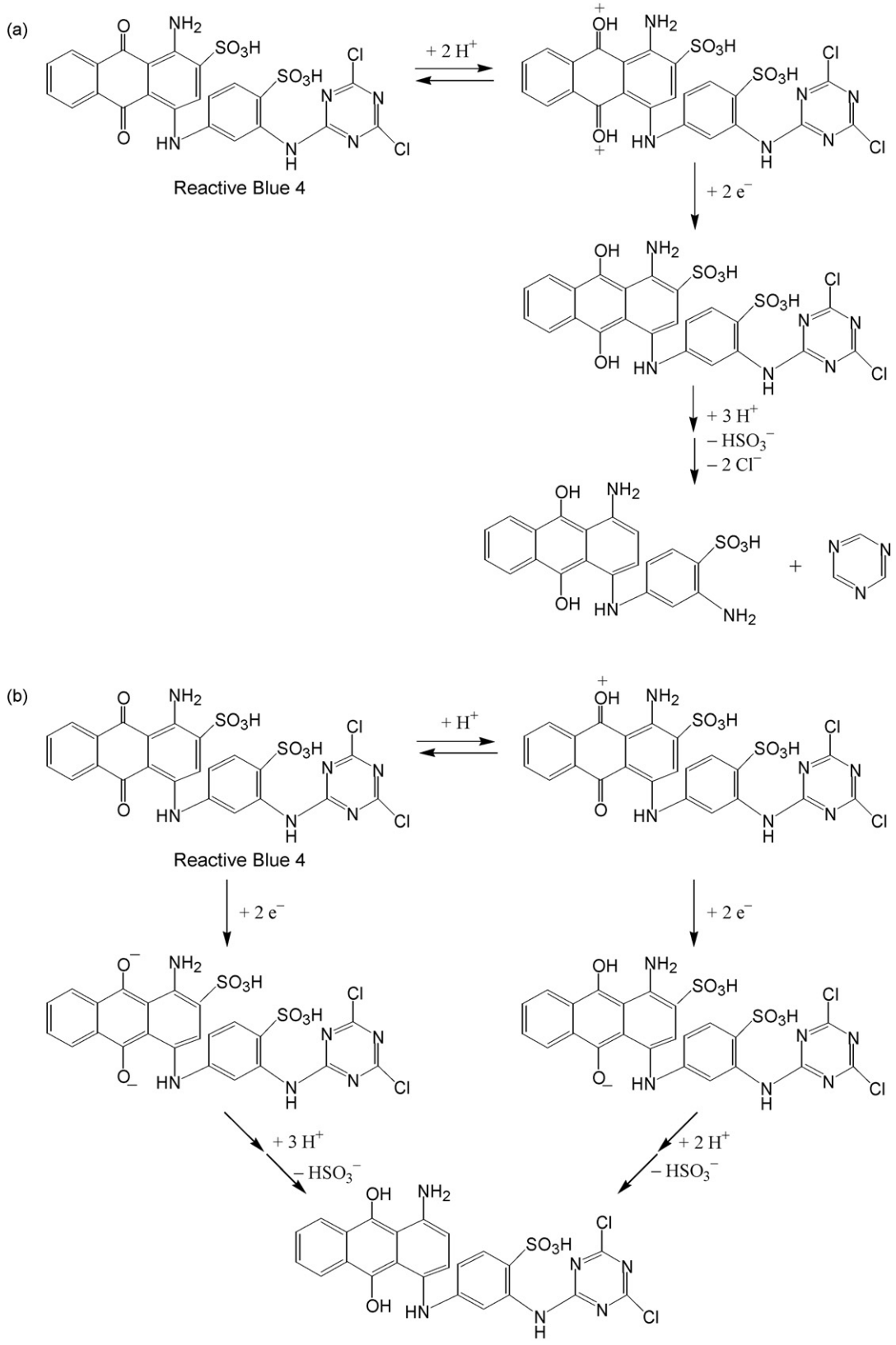

Fig. 9. Initial reaction pathways for the electrochemical reduction of Reactive Blue 4 on reticulated glassy carbon electrode at (a) pH < 8.0 and (b) pH > 8.0. Adapted from Ref. [95].

4. Electrochemical oxidation

Electrochemical oxidation or electro-oxidation (EO) is the most popular electrochemical procedure for removing organic pollutants from wastewaters [35,37,39,42]. This technique has been recently used for decolorizing and degrading dyes from aqueous solutions. It consists in the oxidation of pollutants in an electrolytic cell by

(i) Direct anodic oxidation (or direct electron transfer to the anode), which yields very poor decontamination.
(ii) Chemical reaction with electrogenerated species from water discharge at the anode such as physically adsorbed "active oxygen" (physisorbed hydroxyl radical ($^{\bullet}$OH)) or chemisorbed "active oxygen" (oxygen in the lattice of a metal oxide (MO) anode). The action of these oxidizing species leads to total or partial decontamination, respectively.

The existence of indirect or mediated oxidation with different heterogeneous species formed from water discharge has allowed the proposal of two main approaches for the pollution abatement in wastewaters by EO [39,42,96]:

(i) The electrochemical conversion method, in which refractory organics are selectively transformed into biodegradable compounds, usually carboxylic acids, with chemisorbed "active oxygen".
(ii) The electrochemical combustion (or electrochemical incineration) method, where organics are completely mineralized, i.e., oxidized to CO_2 and inorganic ions, with physisorbed $^{\bullet}$OH. This radical is the second strongest oxidant known after fluorine, with a high standard potential (E^0 = 2.80 V vs. SHE) that ensures its fast reaction with most organics giving dehydrogenated or hydroxylated derivatives up to conversion into CO_2.

In both cases high cell voltages are applied to the electrochemical cell for the simultaneous oxidation of pollutants and water, thus maintaining the anode activity. The use of low cell voltages avoiding O_2 evolution frequently causes the loss of anode activity because some by-products formed from direct anodic oxidation can be adsorbed on its surface and hence, this procedure is not utilized for wastewater treatment in practice. It has been found that the nature of the anode material influences strongly both the selectivity and efficiency of the EO process. To interpret this behaviour, a comprehensive model for organics destruction in acidic medium including the competition with the oxygen evolution reaction has been proposed by Comninellis [96]. The predictions of this model fit quite well with recent results obtained with conductive diamond electrodes such as BDD, which present the highest O_2 overvoltage known [97].

4.1. Model for the organics oxidation with heterogeneous hydroxyl radical

Comninellis [96] explained the different behaviour of electrodes in EO considering two limiting cases: the so-called "active" and "non-active" anodes. Typical examples are Pt, IrO_2 and RuO_2 for the former and PbO_2, SnO_2 and BDD for the latter. The proposed model assumes that the initial reaction in both kind of anodes (generically denoted as M) corresponds to the oxidation of water molecules leading to the formation of physisorbed hydroxyl radical (M($^{\bullet}$OH)):

$$M + H_2O \rightarrow M(^{\bullet}OH) + H^+ + e^- \quad (25)$$

Both the electrochemical and chemical reactivity of heterogeneous M($^{\bullet}$OH) are dependent on the nature of the electrode material. The surface of active anodes interacts strongly with $^{\bullet}$OH and then, a so-called higher oxide or superoxide (MO) may be formed following reaction (26). This may occur when higher oxidation states are available for a metal oxide anode, above the standard potential for oxygen evolution (E^0 = 1.23 V vs. SHE).

$$M(^{\bullet}OH) \rightarrow MO + H^+ + e^- \quad (26)$$

The redox couple MO/M acts as a mediator in the oxidation of organics by reaction (27), which competes with the side reaction of oxygen evolution via chemical decomposition of the higher oxide species from reaction (28).

$$MO + R \rightarrow M + RO \quad (27)$$

$$MO \rightarrow M + (1/2)O_2 \quad (28)$$

In contrast, the surface of a non-active anode interacts so weakly with $^{\bullet}$OH that allows the direct reaction of organics with M($^{\bullet}$OH) to give fully oxidized reaction products such as CO_2 as follows:

$$aM(^{\bullet}OH) + R \rightarrow aM + mCO_2 + nH_2O + xH^+ + ye^- \quad (29)$$

where R is an organic compound with m carbon atoms and without any heteroatom, which needs $a = (2m + n)$ oxygen atoms to be totally mineralized to CO_2. The oxidative reaction (27) with the surface redox couple MO/M is much more selective than the mineralization reaction (29) with physisorbed heterogeneous hydroxyl radical. The latter reaction also competes with the side reactions of M($^{\bullet}$OH) such as direct oxidation to O_2 from reaction (30) or indirect consumption through dimerization to hydrogen peroxide by reaction (31):

$$M(^{\bullet}OH) \rightarrow M + (1/2)O_2 + H^+ + e^- \quad (30)$$

$$2M(^{\bullet}OH) \rightarrow 2M + H_2O_2 \quad (31)$$

A non-active electrode does not participate in the direct anodic reaction of organics and does not provide any catalytic active site for their adsorption from the aqueous medium. It only acts as an inert substrate and as a sink for the removal of electrons. In principle, only outer-sphere reactions and water oxidation are possible with this kind of anode. Hydroxyl radical produced from water discharge by reaction (25) is subsequently involved in the oxidation process of organics.

The above model presupposes that the electrochemical activity (related to the overvoltage for O_2 evolution) and chemical reactivity (related to the rate of organics oxidation) of physisorbed M($^{\bullet}$OH) are strongly linked to the strength of the M–$^{\bullet}$OH interaction. As a general rule, the weaker the interaction, the lower the anode reactivity for organics oxidation with faster chemical reaction with M($^{\bullet}$OH). The BDD anode is the best non-active electrode verifying this behaviour [97], then being proposed as the preferable anode for treating organics by EO. Thanks to the electrogeneration of hydroxyl radical as mediated oxidant, electrochemical oxidation is considered an EAOP.

It should be mentioned that a weaker oxidant as ozone can also be generated from water discharge at the anode (E^0 = −1.51 V vs. SHE) by the following overall reaction [41,42]:

$$3H_2O \rightarrow O_3 + 6H^+ + 6e^- \quad (32)$$

That means that in EO reactive oxygen species (ROS) such as heterogeneous $^{\bullet}$OH by reaction (25), H_2O_2 by reaction (31) and O_3 by reaction (32) are generated, although physisorbed $^{\bullet}$OH is the strongest oxidant of pollutants. This species, however, has so short lifetime that only acts while direct current is supplied to the anode.

When BDD is used, other weaker oxidizing species like peroxodisulphate, peroxodicarbonate and peroxodiphosphate can also be competitively formed with ROS from the anodic oxidation of bisulphate (or sulphate), bicarbonate and phosphate present in the electrolyte as follows [43]:

$$2HSO_4^- \rightarrow S_2O_8^{2-} + 2H^+ + 2e^- \quad (33)$$

$$2HCO_3^- \rightarrow C_2O_6^{2-} + 2H^+ + 2e^- \quad (34)$$

$$2PO_4^{3-} \rightarrow P_2O_8^{4-} + 2e^- \quad (35)$$

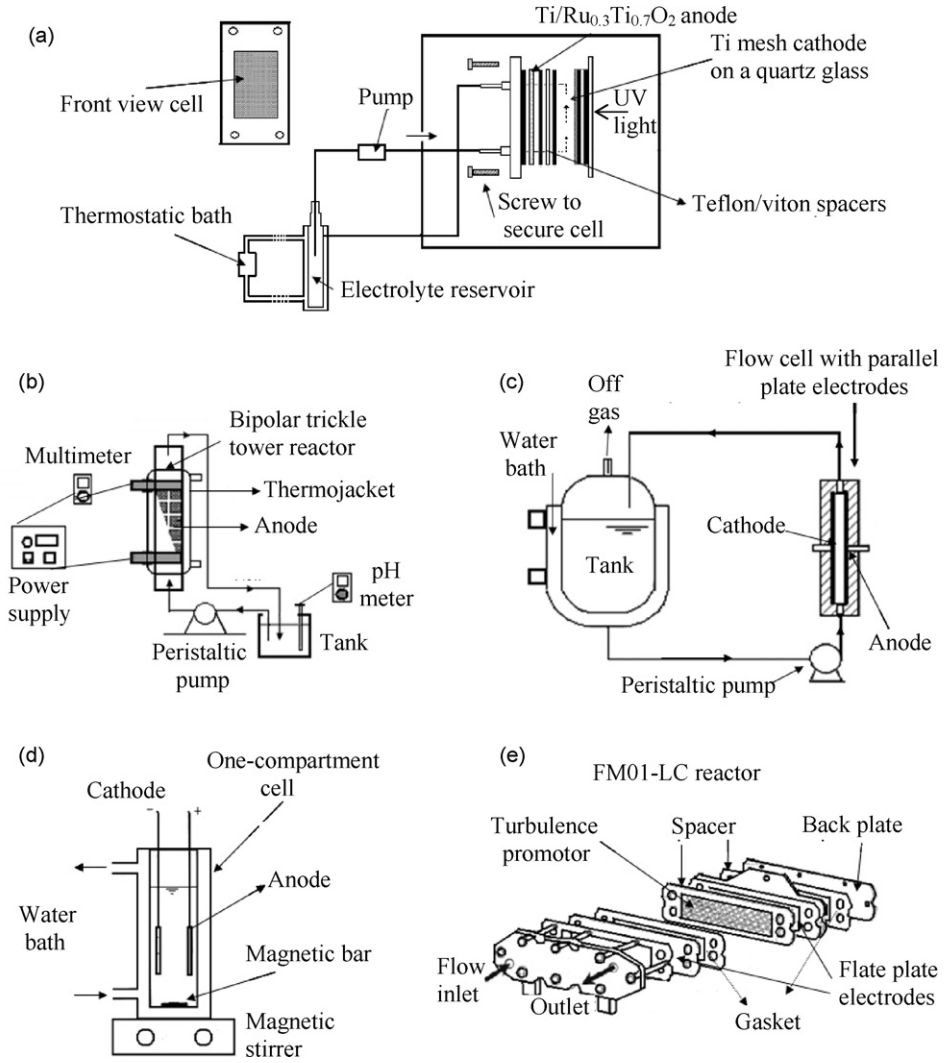

Fig. 10. Sketches of electrochemical plants and cells used in electro-oxidation for removing dyes in batch operation mode. Bench-scaled flow plants with a: (a) photo/electrochemical divided reactor (adapted from Ref. [132]), (b) bipolar trickle tower reactor (adapted from Ref. [133]) and (c) one-compartment cell with parallel plate electrodes (adapted from Ref. [125]). (d) Stirred two-electrode one-compartment tank reactor with a jacket for external thermostatization. Adapted from Ref. [121]. (e) Filter-press flow cell (FM01-LC reactor). Adapted from Ref. [131].

A very different behaviour is found when chloride solutions are treated by EO, since active chlorine species (mainly Cl_2, HClO and/or ClO^-) formed from Cl^- oxidation at the anode can effectively mineralize the dyes and their by-products in competition with ROS. In this section examples will be given to remark the comparative degradation of dyestuffs in several media including Cl^-, although the characteristics of indirect electro-oxidation treatments with active chlorine will be extensively discussed in Section 5.1.

4.2. Electrochemical systems and experimental parameters

A large variety of electrochemical systems have been tested for the treatment of dyeing wastewaters by EO [67,73,90,91,98–136]. Conventional three-electrode cells with two-compartment (see Fig. 8a) or one-compartment and divided or undivided two-electrode cells or tank reactors [67,90,91,98–106,108–124,134] have been widely utilized. Other authors have employed flow cells with parallel electrodes [107,125–132,135,136] and flow plants with a three-phase three-dimensional electrode reactor [73] or a bipolar trickle tower reactor [133]. Fig. 10 illustrates some electrochemical plants and cells designed for this technique operating in batch mode to attain the maximum solution decontamination. The cells are divided or undivided and contain monopolar and sometimes bipolar (see Fig. 10b) electrodes. The hydrodynamics of the cell plays a fundamental role in the mass transport towards the electrodes to efficiently oxidize organics pollutants. Flow cells with planar and monopolar electrodes in a parallel plate configuration such as shown in Fig. 10c and e can reduce the interelectrode gap with the concomitant increase in oxidation rate of pollutants. A good design of these reactors allows optimizing the mass transport coefficient for reaching the maximum current efficiency.

According to the Comninellis model, the most important factor determining the extent of dyes mineralization in EO is obviously the anode material. A high number of electrodes have been tested in this method including polypyrrole [67], granular activated carbon [73], ACF [90,91,98], perovskite-like structures [99], glassy carbon [101], graphite [102,103], Ti/Pt and Pt [91,106–110,117,125], and doped and undoped PbO_2 and mixed metal oxides of Ti, Ru, Ir, Sn and Sb [94,99–101,105,107,111,112,118–123,125,132]. However, synthetic BDD thin films are currently preferred as anodes [67,104,106,109,110,113–116,118,120–131,133–136] by their better oxidative performance. To remark this behaviour, the characteristics of EO and its relevant

application to dyes removal will be examined from a general classification of the anodes used.

The same experimental parameters measured in EC are also determined in EO to quantify the decolorization and degradation attained by synthetic dyes. Thus, the decolorization efficiency or percentage of color removal is obtained from Eq. (9), while the percentages of COD and TOC decays are determined from Eqs. (10) and (11), respectively. COD data are also used to calculate the current efficiency at a given electrolysis time in batch operation mode at constant current as follows:

$$\text{current efficiency}\,(\%) = \frac{(\Delta\text{COD})FV_s}{8It} \times 100 \quad (36)$$

where ΔCOD is the decay in COD (g dm^{-3}) at time t (s), V_s is the solution volume (dm^3), F is the Faraday constant (96,487 C mol^{-1}), I is the applied current (A) and the constant 8 is the oxygen equivalent mass (g equiv^{-1}). Energy consumptions referred to the volume of treated solution (kWh m^{-3}), the dye mass (kWh (kg dye)$^{-1}$) and the amount of COD (kWh (kg COD)$^{-1}$) destroyed are obtained from expressions similar to Eqs. (12), (13) and (15), respectively.

4.3. Metal oxides electrodes

Doped and undoped PbO_2 and mixed metal oxides of Ru, Ti, Sb, Sn and/or Ir, have been widely used as anodes for the electro-oxidation of synthetic dyes. Table 2 summarizes selected results obtained for the destruction of chloride-free dye solutions using these electrodes.

4.3.1. PbO_2 anode

PbO_2 is one of the classical high O_2-overvoltage materials that are expected to perform the overall electrochemical incineration of organics. This behaviour has been clearly confirmed by Panizza and Cerisola [125] when treated 225 mg dm^{-3} COD solutions of Methyl Red in 0.5 M Na_2SO_4 with different anodes using the flow cell of Fig. 10c at 500 mA (corresponding to anode potentials in the O_2 evolution region). Fig. 11a shows a strong dependence of the comparative COD removal on the anode material, decreasing in the order Si/BDD > Ti/PbO_2 > Pt > Ti/$Ti_{0.50}Ru_{0.45}Sn_{0.05}O_2$. The same trend can be seen in Fig. 11b for current efficiency. In the case of Ti/PbO_2, COD decreases to near zero in 11 h, meaning the almost complete oxidation of the azo dye and all its by-products. However, the current efficiency decays from 24 to 7% in 9 h, as

Table 2
Percentage of color and COD decays and energy consumption for the electrochemical oxidation with metal oxides, Pt, carbonaceous and polypyrrole anodes of selected chloride-free dyes solutions.

Dye[a]	C_0/mg dm^{-3}	j[b]/mA cm^{-2}	Electrolysis time/h	Color removal/%	COD decay/%	Energy consumption[c]	Ref.
PbO_2 anode							
Blue Reactive 19	25	50	2	100	95[d]	1.86 kWh m^{-3} for pure electrode and 1.66 kWh m^{-3} for Fe, F-doped electrode at 90% decolorization	[120]
Basic Brown 4	100	30	0.5	100	73	–[e]	[105]
Acid Red 2 (Methyl Red)	225[f]	31.2	11	100	97	–[e]	[125]
Ti/Sb_2O_5–SnO_2 anode							
Acid Orange 7 (Orange II)	750	20	6.25[g]	98	27	–[e]	[121]
Reactive Red 120 (Reactive Red HE-3B)	1500	20	6.25[g]	95	13	–[e]	[122]
Ti/$Ru_{0.3}Ti_{0.7}O_2$ anode							
Reactive Red 198	30	50	3	80	18[d]	95×10^6 kWh (kg dye)$^{-1}$	[132]
Direct Red 81	0.1–1[h]	25	3	100	57–61[d]	0.555 kWh (g TOC)$^{-1}$	[107]
Direct Black 36	0.1[h]	25	3	40	0[d]	–[e]	
Acid Violet 1	0.1[h]	25	3	100	32[d]	–[e]	[112]
Pt anode							
Acid Red 27 (Amaranth)	100	10–20	3	100	10[d]	–[e]	[109]
Reactive Orange 4	100	40	1	91	–[e]	44.1 kWh m^{-3}	[111]
Activated carbon fiber anode							
Acid Red 27 (Amaranth)	80	0.5	8	99	52	–[e]	[90]
Graphite anode							
Vat Blue 1 (Indigo)	200	0.43	0.5	14	–[e]	6.93 kWh m^{-3}	[102]
Polypyrrole anode							
Direct Red 80	350	2	70	100	46	5.46 kWh m^{-3}	[67]

[a] Color index (common) name.
[b] Applied current density.
[c] Different units reported.
[d] Percentage of TOC decay.
[e] Not determined.
[f] Initial COD.
[g] Specific charge passed (Ah dm^{-3}).
[h] mM concentration.

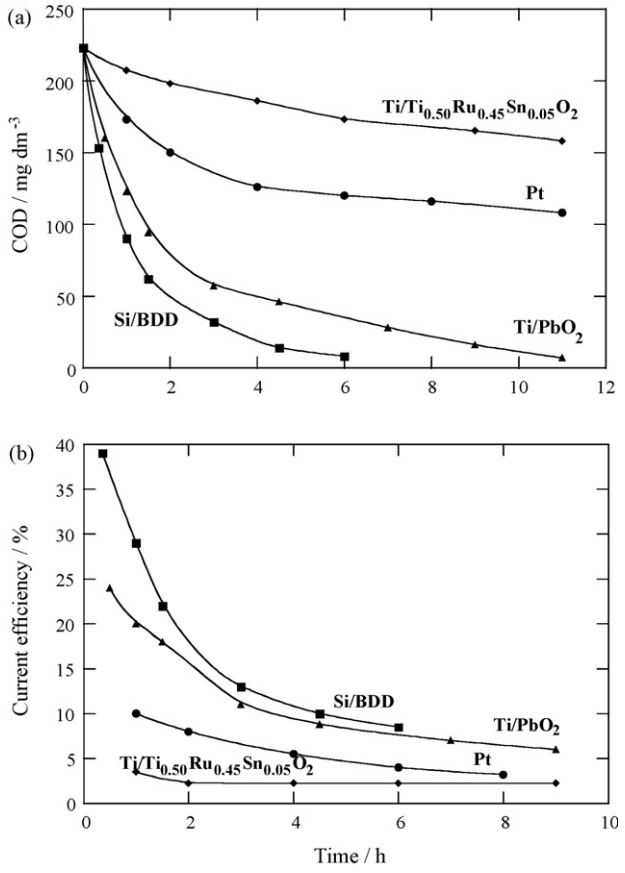

Fig. 11. Comparison of (a) COD removal and (b) current efficiency as function of electrolysis time for the electrochemical oxidation of 300 cm^3 of 225 mg dm^{-3} COD of Methyl Red in the presence of 0.5 M Na_2SO_4 at 25 °C using different anodes of 16 cm^2 area in the cell of Fig. 10c with a stainless steel cathode at 500 mA and flow rate 180 dm^3 h^{-1}. Adapted from Ref. [125].

expected if oxidation intermediates such as aliphatic acids are accumulated and slowly destroyed. These results demonstrate that Methyl Red is incinerated on Ti/PbO_2 and Si/BDD mainly by •OH electrogenerated from water discharge by reaction (25).

An inspection of Table 2 corroborates the great mineralization attained for other dyes in EO with PbO_2. For example, Awad and Abo Galwa [105] studied the electrocatalytic degradation of 50 cm^3 of solutions with 100 mg dm^{-3} of the azo dye Acid Blue 120 or Basic Brown 4 in the presence of 2 g dm^{-3} of different electrolytes (H_2SO_4, NaOH or NaCl) using an undivided conventional cell with a Pb/PbO_2 anode and a stainless steel cathode. After 30 min of electrolysis at 30 mA cm^{-2}, 100% color removal was obtained in all media. However, 42 and 50% dye removal (determined by HPLC) and 37 and 45% COD decay were achieved for Acid Blue 120 and Basic Brown 4, respectively, using H_2SO_4, and higher values of 78 and 76% for dye removal and 80 and 77% for COD decay were attained for the same dyes in NaOH solution. The poor oxidation action of •OH in the above media was enhanced with NaCl, which gave much better performance (>95% of dye and COD removals) due to the additional oxidation of organics with active chlorine species.

Other interesting results have been reported by Andrade et al. [120] who applied pure and Fe and/or F-doped Ti–Pt/β-PbO_2 electrodes to destroy synthetic wastewaters containing 25 mg dm^{-3} of the antraquinone dye Blue Reactive 19 in 0.5 M Na_2SO_4 using a one-compartment filter-press reactor with 5 cm^2 electrodes in batch operation mode. The oxidation rate of this dye was a function of solution pH, flow rate, doping with Fe and/or F, and j. At optimal conditions of 50 mA cm^{-2}, flow rate of 2.4 dm^3 h^{-1} and 25 °C, 90% decolorization efficiency was achieved at only Q = 0.3 Ah dm^{-3} (8 min) and complete color removal was found at Q = 0.4 Ah dm^{-3} (10 min) for all anodes, except for the Fe-doped electrodes that needed greater consumptions of 0.6 Ah dm^{-3} (14 min) and ca. 0.7 Ah dm^{-3} (17 min), respectively. TOC was reduced by 95% in 2 h of electrolysis in most cases. It is important to remark that very low energy consumption of 1.86 kWh m^{-3} for the pure anode and 1.66 kWh m^{-3} for the 1 mM Fe, F-doped electrode was estimated at 90% decolorization efficiency, giving a quite inexpensive cost of approximately US$ 0.20 per m^3 of effluent. Other authors have described the acceleration of Acid Red 14 degradation when EO is performed with a Ti/PbO_2–Co–Bi anode combined with a nanophase TiO_2 catalyst suspended in the electrolyzed solution containing Na_2SO_4 as background electrolyte [100].

4.3.2. Dimensionally stable anode (DSA)-type electrodes

DSAs composed of mixtures of Ti, Ir, Ru, Sn and/or Sb oxides have high surface area and excellent mechanical and chemical resistance even at high current density and in strongly acid media. However, these active anodes show a limited oxidation power to incinerate dyestuffs because of their low ability to electrogenerate •OH, as can be seen in Table 2. This behaviour can also be observed in Fig. 11a, where a Ti–Ru–Sn ternary oxide electrode yields much lower COD removal for a Methyl Red solution than non-active anodes such as Si/BDD and Ti/PbO_2 and even another active anode such as Pt under comparable conditions.

Chen et al. [121–123] utilized a Ti/Sb_2O_5–SnO_2 anode for oxidizing 25–30 cm^3 of solutions of different azo dyes with 2 g dm^{-3} Na_2SO_4. They employed the stirred undivided cell of Fig. 10d with a stainless steel cathode and electrodes of 25 mm × 24 mm × 1.6 mm in dimension. After the consumption of 6.25 Ah dm^{-3} at 20 mA cm^{-2}, 750 mg dm^{-3} of Orange II underwent 98% color removal, but only with 27% COD removal and 16% current efficiency (see Fig. 12), whereas 1500 mg dm^{-3} of Reactive Red HE-3B were decolorized in 95% with 13% COD decay and 11% current efficiency [121,122]. Low mineralization with 26–47% COD abatement, current efficiency between 19 and 48% and about 80% decolorization efficiency were also found for the similar oxidation of 1 g dm^{-3} of 15 reactive dyes at pH 4.7–6.3 and 10 mA cm^{-2} up to 2.4–4.0 Ah dm^{-3} [123]. The same authors

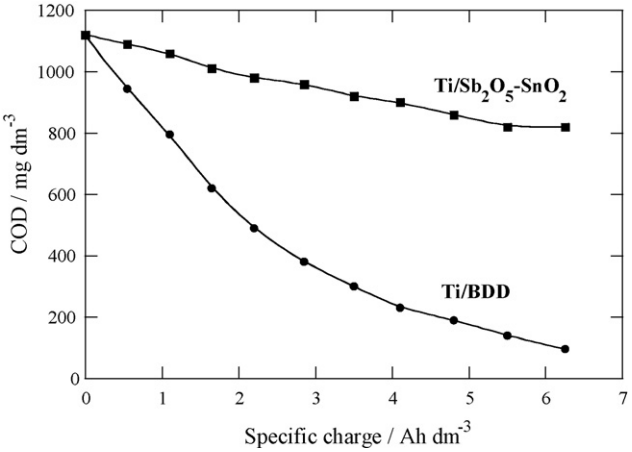

Fig. 12. COD decay for Ti/BDD and Ti/Sb_2O_5–SnO_2 anodes during the electrochemical oxidation of 30 cm^3 of a 750 mg dm^{-3} Orange II solution in 2 g dm^{-3} Na_2SO_4 using the cell of Fig. 10d with a stainless steel cathode at 20 mA cm^{-2} and 30 °C. Adapted from Ref. [121].

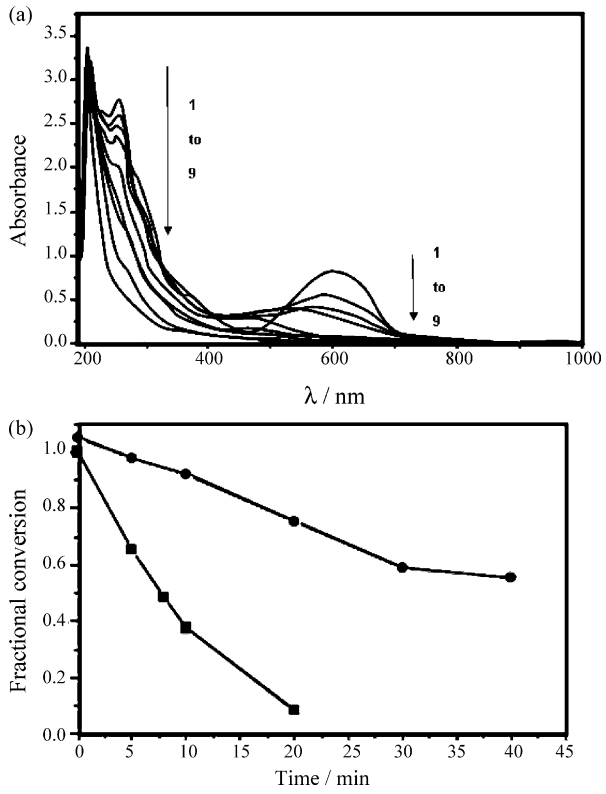

Fig. 13. (a) UV–vis absorption spectra obtained during the electrochemical oxidation of 50 cm^3 of a 680 mg dm^{-3} Reactive Blue 4 solution in 14.2 g dm^{-3} Na_2SO_4 of pH 2.2 in a three-electrode two-compartment cell with a 57.4 cm^2 Ti/SnO_2–SbO_x (3 mol%)–RuO_2 (30 mol%) anode and a 4 cm^2 Pt gauze cathode at E_{anod} = 2.4 V vs. Ag/AgCl for (1) 0 min, (2) 5 min, (3) 8 min, (4) 10 min, (5) 20 min, (6) 30 min, (7) 40 min, (8) 50 min and (9) 60 min. (b) Fractional conversion vs. time at λ: (■) 595 nm and (●) 256 nm. Adapted from Ref. [101].

demonstrate that comparable treatments with a non-active Ti/BDD anode provided much greater mineralization, as illustrated in Fig. 12 for Orange II. Hastie et al. [118] also showed the superiority of Si/BDD anodes on Ti/RuO_2 and Ti/SnO_2 to incinerate this azo dye.

Poor degradation results have also been reported for other mixed metal oxides of Sn and Sb. This has been found, for example, for Carneiro et al. [94,101], who tested the treatment of Reactive Blue 4 solutions with Na_2SO_4 using a three-electrode two-compartment cell with a 57.4 cm^2 Ti/SnO_2–SbO_x (3 mol%)–RuO_2 (30 mol%) anode and a 4 cm^2 Pt gauze cathode at constant potential. Fig. 13a illustrates the decay in UV–vis absorbance recorded for 60 min of treatment of this antraquinone dye at pH 2.2 and anodic potential (E_{anod}) of 2.4 V vs. Ag/AgCl. The fractional conversion at λ = 595 nm (characteristic of the antraquinone) and λ = 256 nm (corresponding to aromatics intermediates) determined from the above spectra is presented in Fig. 13b, showing 100% decolorization when the antraquinone chromophore is completely destroyed at ca. 20 min, and a larger persistence of aromatics intermediates. In contrast, TOC was rapidly reduced by 58% in 10 min, but no greater degradation was achieved for prolonged electrolysis. This phenomenon was attributed to the fast initial oxidation of the dye and its by-products with $^{\bullet}OH$ formed from reaction (25) on the non-active SnO_2 because this radical also reacts with Ti used as substrate promoting the surface passivation by TiO_2 formation and causing the deactivation of the anode.

The use of a Ti/$Ru_{0.3}Ti_{0.7}O_2$ anode has also received great attention in EO, despite its low oxidation power. Pelegrini et al. [119] investigated the electro-oxidation of 30 mg dm^{-3} Reactive Blue 19 solutions of pH 11.0 in a quartz three-electrode cell equipped with this anode, only obtaining 35% decolorization efficiency and 9.6% TOC removal after 2 h of electrolysis at E_{anod} = 1.8 V vs. Ag/AgCl. More recently, Catanho et al. [132] degraded 30 mg dm^{-3} Reactive Red 198 solutions in 0.02 M Na_2SO_4 of pH 5.4 using the electrochemical filter-press reactor of Fig. 10a at liquid flow rate of 18 dm^3 h^{-1} and after 3 h of electrolysis at 50 mA cm^{-2}; they estimated an excessive energy cost of 95 × 10^6 kWh (kg dye)$^{-1}$. On the other hand, Socha et al. [107] treated 60 cm^3 of 0.1–1 mM Direct Red 81 solutions in 0.1 M $NaClO_4$ of pH 7.0 in a conventional divided cell with a 20 cm^2 Ti/$Ru_{0.3}Ti_{0.7}O_2$ anode and a 20 cm^2 Pt cathode at 25 mA cm^{-2} and 60 °C. At 3 h complete color removal, 57–61% TOC decay and a more reasonable energy cost of 0.555 kWh (g TOC)$^{-1}$ were found. Poorer results were obtained by these authors for Direct Black 36 [107] and Acid Violet 1 [112] under similar treatment (see Table 2).

4.4. Pt anode

The destruction of azo dyes (Amaranth, Direct Red 81, Direct Black 36, Acid Orange 7, Methyl Orange and Methyl Red) [90,91,107,109,111,117,125], triphenylmethanes (Bromophenol Blue, Phenol Red, Fuchsin, Methyl Green and Crystal Violet) [117], Indigo [117] and polymeric Poly R-478 [117] has been studied by EO with pure Pt. Ti-supported Pt has also been tested for azo dyes such as Reactive Orange 91, Reactive Red 184, Reactive Blue 182 and Reactive Black 5 [106]. For both anodes the influence of pH [106–108,111], dye content [117,125], temperature [106,107,111], supporting electrolyte [106,107,111], cathode material [109], current density [90,107–109,117,111] and anode potential [91,106] was investigated for optimizing degradation conditions. Many authors also estimated the color removal [91,107,109,111,117,125], current efficiency [125] and decay in COD [91,106,108,125] and/or TOC [91,106–108], which mainly depend on the above parameters. Data collected in Table 2 for these trials show that Pt leads to high decolorization efficiency, but with very low decontamination, because it behaves as an active

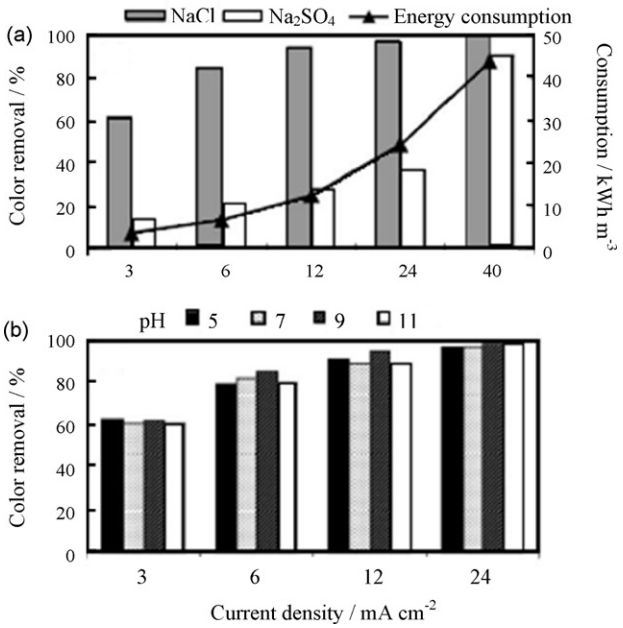

Fig. 14. Color removal and energy consumption vs. current density for 100 mg dm^{-3} of Reactive Orange 4 treated for 1 h in a flow cell with a Ti/Pt plate anode and a Ti plate cathode, both of 486 cm^2 area, in batch operation mode at flow rate of 25 dm^3 h^{-1}. (a) Effect of 20 g dm^{-3} NaCl or 25 g dm^{-3} Na_2SO_4 as supporting electrolyte at pH 9.0. (b) Effect of pH for the NaCl effluent. Adapted from Ref. [111].

anode and small quantity of heterogeneous oxidant •OH is accumulated in its surface during water discharge.

Relevant results have been published by López-Grimau and Gutiérrez [111], who optimized the EO process of 1 dm^3 of 100 mg dm^{-3} Reactive Orange 4 using a flow cell with a 486 cm^2 Ti/Pt anode in batch operation mode at flow rate of 25 dm^3 h^{-1}. Fig. 14 illustrates the effect of supporting electrolyte (20 g dm^{-3} NaCl or 25 g dm^{-3} Na_2SO_4), pH and *j* on color removal and energy consumption after 1 h of electrolysis. For the highest *j* of 40 mA cm^{-2} and pH 9.0 (see Fig. 14a), total decolorization is obtained with NaCl, whereas a high 91% color removal is reached with Na_2SO_4. At lower current densities, the decolorization efficiency is much more favorable for the former. For example, 95% color removal is attained at 12 mA cm^{-2} in presence of NaCl, whereas the Na_2SO_4 effluent only yields a similar result at 40 mA cm^{-2}. That means that oxidation via •OH is effective in Na_2SO_4 at high *j* and hence, in NaCl the oxidation proceeds mainly with active chlorine species. This fact implies an important saving of the energy consumption when decolorizing the NaCl effluent (12.4 kW m^{-3}) in comparison to the Na_2SO_4 one (44.1 kWh m^{-3}). Fig. 14b evidences that decolorization efficiency for NaCl is practically pH-independent and rises with increasing *j*, as expected if greater concentrations of strong oxidants (mainly ClO^- and •OH) are produced.

The positive influence of temperature on EO with Pt has been studied by Socha et al. [107] for Direct Red 81 and Direct Black 36 with 60 cm^3 of solutions containing concentrations from 0.1 to 1 mM of each azo dye in 0.1 M $NaClO_4$ at pH 7.0 and 8.5, treated in a divided Pt/Pt cell with 20 cm^2 electrodes at 25 mA cm^{-2}. The increase in temperature from 25 to 60 °C caused a rise in dye degradation and so, the decolorization of Direct Red 81 proceeded efficiently up to 97% within 2 h, whereas Direct Black 36 was only decolorized in 46% at the same time. Analogous conclusions with the same electrolytic system have been described by these authors for 1-aminonaphthalene-3,6-disulphonic acid, present in the wastewater released during the synthesis of H-acid used in the production of various dyes [108]. In this case, 78% color removal, along with COD and TOC reductions as small as 36 and 18%, respectively, were achieved for a 1 mM pollutant solution of pH 7.0 at optimal temperature of 70 °C after 4 h of electrolysis at 20 mA cm^{-2}.

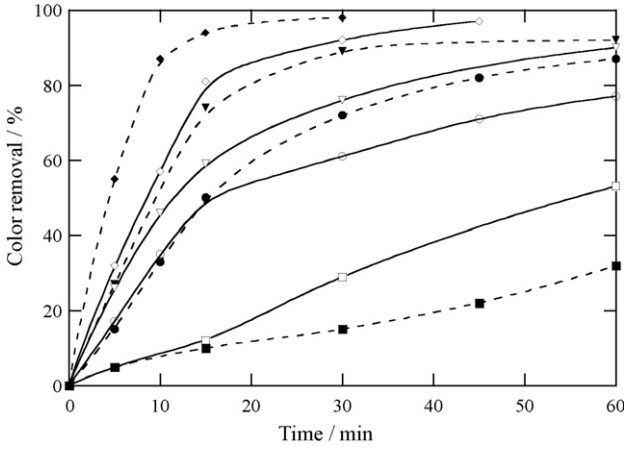

Fig. 15. Color removal for (◆) 12.5 mg dm^{-3} of Bromophenol Blue, (◇) 1.2 mg dm^{-3} of Methyl Orange, (▼) 11.8 mg dm^{-3} of Methyl Green, (▽) 100 mg dm^{-3} of Indigo, (●) 8 mg dm^{-3} of Crystal Violet, (○) 44 mg dm^{-3} of Fuchsin, (□) 90 mg dm^{-3} of Poly R-478 and (■) 18 mg dm^{-3} of Phenol Red in 25 mM succinic acid solutions of pH 4.5 treated by electrochemical oxidation in a stirred undivided Pt/Pt cell at a constant voltage of 5 V and room temperature. Adapted from Ref. [117].

On the other hand, less is known about the influence of the chemical structure of the dye in the EO process with Pt. Fig. 15 shows the comparative evolution of the color removal of eight dye solutions of pH 4.5 treated in a stirred undivided Pt/Pt cell at a cell voltage of 5 V [117]. As can be seen, the triphenylmethane dye Bromophenol Blue is almost completely decolorized in 30 min, while the azo dye Methyl Orange achieves 95% color removal in 45 min. Other triphenylmethanes such as Methyl Green, Crystal Violet and Fuchsin are more slowly removed, attaining 92, 87 and 77% decolorization efficiency in 60 min, respectively. At this time, Indigo is also largely decolorized (90%), but much smaller color removal is found for Poly R-478 (53%) and the triphenylmethane dye Phenol Red (32%). These results confirm that not only the chemical structure influences the process; but also the substituents of the dye strongly affect the decolorization efficiency.

A very limited number of papers have reported some information on the intermediates formed during the EO of dyes on Pt. Hattori et al. [109] detected the accumulation of aliphatic acids such as acetic, maleic and oxalic as final by-products of the treatment of Amaranth dyestuff solutions. Dávila-Jiménez et al. [110] proposed possible fragmentation products of several textile dyes after short electrolysis times by means of HPLC analysis.

Several authors have also compared the efficiency for removing dyes with Pt and other anodes [91,106,107,109,110,125]. It has been found that Pt can be more or less effective depending on the specific dye tested. For example, Fig. 11 shows clearly that the oxidation ability of Si/BDD and Ti/PbO_2 is much greater than Pt for Methyl Red solutions in 0.5 M Na_2SO_4, although the latter yields higher COD removal than a Ti–Ru–Sn ternary oxide anode. On the contrary, Socha et al. [107] reported a slightly better performance using a Ti/$Ti_{0.3}Ru_{0.7}O_2$ electrode than Pt for the EO of Direct Red 81 in 0.1 M $NaClO_4$.

4.5. Carbonaceous and other anode materials

Some anodes composed of carbonaceous materials such as granular activated carbon [73], ACF [90,91,98], glassy carbon [101] and graphite [102,103] have been tested for the EO of dyestuffs. Polypyrrole [67] and a perovskite-like $BaPb_{0.9}Sb_{0.1}O_3$ [99] have also been used as alternative anodes. Selected results listed at the end of Table 2 for these electrodes evidence their low degradation ability. For example, the electrochemical incineration of 80 mg dm^{-3} of Amaranth with 0.1 M Na_2SO_4 in a phosphate buffer of pH 6.6 using the three-electrode two-compartment cell of Fig. 8a led to 99% decolorization efficiency with only 52% COD removal after 8 h of electrolysis at constant *j* of 0.5 mA cm^{-2} [90]. The oxidative performance in this galvanostatic treatment was much greater than under potentiostatic conditions, where 95% color removal and about 35 and 30% of COD and TOC decays, respectively, were obtained in 500 min of electrolysis at E_{anod} = 1.000 V vs. SCE, as can be seen in Fig. 8b [91].

An interesting study of Cameselle et al. [102] was focused to select the best electrolyte for the electrochemical decolorization of Indigo solutions of pH 7.0. They used an undivided tank reactor with two 7.5 cm^2 graphite electrodes for treating 100 cm^3 of 200 mg dm^{-3} of this dye with 0.035 M salt at a cell voltage of 5 V. As can be seen in Fig. 16, the absence of electrolyte and the use of sulphate and nitrate media yields very low color removal in 30 min of electrolysis, being both electrolytes not useful in practice. In contrast, increasing decolorization efficiency of 81, 90, 93 and 98% can be observed for KI, $Na_2S_2O_5$, NaCl and KBr. The lowest energy consumption of 84 kWh m^{-3} was found for NaCl, followed by 92 kWh m^{-3} for KBr, whereas significantly higher values of 123 and 136 kWh m^{-3} were determined for KI and $Na_2S_2O_5$, respectively. Without electrolyte, 14% color removal and 6.93 kWh m^{-3} energy

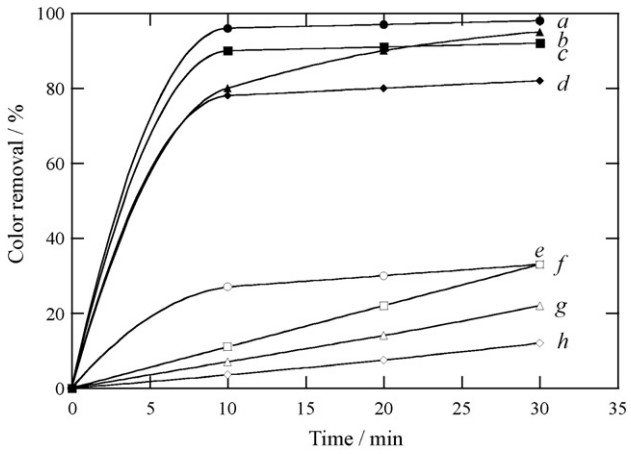

Fig. 16. Electrochemical decolorization of 100 cm^3 of a 200 mg dm^{-3} Indigo solution with 0.035 M of (a) KBr, (b) NaCl, (c) $Na_2S_2O_5$, (d) KI, (e) $MnSO_4$, (f) Na_2SO_4, (g) $NaNO_3$, and (h) without electrolyte at pH 7.0 in a stirred undivided graphite/graphite tank reactor with electrodes of 7.5 cm^2 area at a cell voltage of 5 V and room temperature. Adapted from Ref. [102].

cost under circulation of a $j = 0.43$ mA cm^{-2} were obtained. The better performance in NaCl was related to the mediated oxidation with electrogenerated active chlorine species such as ClO^-.

4.6. Boron-doped diamond electrodes

BDD thin films are relatively new electrode materials that have received great attention, because they possess several technologically important characteristics including an inert surface with low adsorption properties, remarkable corrosion stability even in strongly acidic media and extremely high O_2 evolution overvoltage [41,42]. Thanks to these properties, they are excellent materials for EO. BDD anodes have been defined as non-active electrodes, since it is expected that they do not provide any catalytically active site for the adsorption of reactants and/or products in aqueous media. Hydroxyl radical (BDD($^{\bullet}$OH)) formed from water discharge on their surface from reaction (25) is then considered the responsible species for the electrochemical combustion of organic pollutants, although slower reactions with other ROS (H_2O_2 and O_3) and weaker electrogenerated oxidants (peroxodisulphate, peroxodicarbonate or peroxodiphosphate) are also feasible.

Many papers have demonstrated that the use of a BDD thin film in EO provides total mineralization with high current efficiency of different organics in real wastewaters [41–43]. This synthetic material deposited on several supports has been recently applied to dyestuff treatment. It is important to remark that most studies have been performed with Si-supported devices [109,114,115,118,125–130,135,136], in spite of the difficulties related to their industrial transposition owing to the fragility and the relatively low conductivity of the Si substrate. Some works have tested BDD deposits on Nb support [106,113,120,133], although the large-scale utilization of this metallic substrate is probably unfeasible by its excessive high cost. Samples of small Ti/BDD anodes have also been tested for the destruction of several dyes [104,121–124] since Ti possesses all required features to be a good and inexpensive substrate material. However, a synthetic route to deposit stable diamond films on Ti at industrial scale is not yet available, because cracks appear and cause the detachment of the diamond film during long-term electrolysis.

Table 3 collects the excellent decolorization and degradation results obtained for the EO with diamond anodes of selected chloride-free dyes solutions considering the kind of support utilized. The characteristics of these electro-oxidations are described and discussed below according to this classification, being the last subsection devoted to examine the papers related to BDD electrodes with unspecified support [67,110,116,131,134].

Table 3
Percentage of color and COD removals and energy consumption determined for the electrochemical oxidation with diamond anodes of selected chloride-free dyes solutions.

Dye[a]	C_0/mg dm^{-3}	j[b]/mA cm^{-2}	Electrolysis time/h	Color removal/%	COD decay/%	Energy consumption[c]	Ref.
Ti/BDD anode							
Acid Orange 7 (Orange II)	750	20	6.25[d]	90	92	–[e]	[121]
15 reactive dyes	1000	10	2–4[d]	>95	89–95	8.9–17.9 kWh m^{-3}	[123]
Nb/BDD anode							
Blue Reactive 19	25	50	0.3[d]	95	82[f]	–[e]	[120]
Basic Red 29	40	1	0.03	98	–[e]	–[e]	[133]
Textile wastewater	566[g]	1	8.5	97	92	1.4 kWh (g COD)$^{-1}$	
Si/BDD anode							
Acid Red 27 (Amaranth)	100	80	6.5	100	100, 94[f]	–[e]	[109]
Acid Orange 7 (Orange II)	0.1[h]	20	2.5	100	100	–[e]	[118]
Acid Red 2 (Methyl Red)	200	31.2	6	100	98	–[e]	[125]
Vat Blue 1 (Indigo)	0.29[h]	0.36–80	9–5	100	–[e]	0.47–35 kWh m^{-3}	[126]
Mordant Black 11 (Eriochrome Black T)	100[g]	30	4	100	100, 100[f]	800 kWh m^{-3}	[127]
Acid Orange 52 (Methyl Orange)				100	100, 100[f]		
Direct Red 28 (Congo Red)				100	100, 100[f]		
Acid Blue 22	0.3[h]	20	12	100	97	70 kWh m^{-3}	[136]
BDD with unspecified support							
Direct Red 80	350	1.5	24	100	87	6.65 kWh m^{-3}	[67]
5 textile dyes	500	2.5[i]	2	50–80	60–80	–[e]	[110]
Acid Orange 7	360	10	8	100	90	–[e]	[161]

[a] Color index (common) name.
[b] Applied current density.
[c] Different units reported.
[d] Specific charge passed (Ah dm^{-3}).
[e] Not determined.
[f] Percentage of TOC decay.
[g] Initial COD.
[h] mM concentration.
[i] Anode potential (V vs. SCE).

4.6.1. Ti/BDD electrodes

The effective mineralization of dyes with small Ti/BDD anodes has been demonstrated by the Chen's group [121–124] when degraded 25–30 cm^3 of solutions of Orange II, Reactive Red HE-3B and other 15 reactive dyes using the stirred undivided cell of Fig. 10d with a Ti/BDD anode of 25 mm × 24 mm × 1.6 mm in dimension and a stainless steel cathode of the same area. Fig. 12 shows that COD of a 750 mg dm^{-3} Orange II solution containing 2 g dm^{-3} Na_2SO_4 is reduced by 92% in this cell at 20 mA cm^{-2} and 30 °C after consumption of 6.25 Ah dm^{-3}, being the process much more efficient than with a Ti/Sb_2O_5–SnO_2 anode because of the much higher oxidation ability of BDD(•OH). In this case, 90% color removal and 55% current efficiency was found [121]. Similar treatment of 1500 mg dm^{-3} of Reactive Red HE-3B on Ti/BDD gave 95% COD decay with 47% current efficiency [122]. An analogous study on the degradation of 1 g dm^{-3} of 15 reactive dyes at pH 4.7–6.3 and 10 mA cm^{-2} up to 2.4–4.0 Ah dm^{-3} [121,123] demonstrated that the Ti/BDD anode leads to almost total decolorization (>95%) with COD reduction as high as 88–95%, excellent current efficiency between 51 and 90% and low energy cost from 8.9 to 17.9 kWh m^{-3}.

4.6.2. Nb/BDD electrodes

Azo dyes such as Reactive Orange 91, Reactive Red 184, Reactive Blue 182 and Reactive Black 5 have been effectively mineralized by Sakalis et al. [106] using a batch tank reactor equipped with two Nb/BDD anodes of 14.9 cm × 6.9 cm × 1.0 cm in dimension, alternated between three carbon fleece plates of similar area as cathodes under air bubbling operating in monopolar connection. More than 93% of color removal was found when 500 cm^3 of solutions with 0.5 mM reactive dyes in 10^{-2} M NaCl or Na_2SO_4 of pH 2.0 were electrolyzed at a cell voltage of 12 V for 50 min. Since the treatment using only tap water resulted in 69% decolorization efficiency, the enhancement of dyes destruction by adding NaCl or Na_2SO_4 was ascribed to their parallel reaction with ClO^- and $S_2O_8^{2-}$ formed from Cl^- and HSO_4^- oxidation at the anode, respectively. These authors used the same procedure to show that the COD (150 mg dm^{-3}) and TOC (164 mg dm^{-3}) of a real wastewater of pH 9.0 underwent a significant reduction of 93 and 52%, respectively, by applying 18 V for 30 min. Comparable treatment of this wastewater with Ti/Pt anodes yielded, as expected, worse performance. On the other hand, following their study with Fe and/or F-doped Ti–Pt/β-PbO_2 anodes described in Section 4.3.1, Andrade et al. [120] also showed a slight superiority of a Nb/BDD anode to destroy Reactive Blue 19, since 95% decolorization efficiency and 82% TOC decay were obtained for a 25 mg dm^{-3} dye solution with 0.5 M Na_2SO_4 treated at 50 mA cm^{-2}, flow rate of 2.4 dm^3 h^{-1} and 25 °C for 8 min after the consumption of only Q = 0.3 Ah dm^{-3}.

The flow plant of Fig. 10b with a bipolar trickle tower reactor containing Rasching rings of Nb/BDD as anode of 352 cm^2 total area was employed by Savaş Koparal et al. [133] to decolorize Basic Red 129 solutions. The rise of j from 0.25 to 1 mA cm^{-2} and of pH up to 5.8 accelerated the color removal of 125 cm^3 of 20–60 mg dm^{-3} solutions of this dye in 0.03 M Na_2SO_4, whereas this parameter did not vary for flow rates between 1.49 and 2.87 dm^3 h^{-1}. At 1 mA cm^{-2} and pH 5.8 the process was so efficient that 98% decolorization efficiency was achieved in only 2 min. Similar treatment of a textile wastewater with 566 mg dm^{-3} COD and pH 12.0 was also very effective leading to 97% color removal and 91% COD decay in 8 h with an energy cost of 1.4 kWh (g COD)$^{-1}$. The efficient EO treatment for other wastewater with 8 g O_2 dm^{-3} COD collected from a pigment factory has also been reported using a stirred tank reactor containing two Ni/BDD sheet anodes of 100 cm^2 total area and three Ti sheet cathodes in monopolar connection [113]. In this cell, 500 cm^3 of sample were electrolyzed at 36 mA cm^{-2} to give 100% color removal and 98% COD abatement with 90% current efficiency after passing 50 Ah dm^{-3}.

4.6.3. Si/BDD electrodes

EO of dyes has been more widely investigated with a Si/BDD anode, which shows a much higher oxidizing power than metal oxides and metal anodes [118,125,135]. This can be seen in Fig. 11a, where the COD of 225 mg dm^{-3} of Methyl Red in 0.5 M Na_2SO_4 treated in the flow plant of Fig. 10c at 500 mA decays much more rapidly with this anode than with Ti/PbO_2, Pt and Ti/$Ti_{0.50}Ru_{0.45}Sn_{0.05}O_2$ [125], because Si/BDD possesses higher O_2-overvoltage giving rise to greater production of •OH as the main ROS. The use of Si/BDD led to total decolorization in 3 h and almost complete mineralization in 6 h. The progressive decay in current efficiency from 40 to 8.9% during this time (see Fig. 11b) can be ascribed to the gradual formation of short carboxylic acids, more difficultly oxidizable with BDD(•OH) than aromatic pollutants. This fact was demonstrated by Hattori et al. [109] for the treatment of 50 cm^3 of a 100 mg dm^{-3} Amaranth solution in the presence of 50 g dm^{-3} Na_2SO_4 in a two compartment cell containing two Si/BDD anodes of 1 cm^2 area. These authors found 100% color removal, 100% COD decay and 94% TOC abatement by applying 20 mA cm^{-2} for 6.5 h (Q = 27 Ah dm^{-3}), detecting maleic, acetic and oxalic acids as final by-products, the latter being the most persistent.

Recently, Panizza and Cerisola [136] considered the influence of several experimental variables on the EO efficiency by exploring the mineralization of 300 cm^3 of wastewaters containing Acid Blue 22 and 0.5 M Na_2SO_4 in a flow cell equipped with a Si/BDD anode and a stainless steel cathode of 25 cm^2 geometric areas. A significant rise in current efficiency was obtained with increasing dye concentration from 0.1 to 0.3 mM and flow rate from 100 to 300 dm^3 h^{-1} because the process was controlled by the mass transport of pollutants towards the anode. The same trend for current efficiency was found when j decreased from 80 to 20 mA cm^{-2} due to the lower relative conversion of BDD(•OH) into O_2 and when temperature dropped from 60 to 25 °C owing to the slower chemical decomposition of $S_2O_8^{2-}$ to bisulphate and O_2 as follows:

$$S_2O_8^{2-} + H_2O \rightarrow 2HSO_4^- + (1/2)O_2 \quad (37)$$

At 20 mA cm^{-2}, 25 °C and flow rate of 300 dm^3 h^{-1}, 100% of color and 97% of COD were removed for the 0.3 mM Acid Blue 22 solution in 12 h with 70 kWh m^{-3} energy cost.

Ammar et al. [115] also investigated the effect of current, dye concentration and pH on the EO of 100 cm^3 of Indigo Carmine solutions with 0.05 M Na_2SO_4 at 35 °C in a stirred undivided cell with a 3 cm^2 Si/BDD anode and a 3 cm^2 stainless steel cathode. A faster TOC decay for 220 mg dm^{-3} of the dye at pH 3.0 can be observed in Fig. 17a with increasing current from 100 and 300 mA. This causes the decrease in time needed for total mineralization from 600 to 300 min due to the higher production of BDD(•OH) that accelerates the oxidation of organics. However, the increase in j from 100 to 450 mA yields a rise in specific charge for total decontamination from 10 to 22.5 Ah dm^{-3}, attributed to the existence of a lower relative proportion of BDD(•OH) by the quicker generation of O_2 and other weaker oxidants (O_3, H_2O_2 and $S_2O_8^{2-}$). Fig. 17b shows a rise in the time required for total mineralization from 240 min (Q = 12 Ah dm^{-3}) to 660 min (Q = 33 Ah dm^{-3}) at 300 mA when dye content varies between 110 and 880 mg dm^{-3}, as expected by the presence of more pollutants to be mineralized with the same quantity of electrogenerated oxidizing species. In

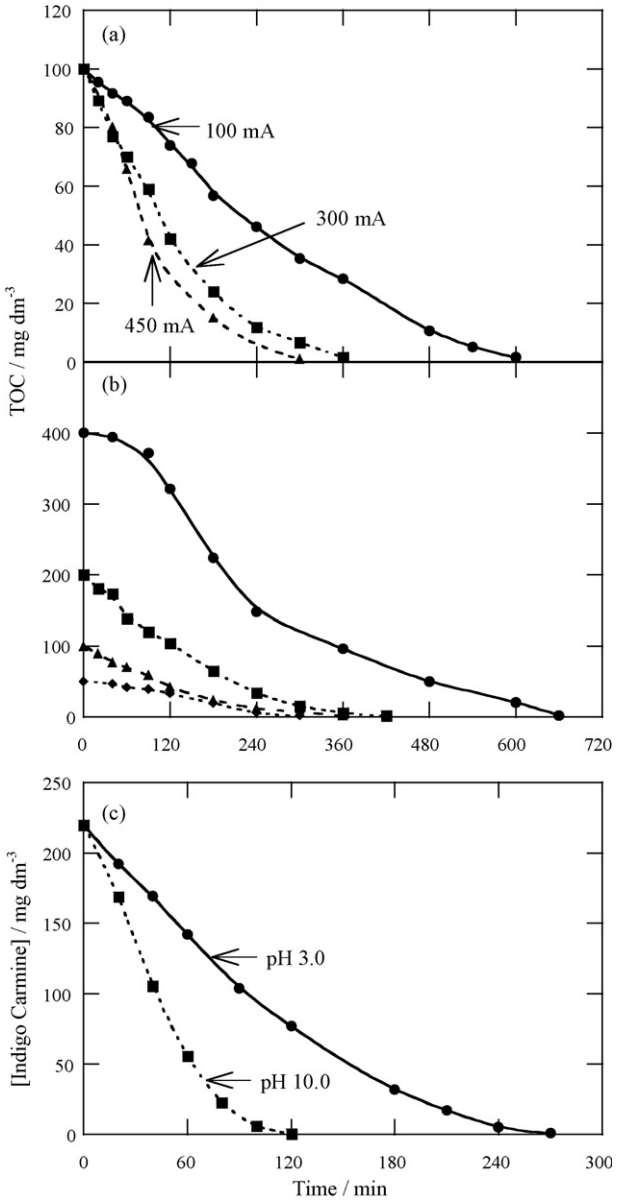

Fig. 17. (a) Influence of current on TOC removal vs. electrolysis time for the electrochemical oxidation of 100 cm^3 of 220 mg dm^{-3} Indigo Carmine solutions in 0.05 M Na_2SO_4 at pH 3.0 and 35 °C using a stirred undivided cell with a 3 cm^2 Si/BDD anode and a 3 cm^2 stainless steel cathode. (b) Effect of initial dye content on TOC abatement at pH 3.0 and 300 mA. Concentration: (●) 880 mg dm^{-3}; (■) 440 mg dm^{-3}; (▲) 220 mg dm^{-3}; (◆) 110 mg dm^{-3}. (c) Indigo Carmine concentration decay at pH 3.0 and 10.0 at 100 mA. Adapted from Ref. [115].

contrast, the 220 mg dm^{-3} Indigo Carmine solution at 100 mA becomes colorless more quickly at pH 10.0 (120 min) than at pH 3.0 (270 min), as can be seen in Fig. 17c, because the electroactive species in alkaline medium (the unprotonated form) is more easily oxidized than that of acid medium (the diprotonated form). A similar effect of current density has also been reported by Faouzi et al. [114] for the degradation of 200 cm^3 of a 5 mM Alizarin Red S solution in 1 M H_2SO_4 at 30, 60 and 90 mA cm^{-2} using an undivided cell with a 10 cm^2 Si/BDD disk anode and a 10 cm^2 Zr plate cathode. Complete decolorization and mineralization was achieved for all j tested after consumption of 28 Ah dm^{-3}.

Cañizares et al. [127] and Faouzi et al. [129] explored the influence of j and initial dye concentration on the mineralization of azo dyes such as Eriochrome Black T, Methyl Orange and Congo Red. They employed an undivided flow cell with a Si/BDD anode and a stainless steel cathode, both of 78 cm^2 geometric area, to degrade high (1800 mg dm^{-3}) and low (100 mg dm^{-3}) COD contents of each dye in 500 cm^3 of solutions containing 5 g dm^{-3} Na_2SO_4 at its original pH, 25 °C and flow rate of 75 dm^3 h^{-1} operating in batch mode at 30 mA cm^{-2}. The oxidation process started with the breakage of the azo group up to Q = 10 Ah dm^{-3}, taking place a large accumulation of carboxylic acids at the final stages of the treatment. The current efficiency was similar for all dyes and mainly depended on their concentration, being bigger for highly loaded than diluted wastes, attributed to the change of the mediated oxidation by $^{\bullet}OH$ and $S_2O_8^{2-}$ in the former media to $S_2O_8^{2-}$ alone in the latter. After 4 h of electrolysis at 30 mA cm^{-2}, all solutions were completely decolorized and mineralized with a high energy cost of about 800 kWh m^{-3}. A similar behaviour has been reported by the same group [128] for the antraquinone dye Alizarin Red treated under comparable conditions. Cañizares et al. [130] also employed the same flow plant for treating the thiazine dye Methylene Blue and the xanthene dye Rhodamine B, typical components of effluents of ink-manufacturing processes, in 0.1 M NaCl, Na_2SO_4 or Na_3PO_4 at neutral pH. As can be seen in Fig. 18a, chloride solutions with 100 mg dm^{-3} COD of each dye are effectively decontaminated in a similar way at 30 mA cm^{-2}, reaching >98% COD removal at 8.25 Ah dm^{-3}. However, Fig. 18b illustrates that at this specific charge, TOC is only reduced by 69% for Methylene Blue and 37% for Rhodamine B, suggesting the generation of by-products with very low oxidizability. Since much slower COD decay was found for the sulphate and

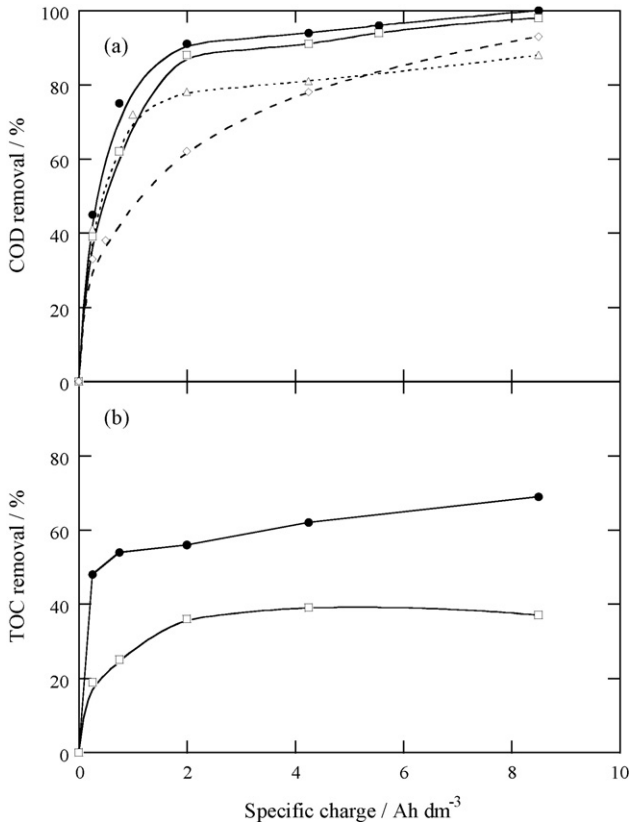

Fig. 18. Percentage of (a) COD and (b) TOC removal as a function of the specific charge passed in the treatment of 0.5 dm^3 of solutions containing (●) Methylene Blue (initial TOC = 33 mg dm^{-3}) and (□, △, ◇) Rhodamine B (initial TOC = 36 mg dm^{-3}) using an undivided flow cell with a Si/BDD anode and a stainless steel cathode, both of 78 cm^2 geometric area, in batch operation mode at 30 mA cm^{-2}, 25 °C and flow rate of 150 dm^3 h^{-1}. Solutions contained 100 mg dm^{-3} of initial COD and (●, □) 0.1 M NaCl, (△) 0.1 M Na_2SO_4, (◇) 0.1 M Na_3PO_4 at neutral pH. Adapted from Ref. [130].

phosphate solutions of Rhodamine B (see Fig. 18a), it was concluded that this dye and its aromatic intermediates react more easily with active chlorine species than with $S_2O_8^{2-}$ and $P_2O_8^{4-}$ formed from reactions (33) and (35), respectively.

Contradictory results on the oxidative role of active chlorine species and $S_2O_8^{2-}$ over dyestuffs have been reported by other authors. When Bechtold et al. [126] investigated the degradation of 2 dm^3 of 0.29 mM Indigo solutions in a divided flow cell with a 12.5 cm^2 Si/BDD anode at flow rate of 480 $dm^3\ h^{-1}$, similar decolorization rate was found using 0.070 M Na_2SO_4 or 2.47 mM NaCl as electrolyte at 3.2 mA cm^{-2}, as expected if oxidation takes place via $^{\bullet}OH$ with minor participation of other oxidants. The sulphate solution achieved 100% color removal for current densities between 0.36 and 80 mA cm^{-2} at decreasing electrolysis times from 9 to 5 h and with increasing energy costs from 0.47 to 35 kWh m^{-3}.

4.6.4. Diamond electrodes with unspecified support

The good performance obtained for remediation of dyes wastewaters with unspecified support diamond electrodes can be deduced from the examples given at the end of Table 3. It is noticeable the preliminary work with this anode published by Dávila-Jiménez et al. [110], who compared the EO process of 50 cm^3 of 500 mg dm^{-3} of five textile dyes (Acid Orange 7, Basic Violet 16, Basic Green 4, Vat Blue 41 and Natural Yellow 28) in a phosphate buffer of pH 7.0 using an unstirred three-electrode one-compartment cell with a BDD, Pt or TiO_2 anode by applying E_{anod} = 2.5 V vs. SCE. After 2 h of treatment, 50–80% color removal and 60–80% COD abatement, depending on the dye, were found for BDD, values much greater than those obtained for the other anodes. On the other hand, Fernandes et al. [116] reported 100% decolorization efficiency and 90% TOC decay for 250 cm^3 of 150–360 mg dm^{-3} Acid Orange 7 solutions in 0.035 M Na_2SO_4 of pH 5.0 in a conventional BDD/Cu cell at 10 mA cm^{-2} for 8 h. These authors also observed the acceleration of decolorization with 0.1 M KCl as background electrolyte owing to reaction with active chlorine species. This behaviour was further confirmed by the same group for real effluents coming from the biotic treatment of Acid Orange 7 under similar experimental conditions [134]. On the contrary, Butrón et al. [131] established the oxidation of Indigo via $^{\bullet}OH$ instead of active chlorine when studying the electrochemical incineration of 1 mM of this dye in 0.05 M NaCl aqueous solution using the filter-press FM01-LC reactor of Fig. 10e with a BDD anode and a Ti/Pt cathode, both of 64 cm^2 geometric area. Long-term electrolysis for 1 dm^3 of the Indigo solution at 5.3 mA cm^{-2} under batch operation mode at Reynolds number of 18,300 for 8 h removed 100% of color and 98% of COD, with an estimated energy consumption as low as 9 kWh m^{-3}.

4.7. Comparative oxidation power of anodes

An inspection of data of Tables 2 and 3 corroborates that most anodes tested in EO for treating chloride-free dye wastewaters provide large decolorization efficiency because they can easily destroy the different chromophore groups of dyestuffs. In contrast, shorter aromatics and aliphatic acids formed during the process can only be mineralized by non-active PbO_2 and conducting diamond electrodes, whereas they are inefficiently removed from solutions by DSA-type electrodes, Pt and carbonaceous materials. Among both non-active anodes, diamond electrodes seem preferable to be utilized in practice since it possesses greater ability to completely mineralize dyes solutions with acceptable energy consumption at least at lab scale. However, the viability of EO with these electrodes for industrial application is not well established yet and more research efforts are needed to clarify several fundamental aspects involving the service lifetime of large-scale BDD electrodes, a total economic study of the process for real wastewaters, the optimization of electrolytic reactors, etc. The highest oxidation power of diamond anodes is due to the production of greater amount of the strongest heterogeneous oxidant $^{\bullet}OH$ and other ROS from water discharge, which can rapidly react with organics up to total mineralization. Additional generation of weaker peroxoderivative oxidants from bisulphate, bicarbonate and phosphate electrolytes at these anodes can also play an important role in the combustion process in chloride-free solutions. However, when chloride is present in treated wastewaters, active chlorine species are easily produced at all anodes, accelerating the destruction of dyes and strongly enhancing the oxidation ability of the electrolytic system in most cases. Some comparative studies with different electrolytes reported in this section have shown the fastest destruction of several dyestuffs in chloride-containing effluents. In the next section the electrochemical degradation of these solutions will be examined in more detail.

5. Indirect electro-oxidation with strong oxidants

Aqueous dyestuffs solutions can be completely decontaminated by indirect electro-oxidation methods involving the homogeneous reaction of organic pollutants with strong oxidants generated during electrolysis. Two approaches are mainly utilized:

(i) The electro-oxidation with active chlorine, where direct anodic oxidation of chloride ion present in the effluent leads to the formation of free chlorine and/or chlorine–oxygen species that can oxidize organic pollutants in the bulk until overall mineralization.
(ii) The electro-Fenton process in which organics can be mineralized with homogeneous $^{\bullet}OH$ formed from Fenton's reaction between added catalytic Fe^{2+} and H_2O_2 electrogenerated from O_2 reduction at a suitable cathode.

In both cases, dyes are also competitively destroyed by direct anodic oxidation and by reaction with heterogeneous $^{\bullet}OH$ and other ROS and weaker oxidants produced from anodic oxidation of water and anions of the electrolyte (see Section 4.1). This section is devoted to clarify the applicability of these mediated electro-oxidation techniques to the decolorization and degradation of synthetic organic dyes, making especial emphasis in the use of electrode materials favouring the generation of chlorine active species or H_2O_2. Other proposed indirect procedures will be also briefly described.

5.1. Electro-oxidation with active chlorine

Chlorine and chlorine–oxygen species such as HClO and ClO^- are traditional chemical strong oxidants for treating industrial wastewaters [35,39]. These agents are also widely employed in the disinfection of drinking water [137]. The electrochemical technology offers an alternative indirect electro-oxidation procedure for the removal of organics pollutants with active chlorine species generated from direct oxidation of chloride ion at suitable anodes. This method differs from EO in the use of contaminated chloride-containing solutions to produce on-site active chlorine during electrolysis. It presents as major advantages [35,137,138]:

(i) the transport and storage of dangerous chlorine for water treatment is avoided;
(ii) faster destruction of organic matter than in chemical oxidation;
(iii) the total costs are much lower than conventional chemical technology.

Several disadvantages are [137,139,140]:

(i) the formation of undesirable toxic chloro-organic derivatives such as chloroform;
(ii) the electrogeneration of chlorine–oxygen by-products such as ClO_2^-, ClO_3^- and ClO_4^-, which have a high health-risk for living beings.

Fundamentals and applications of this mediated electro-oxidation method to the treatment of synthetic and real dyeing wastewaters are discussed in subsections below.

5.1.1. Electrogeneration of active chlorine species

It is well-known [141–144] that electrolysis of chloride aqueous solutions in an undivided cell involves the direct oxidation of chloride ion at the anode to yield soluble chlorine:

$$2Cl^- \rightarrow Cl_{2(aq)} + 2e^- \quad (38)$$

and the reduction of water at the cathode giving hydroxide ion and hydrogen gas from reaction (2). If the local concentration of dissolved chlorine exceeds its solubility, then supersaturation drives the formation of bubbles of chlorine gas. As electrogenerated chlorine diffuses away from the anode, it can react with chloride ion to form trichloride ion:

$$Cl_{2(aq)} + Cl^- \rightleftarrows Cl_3^- \quad (39)$$

or is rapidly hydrolyzed to be disproportionated to hypochlorous acid and chloride ion:

$$Cl_{2(aq)} + H_2O \rightleftarrows HClO + Cl^- + H^+ \quad (40)$$

In the bulk solution this acid is in equilibrium with hypochlorite ion (pK_a = 7.55 [141]) as follows:

$$HClO \rightleftarrows ClO^- + H^+ \quad (41)$$

Fig. 19 shows the speciation diagram for active chlorine species ($Cl_{2(aq)}$, Cl_3^-, HClO and ClO^-) calculated during the electrolysis of 0.1 M NaCl with a conversion of 0.2 for Cl^- [145]. Cl_3^- is formed in very low concentration up to pH ca. 4.0, while the predominant species is $Cl_{2(aq)}$ until pH near 3.0, HClO in the pH range 3–8 and ClO^- for pH > 8.0. The mediated oxidation of dyes with these species is then expected to be faster in acidic than in alkaline media because of the higher standard potential of $Cl_{2(aq)}$ (E^0 = 1.36 V vs. SHE) and HClO (E^0 = 1.49 V vs. SHE) than ClO^- (E^0 = 0.89 V vs. SHE). Since most electrolyses in undivided cells are treated in alkaline medium, the general mineralization of organic dyes is commonly referred to the only chemical action of ClO^- as follows [143,146]:

$$Dye + ClO^- \rightarrow CO_2 + H_2O + Cl^- \quad (42)$$

The concentration of electrogenerated ClO^- can be limited by its anodic oxidation to chlorite ion from reaction (43) and consecutive oxidation of this species to chlorate and perchlorate ions from reactions (44) and (45), respectively [141–144]:

$$ClO^- + H_2O \rightarrow ClO_2^- + 2H^+ + 2e^- \quad (43)$$

$$ClO_2^- + H_2O \rightarrow ClO_3^- + 2H^+ + 2e^- \quad (44)$$

$$ClO_3^- + H_2O \rightarrow ClO_4^- + 2H^+ + 2e^- \quad (45)$$

It is also possible the loss of ClO^- by reduction to chloride ion at the cathode:

$$ClO^- + H_2O + 2e^- \rightarrow Cl^- + 2OH^- \quad (46)$$

and from the following waste reactions in the bulk solution:

$$2HClO + ClO^- \rightarrow ClO_3^- + 2Cl^- + 2H^+ \quad (47)$$

$$2ClO^- \rightarrow 2Cl^- + O_2 \quad (48)$$

$$ClO^- + H_2 \rightarrow Cl^- + H_2O \quad (49)$$

The rates of electrode reactions (38) and (43)–(46) are a function of the electrocatalytic activity of the anode, chloride concentration, stirring or flow rate, temperature and current density. In contrast, the homogeneous chemical reaction (42) depends on the diffusion rate of organic pollutants into the solution regulated by the stirring or flow rate, temperature and pH, being chemical waste reactions (47)–(49) strongly enhanced as temperature rises [146].

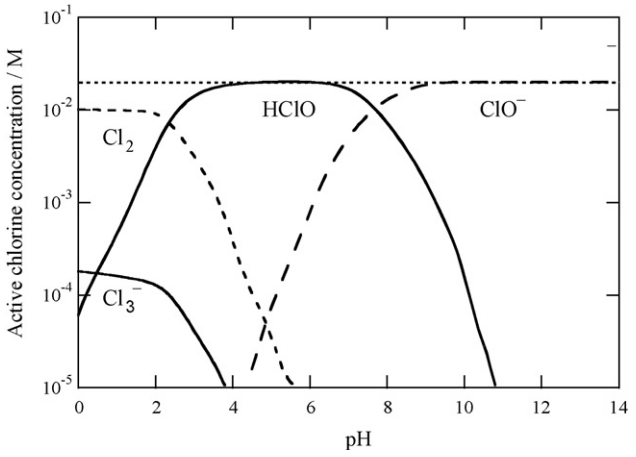

Fig. 19. Speciation diagram for the chlorine–water system calculated for the electrolysis of 0.1 M chloride ion at 25 °C in an undivided cell with a conversion of 0.2. Adapted from Ref. [145].

5.1.2. Experimental systems

Analogous electrochemical systems to those reported above for EO (see Section 4.2) are utilized in the indirect electro-oxidation treatment of dyeing solutions with active chlorine. The decolorization efficiency, percentages of COD and TOC decays, energy consumptions and current efficiency are then obtained in a similar way, by means of the corresponding Eqs. (9)–(12), (15) and (36), to confirm their effectiveness.

In electro-oxidation with active chlorine, however, a special attention merits the kind of anode material chosen, because it determines the predominant oxidants produced during the electrolysis of chloride solutions. Non-active conductive diamond electrodes, the most effective anodes in EO, are not useful for this technique since they generate appreciable amounts of ROS and other oxidants species such as peroxodisulphate, peroxodicarbonate and peroxodiphosphate [43,139]. While some authors [106,116,130] have described acceleration in dyes destruction with BDD anodes from chloride solutions in comparison to other electrolytes (see, for example, Fig. 18a), others [126,131] have considered negligible the generation of active chlorine, as discussed in Sections 4.6.3 and 4.6.4. The use of another non-active anode like PbO_2 provides a slightly better performance for dyestuffs degradation in chloride solutions [105,147].

The opposite behaviour is found for active anodes having much higher electrocatalytic power for oxidizing chloride ion than for generating ROS. Among these materials, DSA-type electrodes [135,141–144,146,148–156], metals such as Pt and Pt–Ir [111,157–161] and graphite [102,162–164] have been positively checked for treating organic dye solutions mediated with active chlorine and their characteristics will be separately detailed below. The good performances for these systems can be observed in the selected results collected in Table 4, which are superior to those

Table 4
Percentage of color and COD decays and energy consumption for the indirect electro-oxidation with active chlorine of selected dyes in chloride solutions using undivided cells with DSA-type electrodes, metals and graphite as anodes at 20–30 °C.

Dye[a]	C_0/mg dm^{-3}	Experimental conditions	j[b]/mA cm^{-2}	Color removal/%	COD decay/%	Energy consumption[c]	Ref.
Ti/RuO_2 anode							
Basic Blue 9 (Methylene Blue)	80	1.2 g dm^{-3} Cl^-, natural pH, for 95 min	20	100	94	–[d]	[135]
Reactive Black 5B (Procion Black 5B)	1624[e]	3.61 g dm^{-3} Cl^-, pH 10.6, residence time 27 min	25	100	74	16.3 kWh (g COD)$^{-1}$	[146]
Acid Blue 113	160	1.74 g dm^{-3} NaCl, pH 9, for 90 min	10	–[d]	80	61.3 kWh (kg COD)$^{-1}$	[150]
Ti/TiO_2–RuO_2 anode							
Acid Brown 14	330	0.58 g dm^{-3} NaCl, pH 7, for 2.5 h	30	100	67	–[d]	[155]
Ti/TiO_2–SnO_2 anode							
Acid Brown 14	330	0.58 g dm^{-3} NaCl, pH 7, for 2.5 h	30	100	60	–[d]	[155]
Ti/TiO_2–RuO_2–PbO_2 anode							
Acid Brown 14	330	0.58 g dm^{-3} NaCl, pH 7, for 2.5 h	30	100	42	–[d]	[155]
Ti/TiO_2–RuO_2–IrO_2 anode							
Reactive Black 5	100	1.5 g dm^{-3} NaCl, pH 6.2–6.5, for 2 h	36	100	53, 26[f]	450 kWh (kg COD)$^{-1}$	[143]
Reactive Blue 19				100	53, 22[f]	366 kWh (kg COD)$^{-1}$	
Reactive Red 141				100	82, 44[f]	192 kWh (kg COD)$^{-1}$	
Pt anode							
Reactive Orange 4	1000	20 g dm^{-3} NaCl, pH 9, for 10 h	24	100	81, 81[f]	698 kWh m^{-3}	[111]
Ti/Pt–Ir anode							
(Red Procion H-EXGL)	600	16.25 g dm^{-3} NaCl, pH 11.5, for 16 min	26	100	–[d]	4.40 kWh m^{-3}	[160,161]
Graphite anode							
Vat Blue 1 (Indigo)	200	30 g dm^{-3} NaCl, natural pH, for 2 h	5[g]	90	–[d]	1.84 kWh m^{-3}	[102]

[a] Color index (common) name.
[b] Applied current density.
[c] Different units reported.
[d] Not determined.
[e] Initial COD.
[f] Percentage of TOC decay.
[g] Applied cell voltage (V).

given in Table 2 for the EO processes with the same kind of anodes using chloride-free solutions. Although there is not enough comparative data in the literature to establish the best kind of anode for this technique, DSA-type electrodes are usually preferred due to their high stability and large production of oxidant ClO^- that can reach current efficiencies as high as 81–93%, as found for the electrolysis of 0.5 M NaCl with Ti/RuO_2 and Ti/(Ru + Pt)oxides between 100 and 600 mA cm^{-2} [149].

5.1.3. DSA-type electrodes

A reduced number of papers have compared the color removal and COD reduction of some azo and disperse dyes with active chlorine produced at several DSA-type anodes. Recently, Mohan et al. [154,155] used a stirred undivided tank reactor equipped with an expanded mesh of 10 cm^2 of Ti coated with TiO_2–RuO_2–PbO_2, TiO_2–SnO_2 or TiO_2–RuO_2 as anode and a 10 cm^2 stainless steel cathode to electrolyze 75 cm^3 of a 330 mg dm^{-3} Acid Brown 14 solution in 0.58 g dm^{-3} NaCl at pH 7.0, 30 mA cm^{-2} and room temperature. For these trials, Fig. 20 evidences that such anodes yield a more rapid COD decay in the sequence Ti/TiO_2–RuO_2–PbO_2 < Ti/TiO_2–SnO_2 < Ti/TiO_2–RuO_2, thus giving 100% decolorization efficiency and increasing decontamination of 42, 62 and 67% at 150 min. Other relative oxidation powers for DSA-type electrodes and metal anodes have been reported by Szpyrkowicz et al. [141] when examined the treatment of 700 cm^3 of a mixture of 0.181 g dm^{-3} of Disperse Yellow 126, 0.034 g dm^{-3} of Disperse Red 74 and 0.158 g dm^{-3} of Disperse Blue 139 in 0.1 M NaCl using a stirred undivided cell with a 100 cm^2 plate anode at 20 mA cm^{-2} and 25 °C for 40 min. Under these conditions, the use of a Ti/TiO_2–RuO_2 anode gave 42% color removal, 26% COD abatement and 60% current efficiency, obtaining better performances for Ti/TiO_2–RhO_x (47% color and 29% COD decays) and Ti/Pt–Ir (50% color and 39% COD decays). More results are then needed to ascertain the relative electrocatalytic activity of the large variety of DSA-type electrodes available for the electro-oxidation of organic dyes mediated with active chlorine.

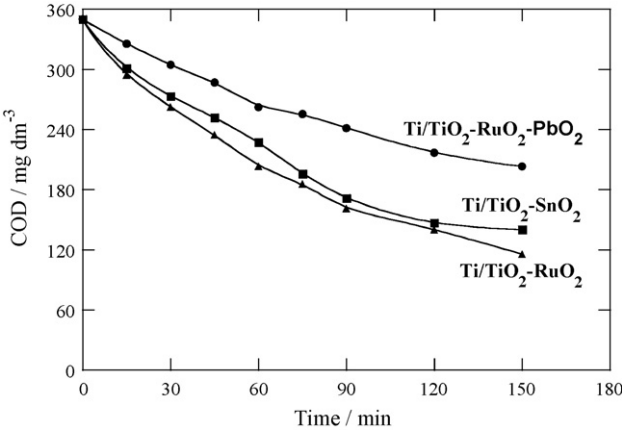

Fig. 20. Comparative COD abatement for 10 cm^2 Ti/TiO_2–RuO_2–PbO_2, Ti/TiO_2–SnO_2 and Ti/TiO_2–RuO_2 anodes during the indirect electro-oxidation with active chlorine of 75 cm^3 of a 330 mg dm^{-3} Acid Brown 14 solution in 0.58 g dm^{-3} NaCl of pH 7.0 using a stirred undivided tank reactor with a 10 cm^2 stainless steel cathode at 30 mA cm^{-2} and room temperature. Adapted from Ref. [155].

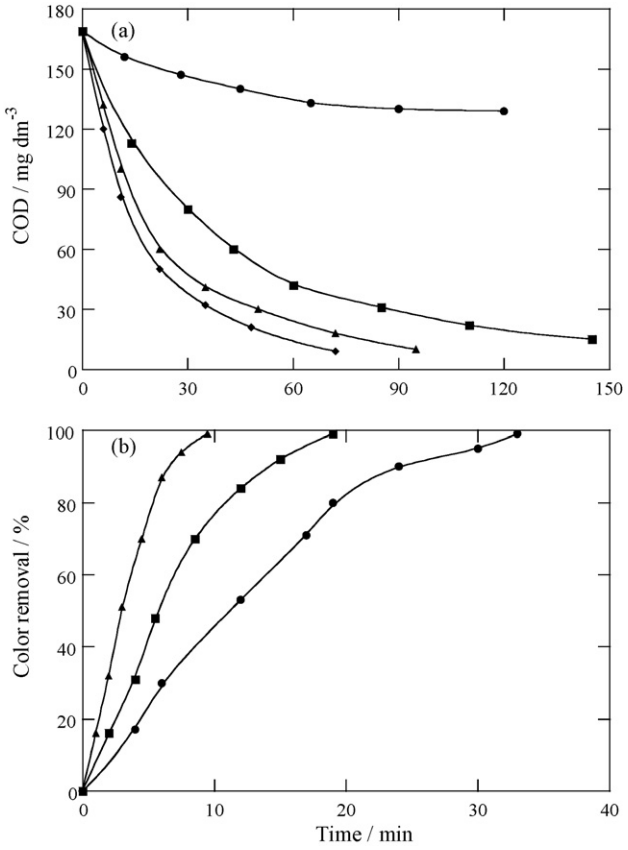

Fig. 21. (a) COD decay with time for the indirect electro-oxidation with active chlorine of 500 cm^3 of 80 mg dm^{-3} Methylene Blue solutions in 0.5 M Na_2SO_4 (●) without chloride and with (■) 0.6 g dm^{-3}, (▲) 1.2 g dm^{-3} and (◆) 2.0 g dm^{-3} of Cl^- using the cell of Fig. 10c with a 50 cm^2 Ti/RuO_2 anode and a 50 cm^2 stainless steel cathode at 20 mA cm^{-2}, 20 °C and a flow rate of 180 dm^3 h^{-1}. (b) Influence of current density on color removal for the same dye solution with 0.5 M Na_2SO_4 and 1.2 g dm^{-3} Cl^- at (●) 20 mA cm^{-2}; (■) 40 mA cm^{-2} and (▲) 60 mA cm^{-2}. Adapted from Ref. [135].

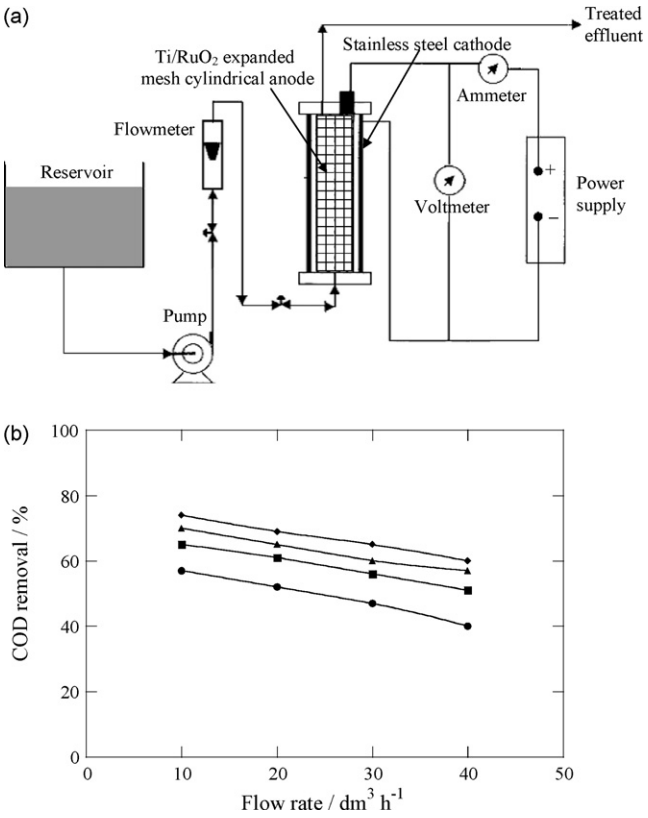

Fig. 22. (a) Scheme of the pilot electrochemical plant with a cylindrical flow reactor equipped with a Ti/RuO_2 coated expanded mesh anode of 10 cm height × 5 cm diameter and a stainless steel cathode of 10 cm height × 7 cm diameter used for the indirect electro-oxidation with active chlorine of Procion Black 5B in continuous mode operation. (b) Effect of current density on COD abatement vs. flow rate for 1264 mg dm^{-3} COD of this dye and 3.86 g dm^{-3} NaCl at pH 10.6. (●) 10 mA cm^{-2}; (■) 15 mA cm^{-2}; (▲) 20 mA cm^{-2}; (◆) 25 mA cm^{-2}. Adapted from ref. [146].

The effect of operating parameters such as Cl^- concentration, current density, stirring or flow rate, pH and temperature on the color and COD decays of synthetic dyestuffs effluents has been extensively studied [135,142–144,146,149,150,154,155]. Higher Cl^- content promotes faster destruction of dyes because of the formation of greater concentration of active chlorine species from reactions (38)–(41) with the consequent detrimental in ROS production. This behaviour is illustrated in Fig. 21a for the treatment of 500 cm^3 of 80 mg dm^{-3} Methylene Blue solutions in 0.5 M Na_2SO_4 using the system of Fig. 10c with a 50 cm^2 Ti/RuO_2 anode at 20 mA cm^{-2} [135]. A quicker COD removal can be observed as more Cl^- concentration is added until 2.0 g dm^{-3}. Increasing j also accelerates dyes mineralization due to the concomitant rise in rate of all electrode reactions to produce more oxidizing species. As an example, Fig. 21b shows that the above Methylene Blue solution with 1.2 g dm^{-3} Cl^- becomes completely decolorized in 33 min at 20 mA cm^{-2} and much more rapidly, in about 10 min, at a higher current density of 60 mA cm^{-2}.

A large influence of stirring in batch tank reactors and liquid flow rate in continuous flow systems on the mediated electro-oxidation process of dyes has been described provided that they affect the transport of active species and/or the residence time in the cell. Szpyrkowicz et al. [142] concluded that increasing stirring favours the decolorization efficiency of a mixture of disperse dyes in 0.1 M NaCl using a Ti/TiO_2–RhO_x anode, although their mineralization reactions are decelerated causing less COD abatement. A relevant study on the treatment of the azo dye Procion Black 5B has been reported by Raghu and Ahmed Basha [146] using the pilot flow plant of Fig. 22a with a reactor consisting of two cylindrical electrodes of 10 cm height, an inner Ti/RuO_2 expanded mesh anode of 5 cm diameter and an outer stainless steel cathode of 7 cm diameter. Experiments involved the degradation of a 1264 mg dm^{-3} COD solution of this azo dye in 3.86 g dm^{-3} NaCl of pH 10.6 in a single pass by varying the liquid flow rate between 10 and 40 dm^3 h^{-1}. Fig. 22b illustrates that COD reduction increases with increasing j from 10 to 25 mA cm^{-2}, as expected from the faster generation of oxidant ClO^-, but it undergoes a gradual fall as flow rate rises due to the shorter residence time in the reactor, directly related to electrolysis time. For the highest j of 25 mA cm^{-2} and the lowest flow rate of 10 dm^3 h^{-1} (residence time 27 min), 100% color removal was attained, along with the greatest COD decay (74%) and energy cost (16.3 kWh (g COD)$^{-1}$).

Several studies have reported higher COD destruction when the dyeing solution varies from acidic to alkaline conditions. For example, Mohan et al. [150] found that 100 cm^3 of 160 mg dm^{-3} of the azo dye Acid Blue 113 containing 1.74 g dm^{-3} NaCl, electrolyzed in a stirred undivided cell equipped with a Ti/RuO_2 anode at 10 mA cm^{-2}, are more rapidly mineralized at pH 9.0 than at pH 7.0 or 4.0. At pH 9.0 COD was reduced by 80% in 90 min with low energy consumption of 61.3 kWh (kg COD)$^{-1}$. This behaviour evidences the complexity of chemical mineralization reactions and wastes reactions (47)–(49) involved in the mediated oxidation process, since the degradation rate should be greater in acidic medium with $Cl_{2(aq)}$ and HClO as active species than in alkaline

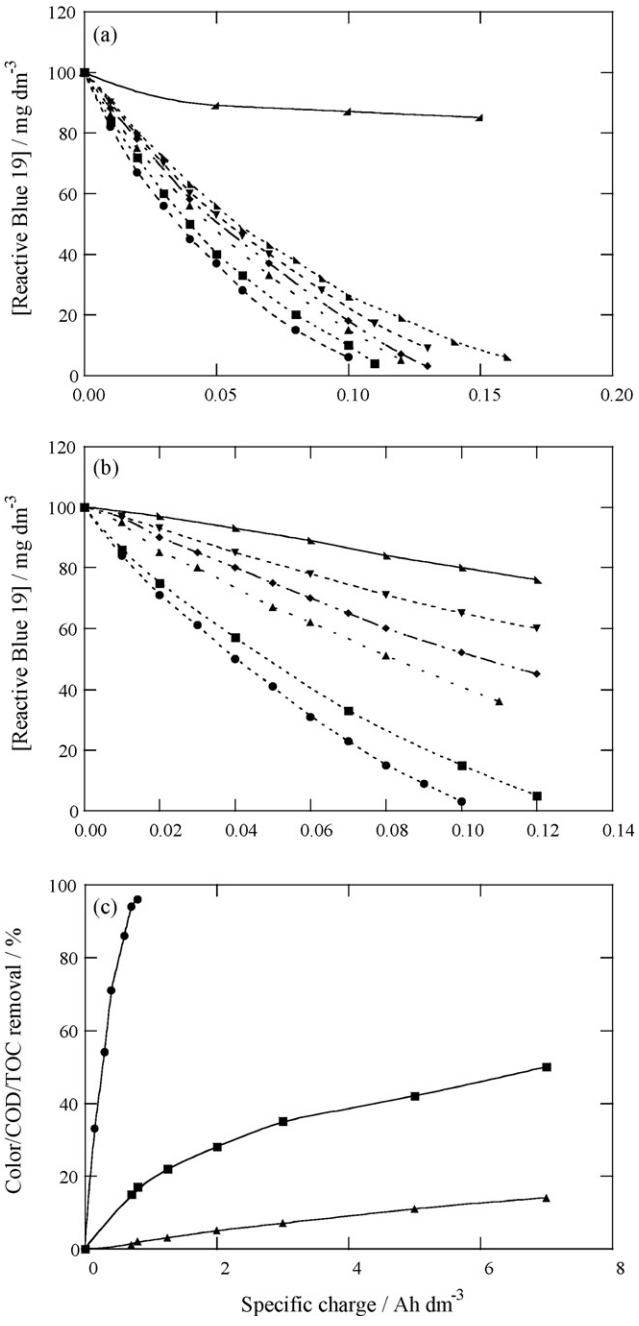

Fig. 23. Effect of (a) pH and (b) temperature on dye concentration decay for 1 dm^3 of 100 mg dm^{-3} Reactive Blue 19 solutions with 1.5 g dm^{-3} NaCl by indirect electro-oxidation with active chlorine in a stirred undivided tank reactor with a Ti/TiO_2–RuO_2–IrO_2 mesh anode and a stainless steel plate cathode, both of 27.2 cm^2 area, at 21.66 mA cm^{-2}. In plot (a), initial pH: (●) 4.0; (■) 5.0; (▲) 6.0; (◆) 7.0; (▼) 8.0; (◣) 9.0; (◢) 10.0 and 30 °C. In plot (b), pH 6.0 and temperature: (●) 25 °C; (■) 30 °C; (▲) 35 °C; (◆) 45 °C; (▼) 55 °C and (◣) 65 °C. In plot (c), change of (●) color, (■) COD and (▲) TOC removal with specific charge for a 400 mg dm^{-3} dye solution containing 1.5 g dm^{-3} NaCl at pH 6.0, 21.66 mA cm^{-2} and 25 °C. Adapted from Ref. [144].

solutions where the less potent ClO^- acts as oxidant. This trend has been confirmed by Rajkumar et al. [144] in an accurate study on the direct reaction of the antraquinone dye Reactive Blue 19 with active chlorine produced at a Ti/TiO_2–RuO_2–IrO_2 mesh anode. Fig. 23a illustrates the expected deceleration for the removal rate of 100 mg dm^{-3} of the dye with increasing pH from 4.0 to 10.0, determined during the electrolysis of 1 dm^3 of 1.5 g dm^{-3} NaCl solutions in a stirred undivided tank reactor containing this anode and a stainless steel plate cathode, both of 27.2 cm^2 area, at 21.66 mA cm^{-2} and 30 °C. These authors also found that Reactive Blue 19 at pH 6.0 disappears more slowly when temperature rises from 25 to 65 °C, as can be seen in Fig. 23b. This phenomenon was attributed to increasing loss of ClO^- via the cathode reaction (46) and waste reactions (47)–(49). While these results confirm the feasibility of rapid decolorization of reactive dyeing solutions with active chlorine at pH < 7.0 and 25 °C, very slow mineralization of by-products formed in acid medium was detected. Fig. 23c shows that a 400 mg dm^{-3} dye solution in the presence of 1.5 g dm^{-3} NaCl at pH 6.0 and 25 °C can attain overall color removal at a low Q value of 0.8 Ah dm^{-3}, but with so poor mineralization that COD and TOC decays as low as 50 and 14%, respectively, are obtained even after prolonging electrolysis to 7.0 Ah dm^{-3}. According to this behaviour, high energy costs (ca. >200 kWh $(kg\ COD)^{-1}$) were determined for the mediated electro-oxidation of acidic solutions with 100 mg dm^{-3} of several reactive dyes under similar conditions [143] (see Table 4).

On the other hand, the expected formation of chlorinated derivatives from the attack of active chlorine on the organic dye has been confirmed in some cases by GC–MS analysis of electrolyzed solutions. Donaldson et al. [151] detected the leuco dye 4,6-dichloro-7-dimethylamino-3*H*-phenothiazin-3-one as the main dichloroaromatic intermediate of Methylene Blue during its electro-oxidation in chloride solutions using a DSA anode. For a mixture of Disperse Yellow, Disperse Red 74 and Disperse Blue 139 in 0.1 M NaCl at pH 4.0 with a Ti/TiO_2–RhO_x anode, Szpyrkowicz et al. [142] identified a high number of mono- and di-chlorinated intermediates such as 2-chloro-2-methylbutane, *cis*-3-chloropropanate, 2-chloroethenylbenzene, *cis*-1,3-dichlorocyclopentane and *trans*-1,2-dichlorocyclopentane. In contrast, no chlorinated derivatives were found by Rajkumar and Kim [143] for Reactive Blue 19 in 1.5 g dm^{-3} NaCl at pH 6.0 under degradation with a Ti/TiO_2–RuO_2–IrO_2 mesh anode. From detected intermediates, these authors proposed the reaction sequence of Fig. 24 assuming that $Cl_{2(aq)}$, HClO and/or ClO^- are the oxidizing agents. The initial attack of these species gives rise to the breaking of the dye molecule into 1-aminoantraquinone and benzene. The former is then transformed into 2-hydroxy-1,4-naphtaquinone, which is subsequently degraded to a mixture of 1,3-indanone, phthalic anhydride, phthalimide and phthalide. Benzene is oxidized in parallel to benzoic acid via benzyl alcohol and benzaldehyde. Further destruction of the above by-products leads to lower molecular weight species that are finally converted into CO_2.

The effectiveness of electrogenerated active chlorine for the remediation of industrial effluents has been confirmed by Vaghela et al. [153] with an undivided flow filter-press cell equipped with a 50 cm^2 expanded DSA anode and an 88 cm^2 stainless steel plate cathode in continuous operation mode. At 100 mA cm^2 and flow rate of 5 cm^3 min^{-1} they found total decolorization and 53% COD reduction for a reactive azo dye wastewater from a leading textile industry initially containing 5957 mg dm^{-3} COD and 16.7% (w/v) NaCl at pH 7.2. An excellent performance of this procedure has also been reported by Muthukumar et al. [152] when treating another textile reactive dye effluent with ca. 3000 mg dm^{-3} COD and 32 g dm^{-3} NaCl at pH 12.0 by a batch flow system containing a bipolar stack cell with 11 bipolar Ti/RuO_2 electrodes of 0.181 dm^2 total area. These authors determined 74% COD removal with 42 kWh $(kg\ TOC)^{-1}$ energy consumption after 8 h of electrolysis of 1.5 dm^3 of this wastewater under optimal conditions of 50 mA cm^{-2} and flow rate of 80 dm^3 h^{-1}.

5.1.4. Metal anodes

The use of Ti/Pt in indirect electro-oxidation with active chlorine can also yield rapid decolorization and large decontami-

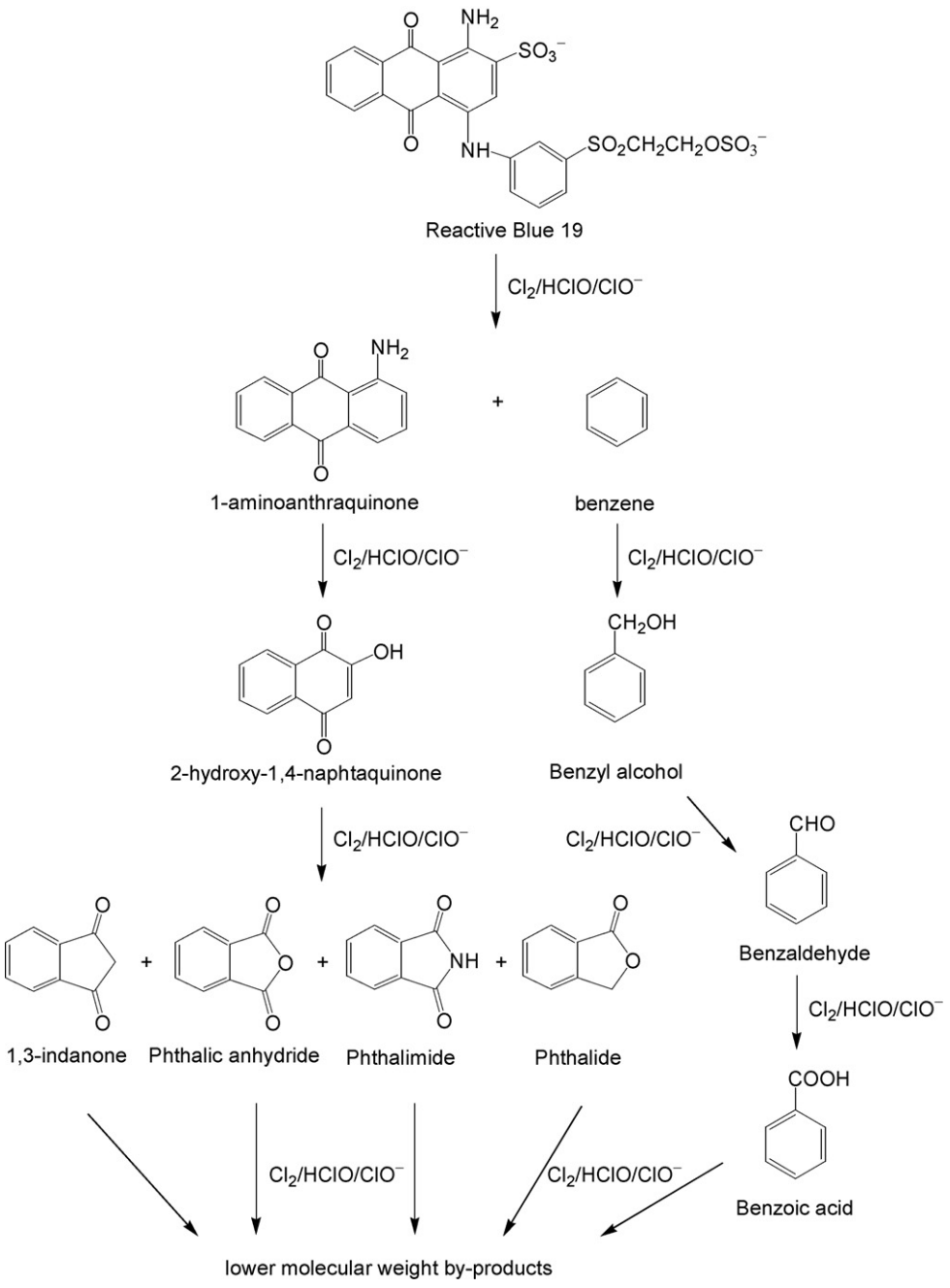

Fig. 24. Proposed reaction pathway for the indirect electro-oxidation with active chlorine of the dye Reactive Blue 19 under the experimental conditions of Fig. 23.

nation of highly concentrated dyes effluents. This has been shown by López-Grimau and Gutiérrez [111] following their comparative study on the degradation of Reactive Orange 4 in Na_2SO_4 and NaCl effluents described in Section 4.4 and illustrated in Fig. 14. A flow cell containing 486 cm^2 Ti/Pt anode flow rate was utilized to treat 4 dm^3 of 1 g dm^{-3} of this dye in 20 g dm^{-3} NaCl at pH 9.0, 24 mA cm^{-2} and flow rate of 25 dm^3 h^{-1} in batch operation mode. Total color removal of this effluent was attained in 90 min, but mineralization was much slower and after 10 h of treatment, 81% of COD and TOC decays were reached, with a very high energy cost of 698 kWh m^{-3}. From these results, these authors inferred that this method can only be attractive for decolorizing dyeing effluents because conventional biological treatment is unable to remove their color satisfactorily. In a similar way, Vlyssides et al. [157] also proposed the application of mediated electro-oxidation with a Ti/Pt anode to color removal of textile dyestuff wastewaters with high Cl^- content as pre-treatment stage for biological post-treatment.

More recently, the performance of stirred undivided [160] and divided [161] tank reactors containing a 100 cm^2 Ti plate coated with Pt (70 mol%) and Ir (30 mol%) as metal anode and a 100 cm^2 stainless cathode has been checked for the decolorization of 600–800 cm^3 of 0.6 g dm^{-3} of the reactive dye Red Procion H-EXGL in 16.25 g dm^{-3} NaCl at pH 11.6, 26 mA cm^{-2} and temperatures of 10–80 °C. These trials revealed that the dye is not oxidized at the Ti/Pt–Ir anode, but only reacts with active chlorine agents in the solution bulk. In the undivided cell, total decolorization was more rapidly attained with raising temperature from 10 to 40 °C due to the acceleration of all electrode and chemical reactions, without significant pH change. A much faster color removal was found for the anolyte of the divided cell since its pH suddenly dropped to ca.

6 by the uncompensated reactions (38), (40) and (41) favouring the dye oxidation with HClO instead of its slower reaction with ClO^- taking place in alkaline medium. By raising the temperature from 10 to 80 °C in this system, the rate for dye decay increased up to 40 °C, whereupon it became gradually slower because of the fall in solubility of $Cl_{2(aq)}$ formed from reaction (38). Lower energy costs for total color removal were then found for the divided cell up to 40 °C and for the undivided system at greater temperature. These findings evidence the need of optimizing the configuration of the electrolytic system and parameters such as pH and temperature to obtain the highest oxidation ability of electrogenerated active chlorine.

5.1.5. Graphite anode

The studies on indirect electro-oxidation with active chlorine performed with a graphite anode have been focused to mainly characterize the decolorization process of several organic dyes such as Indigo [102], Congo Red [162] and Methyl Orange [163]. The two latter, for example, exhibited a fast color removal that increased with raising Cl^- concentration, current density and temperature from 20–25 to 40–45 °C and with decreasing pH, as expected if they react with $Cl_{2(aq)}$, HClO and/or ClO^- (see Section 5.1.3) with small participation of their direct anodic oxidation on graphite. It is also noticeable the scale-up carried out by Cameselle et al. [102] for the treatment of 0.2 g dm^{-3} Indigo in 30 g dm^{-3} NaCl at natural pH using 20 dm^3 solutions in a stirred undivided graphite/graphite cell with 500 cm^2 electrodes separated 50 cm. After application of a cell voltage of 5 V at room temperature for 2 h, 90% decolorization efficiency with a very low energy consumption of 1.86 kWh m^{-3} was determined. This corroborates again the feasibility of using mediated oxidation with electrogenerated active chlorine as a very attractive method for an efficient and low cost color removal of industrial dyeing wastewaters.

5.2. Electro-Fenton method

Hydrogen peroxide is a "green" chemical that leaves oxygen gas and water as by-products, although it can be hazardous owing to its comburent character. It is used to bleach pulp and paper and textiles, clean electronic circuits and delignify agricultural wastes, as well as disinfectant in medical and industrial applications and as oxidant in synthesis and wastewater treatment [165,166]. However, the direct remediation of wastewaters with H_2O_2 is limited by its low oxidation power, since it can only attack reduced sulphur compounds, cyanides, chlorine (it is reduced to chloride ion) and certain organics such as aldehydes, formic acid and some nitro-organic and sulpho-organic compounds. For this reason, H_2O_2 is commonly activated in acidic effluents with Fe^{2+} ion as catalyst (Fenton's reagent) to give homogenous $^\bullet OH$ as strong oxidant of organics [167]. This procedure has been developed in the traditional Fenton method. An important disadvantage of this chemical technique is the fast consumption of the Fenton's reagent giving partial mineralization of organic pollutants. This problem can be solved by an emerging EAOP such as EF, where H_2O_2 is directly electrogenerated at the cathode of the cell from O_2 gas reduction. The major advantages of this indirect electro-oxidation method are [39,168,169]:

(i) the on-site production of H_2O_2 avoids its dangerous transport and storage;
(ii) higher degradation rate of organic pollutants than in traditional Fenton method because of the continuous regeneration of Fe^{2+} at the cathode;
(iii) the feasibility of overall mineralization with relative low cost if operational parameters are optimized.

However, the following disadvantages are emphasized [39,167,170]:

(i) limitation of its application to acidic wastewaters, usually within the pH range 2–4;
(ii) high amounts of chemicals are spent for acidifying effluents before decontamination and/or for neutralizing treated solutions before disposal.

Recently, the EF treatment of dyeing solutions has received increasing attention, but the studies have only been focused to show the viability of the method for synthetic effluents at lab scale.

5.2.1. Generation of homogeneous hydroxyl radical

It is known since 1882 that hydrogen peroxide can be accumulated in aqueous medium from the cathodic reduction of dissolved O_2 gas at carbonaceous electrodes with high surface area [166,171]. The corresponding two-electron reaction with E^0 = 0.68 V vs. SHE can be written as follows:

$$O_{2(g)} + 2H^+ + 2e^- \rightarrow H_2O_2 \quad (50)$$

and takes place more easily than the four-electron reduction of this gas to water (E^0 = 1.23 V vs. SHE). Hydrogen peroxide production and stability depend on factors such as cell configuration, the cathode used and operational conditions. Electrochemical reduction at the cathode surface by reaction (51) and in much lesser extent disproportion in the bulk by reaction (52) are general parasite reactions that result in the loss of product or a lowering of current efficiency [172]:

$$H_2O_2 + 2e^- \rightarrow 2OH^- \quad (51)$$

$$2H_2O_2 \rightarrow O_{2(g)} + 2H_2O \quad (52)$$

Furthermore, in an undivided cell H_2O_2 is oxidized to O_2 via hydroperoxyl radical ($HO_2^\bullet$) as intermediate by the following reactions [173]:

$$H_2O_2 \rightarrow HO_2^\bullet + H^+ + e^- \quad (53)$$

$$HO_2^\bullet \rightarrow O_{2(g)} + H^+ + e^- \quad (54)$$

The EF treatment of dyeing wastewaters involves the continuous generation of H_2O_2 from dissolved O_2 directly injected as pure gas or air, which is efficiently reduced at RVC [172], carbon felt [1,174–179], ACF [180,181], three-dimensional graphite [182], graphite cloth [183], graphite–polytetrafluoroethylene (PTFE) [184,185], Pt–carbon [186] and carbon–PTFE O_2-diffusion [187] cathodes via reaction (50). A small catalytic quantity of Fe^{2+} is then added to the acidic contaminated solution to generate Fe^{3+} and $^\bullet OH$ according to the classical Fenton's reaction (55) with a second-order rate constant (k_2) of 63 M^{-1} s^{-1} [167,188]:

$$Fe^{2+} + H_2O_2 \rightarrow Fe^{3+} + {}^\bullet OH + OH^- \quad (55)$$

Reaction (55) can be propagated by the catalytic behaviour of the Fe^{3+}/Fe^{2+} system. Thus, Fe^{2+} is continuously regenerated from the reduction of Fe^{3+} at the cathode (E^0 = 0.77 V vs. SHE) from reaction (56) or in the medium by electrogenerated H_2O_2 from Fenton-like reaction (57) with $k_2 = 8.4 \times 10^{-6}$ M^{-1} s^{-1}, by $HO_2^\bullet$ from reaction (58) with $k_2 = 2 \times 10^3$ M^{-1} s^{-1} and/or by organic radical intermediates $R^\bullet$ from reaction (59) [167–169]:

$$Fe^{3+} + e^- \rightarrow Fe^{2+} \quad (56)$$

$$Fe^{3+} + H_2O_2 \rightarrow Fe^{2+} + H^+ + HO_2^\bullet \quad (57)$$

$$Fe^{3+} + HO_2^{\bullet} \rightarrow Fe^{2+} + H^+ + O_2 \quad (58)$$

$$Fe^{3+} + R^{\bullet} \rightarrow Fe^{2+} + R^+ \quad (59)$$

As a result of the efficient Fe^{2+} regeneration from reaction (56), Fe^{3+} can also be directly added to dyes effluents yielding similar decontamination to Fe^{2+} as initial catalyst [1,178]. However, a part of $^{\bullet}OH$ formed in the medium is lost by its reaction with Fe^{2+} from reaction (60) with $k_2 = 3.2 \times 10^8\ M^{-1}\ s^{-1}$ and H_2O_2 from reaction (61) with $k_2 = 2.7 \times 10^7\ M^{-1}\ s^{-1}$:

$$Fe^{2+} + {}^{\bullet}OH \rightarrow Fe^{3+} + OH^- \quad (60)$$

$$H_2O_2 + {}^{\bullet}OH \rightarrow HO_2^{\bullet} + H_2O \quad (61)$$

The rate of Fenton's reaction (55) can also drop by oxidation of Fe^{2+} in the bulk with $HO_2^{\bullet}$ from reaction (62) with $k_2 = 1.2 \times 10^6\ M^{-1}\ s^{-1}$ and at the anode by reaction (63) if an undivided cell is used:

$$Fe^{2+} + HO_2^{\bullet} \rightarrow Fe^{3+} + HO_2^- \quad (62)$$

$$Fe^{2+} \rightarrow Fe^{3+} + e^- \quad (63)$$

In an undivided electrolytic cell organics contained in the wastewater can undergo simultaneous oxidation with heterogeneous $^{\bullet}OH$ produced at the anode from reaction (25) and with homogeneous $^{\bullet}OH$ formed in the medium from Fenton's reaction (55). The degradative action of the former is usually disregarded for most anodes, expect in the case of BDD because of the much higher oxidation power of BDD($^{\bullet}OH$) [187]. Parallel slower destruction of pollutants with other ROS such as H_2O_2, $HO_2^{\bullet}$ and O_3 formed from reactions (50), (53) and (32), respectively, and weaker oxidants like $S_2O_8^{2-}$ when using BDD (see Section 4.1) is also possible. Moreover, final carboxylic acids form complexes with iron ions that are difficultly mineralized with $^{\bullet}OH$ [178,187,189,190].

5.2.2. Electrochemical systems and experimental conditions

The EF technology utilizes the same electrochemical systems as the other electro-oxidation methods, but differs in the additional use of pure O_2 gas or air that is bubbled through the solution or directly injected to the carbonaceous cathode for producing H_2O_2 from reaction (50). Three-electrode divided [1,174,175] or undivided [176,179,184,185] cells, two-electrode tank reactors with two-compartment [172,186] or one-compartment [177,178,180,181,186,187] and two-electrode divided [182] or undivided [183] flow cells, have been tested for treating dyes. Examples of undivided cells with carbon felt [178], graphite-PTFE [184] and O_2-diffusion [173] cathodes are presented in Fig. 25a–c, respectively.

Dyeing solutions are usually saturated with O_2 or air under vigorous stirring or high liquid flow rate to obtain the maximum accumulation of H_2O_2. This is also achieved with an O_2-diffusion cathode if it is feed with an excess of pure O_2 gas. The initial pH of effluents treated by EF is always regulated to a value near 3.0, close to the optimum pH of 2.8 for Fenton's reaction (55) [167], to ensure the fastest generation of homogeneous $^{\bullet}OH$. Other parameters affecting the production of this radical from reactions (50) and (55) are optimized in each system such as E_{cat} or current and Fe^{2+} or Fe^{3+} concentration.

A similar H_2O_2 production has been found at pH 3.0 by applying a constant E_{cat} between −0.5 and −1.0 V vs. SCE, whereas at more negative cathodic potentials this species is unstable since it is reduced to OH^- by reaction (51) [1,179,184,185]. Fig. 26a shows the change of H_2O_2 concentration with time during the electrolysis of 200 cm^3 of 0.1 M Na_2SO_4 at pH 3.0 in a three-electrode cell similar to that of Fig. 25b, with a 1 cm^2 Pt anode and a 7.6 cm^2 carbon felt cathode. A continuous accumulation of H_2O_2 up to 0.47 mM at 310 min of electrolysis at $E_{cat} = -1.0$ V vs. SCE can be observed without iron catalyst. In contrast, in the presence of 0.1 mM Fe^{3+}, less H_2O_2 is accumulated in the bulk since part of it is destroyed by Fe^{3+} and regenerated Fe^{2+} from reactions (57) and (55), respectively. Fig. 26a also illustrates that when 0.1 mM Fe^{2+} is added to the medium, this ion attains rapidly a steady content of ca. 5×10^{-3} mM, similar to that obtained from its regeneration starting from 0.1 mM Fe^{3+}. Analogous results have been reported by Zhou et al. [184,185] using a Pt/graphite-PTFE cell, indicating that very small quantity of catalytic Fe^{2+} or Fe^{3+} is needed in the EF method. A different behaviour can be seen in Fig. 26b for the electrolysis of 100 cm^3 of 0.05 M Na_2SO_4 solutions at pH 3.0 in the two-electrode undivided cell of Fig. 25c equipped with a 10 cm^2 Pt anode and a 3 cm^2 carbon-PTFE O_2-diffusion cathode [190]. Under these conditions, H_2O_2 is gradually accumulated during 3 h up to reach an increasing steady content with increasing current at 450 mA (curve *a*), 300 mA (curve *b*) and 100 mA (curve *e*). The steady H_2O_2 concentration is attained just when its electrogeneration rate from reaction (50) becomes equal to its oxidation rate to O_2 from reactions (53) and (54). When 1.0 mM Fe^{2+} is added to this system, H_2O_2 destruction is accelerated by the action of reactions (55) and (57), as can be deduced by comparing curves *b* and *c* of Fig. 26b determined at 300 mA. This behaviour has also been described by Wang et al. [180] operating with an undivided RuO_2/ACF cell. Results of Fig. 26a and b evidence the complexity of reactions involved in EF to produce homogeneous $^{\bullet}OH$.

While the decolorization efficiency and percentages of COD and/or TOC removals for synthetic organic dyes treated by EF have been determined in most papers from Eqs. (9)–(11), the current efficiency and energy consumption for this process has been disregarded. Several authors have detected by GC–MS and HPLC the oxidation intermediates coming from the reaction of dyestuffs with homogeneous $^{\bullet}OH$. The kinetics for some dyes decays has also been measured, allowing calculating the corresponding pseudo-first-order (k_1) and/or second-order ($k_2 = k_1/[^{\bullet}OH]$) rate constants [1,174–178]. Data collected in Table 5 show that k_1-values between 3.2×10^{-2} and $7.0 \times 10^{-3}\ s^{-1}$ and k_2-values between 2×10^9 and $2 \times 10^{10}\ M^{-1}\ s^{-1}$ are obtained for several organic dyes. That means that 10^{-12} to 10^{-13} M $^{\bullet}OH$ concentration ($=k_1/k_2$) is formed under steady state conditions.

5.2.3. Treatment of dyes

Table 6 summarizes relevant results obtained for the EF degradation of several synthetic organic dyes in 0.05–0.10 M Na_2SO_4 solutions of pH 3.0 in undivided electrolytic cells. An examination of these data reveals that this EAOP provides total decolorization and almost complete mineralization (>98% TOC abatement) in most cases. The degradative performance of EF is then similar to that of EO with diamond anodes (see Table 3), but much better than that of indirect electro-oxidation with active chlorine (see Table 4), also avoiding the production of undesirable toxic chlorinated derivatives.

Shen et al. [186] utilized a two-chamber cell connected with a K_2SO_4 electrolyte bridge to demonstrate the better performance of the EF degradation of 500 cm^3 of 60 mg dm^{-3} of the azo dye Acid Red 14 with 50 mM Fe^{2+} and 0.05 M Na_2SO_4 at pH 3.0 saturated with air in the cathodic chamber with a Pt–carbon cathode in comparison to the EO of the same solution in the anodic chamber with a graphite electrode. After 80 min of electrolysis at 58 mA, the former yielded 66% COD removal, a value higher than 56% obtained for the latter. From the intermediates detected in the EF process, they proposed the reaction sequence depicted in Fig. 27 considering the homogeneous $^{\bullet}OH$ as the main oxidant. As can be seen, the

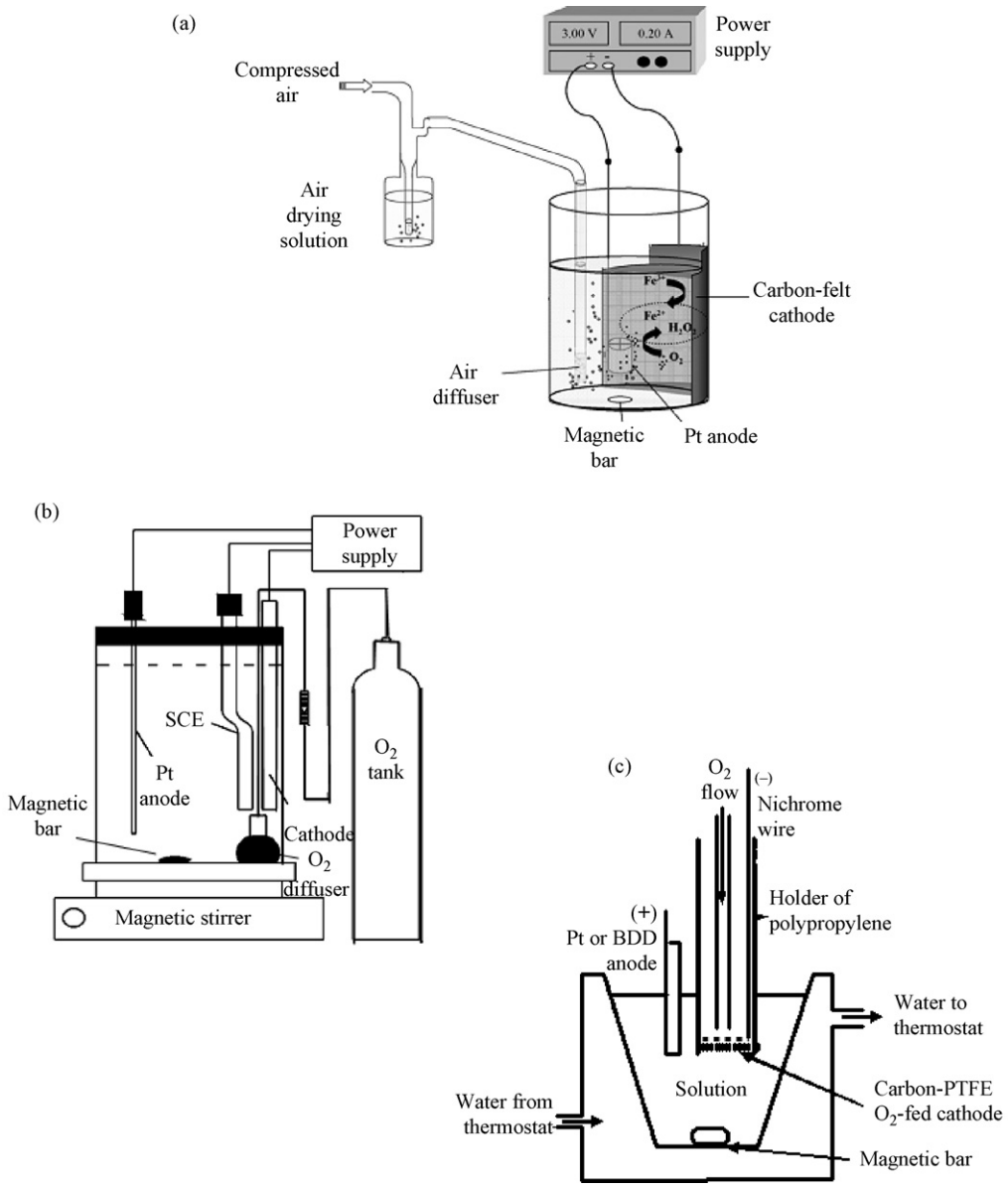

Fig. 25. Schemes of bench-scaled electrochemical systems with open and undivided tank reactors utilized for the electro-Fenton treatment of dyeing solutions with H_2O_2 electrogeneration. (a) Stirred two-electrode cell with a carbon felt cathode and bubbling of compressed air. Adapted from Ref. [178]. (b) Stirred three-electrode cell with a graphite-PTFE cathode and continuous injection of pure O_2 to the solution. Adapted from Ref. [184]. (c) Stirred two-electrode cell with a carbon-PTFE diffusion cathode directly fed with pure O_2. Adapted from Ref. [173].

–OH group of Acid Red 14 is initially oxidized to =O and its C–N=N– bond is broken to give the undetected intermediates A and B, which are rapidly transformed into hydroxymethyl-phenyloxime, phthalic anhydride and salicylic acid with loss of SO_4^{2-}. The former is then oxidized to 2-nitroethanol, 2-nitro-2-propanol, benzoic acid and ethane-1,1,2-tricarboxylic acid, while phthalic anhydride evolves to 5-oxotetrahydrofuran-2,3-dicarboxylic acid. Subsequent degradation of these species, with release of NO_3^- from nitrocompounds, leads to short-linear carboxylic acids such as 3-ketoadipic, 2-ketoglutaric, succinic, malonic, ketomalonic and oxalic, which are finally mineralized to CO_2.

The reactivity of homogeneous $^{\bullet}OH$ in EF has been clarified by the Oturan's group [176–178] using the undivided tank reactor of Fig. 25a equipped with a small 4.5–5.5 cm^2 Pt sheet or cylinder as anode, centred in the cell, and surrounded by a larger 60 cm^2 carbon felt cathode. A strong inhibition for the oxidation process of 500 cm^3 of air-saturated 1.0 mM Direct Orange 61 solutions in 0.05 M Na_2SO_4 of pH 3.0 was found with raising Fe^{2+} concentration in the above two-electrode cell, attributed to the concomitant loss in $^{\bullet}OH$ as a result of the rise in rate of the parasite reaction (60) [177]. This phenomenon can be observed in Fig. 28a since increasing 0.1, 0.2 and 0.5 mM Fe^{2+} causes decreasing TOC removal of 96, 63 and 55% after 8 h of electrolysis at 100 mA. The fastest decay for Direct Orange 61 with the most favorable 0.1 mM Fe^{2+} as catalyst was obtained for a 0.05 mM dye solution operating at 60 mA. Under these optimum conditions, Fig. 28b shows that solution is decolorized in 50 min while the compound reacts with homogeneous $^{\bullet}OH$ following a pseudo-first-order kinetics with $k_1 = 5.0 \times 10^{-3}\ s^{-1}$. For this reaction, a k_2-value of $2.1 \times 10^{10}\ M^{-1}\ s^{-1}$ was determined from the competition kinetics method, indicating that it is attacked with 2.4×10^{-13} M $^{\bullet}OH$ in average. The production of a similar small, but very effective $^{\bullet}OH$ concentration has been corroborated by this group from the decay kinetics of Yellow Drimaren, Congo Red and Methylene Blue under

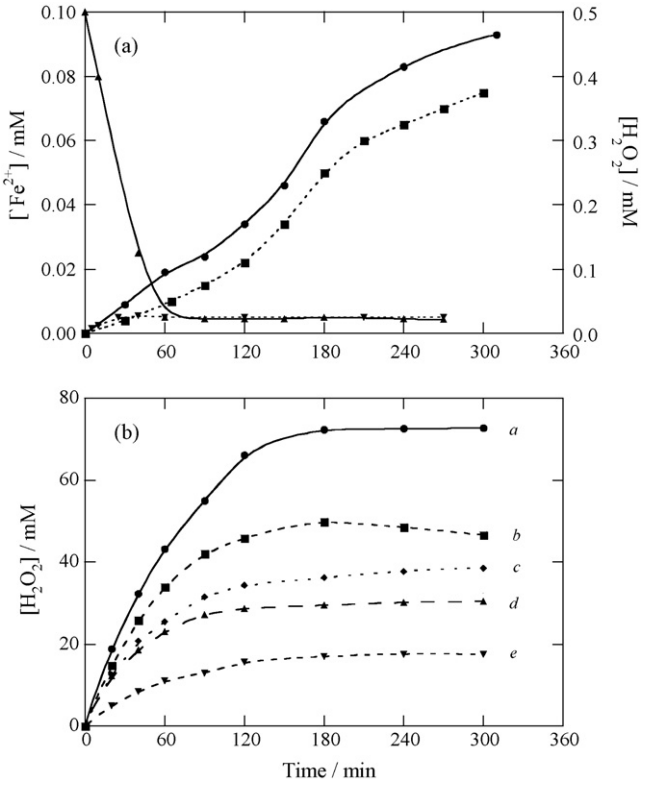

Fig. 26. (a) Change of the concentration of (▲, ▼) Fe^{2+} and (●, ■) accumulated hydrogen peroxide with electrolysis time for 200 cm^3 of 0.1 M Na_2SO_4 solutions of pH 3.0 in a three-electrode Pt/graphite felt cell similar to that of Fig. 25b at E_{cat} = −1.0 V vs. SCE and room temperature. (●) Without iron ions and with (■, ▼) 0.1 mM Fe^{3+} and (▲) 0.1 mM Fe^{2+}. Data from Ref. [179]. (b) Evolution of hydrogen peroxide concentration accumulated during the electrolysis of 100 cm^3 of 0.05 M Na_2SO_4 solutions of pH 3.0 at 25 °C in the Pt/O_2 diffusion cell of Fig. 25c. (*a*, *b* and *e*) Without Fe^{2+}; (*c* and *d*) with 1.0 mM Fe^{2+} and (*d*) under a 6 W UVA irradiation. Applied current: (*a*) 450 mA, (*b*, *c* and *d*) 300 mA and (*e*) 100 mA. Adapted from Ref. [190].

comparable conditions in a three-electrode cell [176]. The constant generation of this oxidant at constant E_{cat} can also explain the decay in k_1 with increasing Reactive Red 120 [174] and Reactive Black 5 [175] concentrations from 20 to 100 mg dm^{-3} using a similar three-electrode divided Pt/carbon felt cell (see Table 5). In contrast, Direct Orange 61 was more efficiently mineralized as its concentration raised, obtaining the quickest degradation rate for 0.53 mM at 250 mA with 98% TOC removal in 6 h [177]. This effect can be simply related to the quicker reaction of greater amount of •OH with organic pollutants in detrimental of its parasite reactions.

Recently, the Oturan's group has demonstrated that the EF treatment of 250 cm^3 of 0.5 mM Malachite Green with 0.2 mM Fe^{3+} or Fe^{2+} as catalyst at pH 3.0 yielded total color removal in 22 min and overall mineralization in 9 h using the two-electrode cell of Fig. 25a at 200 mA [178]. The decay of this dye followed pseudo-first-order kinetics and its k_1 value increased from 1.7×10^{-3} to 4.0×10^{-3} s^{-1}, when the current varied from 60 to 200 mA, as expected by the faster production of •OH from Fenton's reaction (55) due to the enhancement of H_2O_2 electrogeneration via reaction (50). Analysis of treated solutions allowed detecting aromatic intermediates such as 4-dimethylaminobenzophenone, 4-aminophenol, benzoic acid, 4-aminobenzoic acid, 4-nitrocatechol and quinones, which are oxidized to final carboxylic acids such as oxalic, maleic, fumaric, glycolic and formic, with release of NO_3^-, NO_2^- and NH_4^+ ions.

Similar effects of current and catalytic Fe^{2+} and dye concentrations have been reported by other authors. For example, Wang et al. [180] studied the EF treatment of 500 cm^3 of O_2-saturated solutions with 200 mg dm^{-3} of the azo dye Acid Red 14 and different Fe^{2+} contents in 0.05 M Na_2SO_4 of pH 3.0 using an undivided RuO_2/ACF cell at constant current. After 6 h of electrolysis at 500 mA in the presence of 1.0 mM Fe^{2+}, complete decolorization and 73% TOC removal were determined. TOC decay gradually increased with raising current from 120 to 500 mA and Fe^{2+} concentration up to 1.0 mM, but mineralization was decelerated at greater Fe^{2+} contents due to the higher consumption of •OH from reaction (60). Zhou et al. [184,185] analyzed the EF process of 100 cm^3 of Methyl Red solutions with the three-electrode Pt/graphite-PTFE cell of Fig. 25b with electrodes of 1 cm^2 area, concluding that the best performance takes place for 0.1 M Na_2SO_4, 0.2 mM Fe^{2+}, pH 3.0 and E_{cat} = −0.55 V vs. SCE. Under these optimum conditions, a solution with 20 mg dm^{-3} of the dye became colorless in 20 min, whereas at higher concentration of 100 mg dm^{-3} only

Table 5
Pseudo-first-order and absolute second-order rate constants determined for the reaction of synthetic organic dyes with homogeneous •OH formed during the electro-Fenton process in sulphuric acid solutions of pH 3 using two- and three-electrode Pt/carbon felt cells.

Dye[a]	C_0/mM	Treated solution	Current/mA	E_{cat}[b]/V vs. SCE	$k_1 \times 10^3/s^{-1}$	$k_2 \times 10^{-10}$/ M^{-1} s^{-1}	Ref.
Undivided cell							
Acid Red 2 (Methyl Red)	0.04	110 cm^3, 0.5 mM Fe^{3+}, room temperature		−0.50	7.0	–[c]	[1]
Acid Orange 52 (Methyl Orange)	0.10				4.2		
(Yellow Drimaren)	0.25	125 cm^3, 0.5 mM Fe^{3+}, room temperature		−0.50	2.3	1.4	[176]
Direct Red 28 (Congo Red)	0.25				0.92	0.55	
Basic Blue 9 (Methylene Blue)	0.25				0.40	0.24	
Direct Orange 61	0.05	500 cm^3, 0.05 M Na_2SO_4 and 0.1 mM Fe^{2+}, room temperature	60		5.0	2.1	[177]
Basic Green 4 (Malachite Green)	0.50	250 cm^3, 0.05 M Na_2SO_4 and 0.2 mM Fe^{2+}, room temperature	60		1.7	–[c]	[178]
			200		4.0	–[c]	
Divided cell							
Reactive Red 120	20[d]	250 cm^3, 0.04 mM Fe^{2+}, 30 °C		−0.55	3.3	–[c]	[174]
	100[d]	250 cm^3, 0.20 mM Fe^{2+}, 30 °C			0.97	–[c]	
Reactive Black 5	20[d]	250 cm^3, 0.07 mM Fe^{2+}, 30 °C		−0.55	3.1	–[c]	[175]
	100[d]	250 cm^3, 0.35 mM Fe^{2+}, 30 °C			0.32	–[c]	

[a] Color index (common) name.
[b] Cathode potential.
[c] Not determined.
[d] Initial concentration in mg dm^{-3}.

Table 6
Percentage of color removal and TOC decay for the electro-Fenton treatment of synthetic organic dyes in sulphuric acid solutions with 0.05–0.10 M Na_2SO_4 of pH 3 using different two- and three-electrode undivided cells.

Dye[a]	C_0/mg dm^{-3}	Treated solution	Current/mA	Electrolysis time/h	Color removal/%	TOC decay/%	Ref.
Pt/carbon felt cell							
Direct Orange 61	0.53[b]	500 cm^3, 0.1 mM Fe^{2+}, room temperature	250	6	100	98	[177]
Basic Green 4 (Malachite Green)	0.50[b]	250 cm^3, 0.2 mM Fe^{2+}, room temperature	200	9	100	100	[178]
Acid Orange 7 (Orange II)	0.02[b]	200 cm^3, 0.1 mM Fe^{3+}, room temperature	−0.50[c]	2	97	–[d]	[179]
Graphite cloth/graphite cloth cell							
Acid Orange 7 (Orange II)	50	400 cm^3, 0.2 mM Fe^{2+}, room temperature	300[e]	1	100	63	[183]
Pt/graphite–PTFE cell							
Acid Red 2 (Methyl Red)	20	100 cm^3, 0.2 mM Fe^{2+}, room temperature	−0.55[c]	0.33	100	–[d]	[184]
	100				74	–[d]	
Pt/O_2 diffusion cell							
Acid Blue 64 (Indigo Carmine)	220	100 cm^3, 1.0 mM Fe^{2+}, 35 °C	100	9	100	49	[187]
BDD/O_2 diffusion cell							
Acid Blue 64 (Indigo Carmine)	220	100 cm^3, 1.0 mM Fe^{2+}, 35 °C	100	13	100	100	[187]
RuO_2/ACF cell							
Acid Red 14	200	500 cm^3, 1.0 mM Fe^{2+}, room temperature	500	6	100	73	[180]

[a] Color index (common) name.
[b] mM concentration.
[c] Cathode potential (V vs. SCE).
[d] Not determined.
[e] Cathodic current density (mA cm^{-2}).

74% color removal was attained at the same time. Daneshvar et al. [179] showed that the rate in color removal of 0.02 mM Orange II solutions with 0.1 mM Fe^{3+} in 0.050 M $NaClO_4$, Na_2SO_4 or NaCl at pH 3.0 and E_{cat} = −0.50 V vs. SCE using a Pt/carbon felt cell like in Fig. 25b is also affected by the anion of the electrolyte. The decolorization efficiency decreased in the sequence $ClO_4^- > Cl^- > SO_4^{2-}$, which was explained by the formation of chloro- or sulphate-complexes with Fe(II) that decreases the free Fe^{2+} concentration in the bulk and consequently inhibits Fenton's reaction (55).

The influence of the anode on the oxidation power of EF in undivided cells has been evidenced by Flox et al. [187] when studying the comparative treatment of 100 cm^3 of acidic aqueous solutions containing up to 0.9 g dm^{-3} of Indigo Carmine with the Pt/O_2 and BDD/O_2 cells of Fig. 25c. As can be seen in Fig. 29a, the application of this method in the Pt/O_2 cell at 100 mA provides partial mineralization of 100 mg dm^{-3} of the dye with 1.0 mM Fe^{2+} at pH 3.0, only reaching 49% TOC decay in 9 h. In contrast, the same solution treated in the BDD/O_2 cell yields 91% TOC reduction at this time and complete decontamination with loss of NH_4^+ at 13 h. This procedure gave similar degradation rate in the pH range 2.0–4.0, which increased with increasing current and initial dye content. Indigo Carmine always followed a pseudo-zero-order decay and disappeared at the same time as its identified aromatic derivatives isatin 5-sulphonic acid, indigo and isatin. Kinetic results corroborated the destruction of the dye and its aromatic intermediates mainly by $^{\bullet}OH$ formed in the bulk from Fenton's reaction (55). Oxalic and oxamic acids were detected as the most persistent carboxylic acids, present in the medium in the form of Fe(III)–oxalate and Fe(III)–oxamate complexes [189]. Fig. 29b and c show a slow reaction of both complexes with heterogeneous Pt($^{\bullet}OH$) and homogeneous $^{\bullet}OH$ generated in the Pt/O_2 cell by reactions (25) and (55), respectively, whereas they are very quickly destroyed with heterogeneous BDD($^{\bullet}OH$) in the BDD/cell up to total removal. The much greater ability of BDD($^{\bullet}OH$) than Pt($^{\bullet}OH$) to oxidize final Fe(III) complexes then explains the feasibility of achieving faster and overall mineralization in EF with a BDD anode.

5.3. Other indirect electrochemical techniques

Several attempts have been made to check other novel mediated electro-oxidation methods for dyestuffs removal. In this scenario it is noticeable the catalytic use of the Co^{3+}/Co^{2+} system to form homogeneous $^{\bullet}OH$ from electrogenerated H_2O_2 by the Fenton-like reaction [191]:

$$Co^{2+} + H_2O_2 \rightarrow Co^{3+} + {}^{\bullet}OH + OH^- \quad (64)$$

This electro-Fenton like "electro Co^{2+}–H_2O_2 system" was tested with a stirred three-electrode undivided Pt/graphite cell, similar to that of Fig. 25b, containing 50 cm^3 of an air-saturated solution with 0.1 mM of the xanthene dye Bromopyrogallol Red with $CoSO_4$ as catalyst in 0.2 M phosphate buffer solution [192]. Under optimized conditions of pH 4.0, 0.1 mM Co^{2+} and E_{cat} = −0.75 V vs. SCE, color was completely removed in 10 min and the initial COD of 3320 mg dm^{-3} was reduced by 96% in 30 min. It was also found that this electro-Fenton like "electro Co^{2+}–H_2O_2 system" possessed about 10 times higher oxidation ability than its comparable EF treatment with 3.0 mM Fe^{2+}. This was associated with the stronger catalytic activity of Co^{2+} towards the decomposition of H_2O_2 from reaction (64) than Fe^{2+} from reaction (55). However, an excessive Fe^{2+} concentration in EF was used leading to a loss of $^{\bullet}OH$ via reaction (60). A recent study of Pimentel et al. [193] on the EF degradation of 330 cm^3 of 0.33 mM phenol solutions with 0.1 mM Fe^{2+} or 0.1 mM Co^{2+} in 0.05 M Na_2SO_4 of pH 3.0 using an undivided Pt/carbon felt cell like of Fig. 25a has shown that both ions yield similar TOC reduction of 80 and 78%, respectively, after 4 h of electrolysis at 100 mA.

On the other hand, the decolorization of dyes Rhodamine B, Methyl Orange and Chicago Sky Blue in an aqueous KCl effluent has been studied at lab scale in a cylindrical flow cell equipped with two stainless steel rings of 6 and 53 mm diameter, respectively, and 50 mm length under generation of a pulsed streamer corona discharge with 0–30 kV voltage amplitude, 25 Hz pulse frequency and 6 nF capacitance [194]. This causes the production of ROS such as $^{\bullet}OH$, $^{\bullet}O$, H_2O_2, etc., being the oxidation process strongly

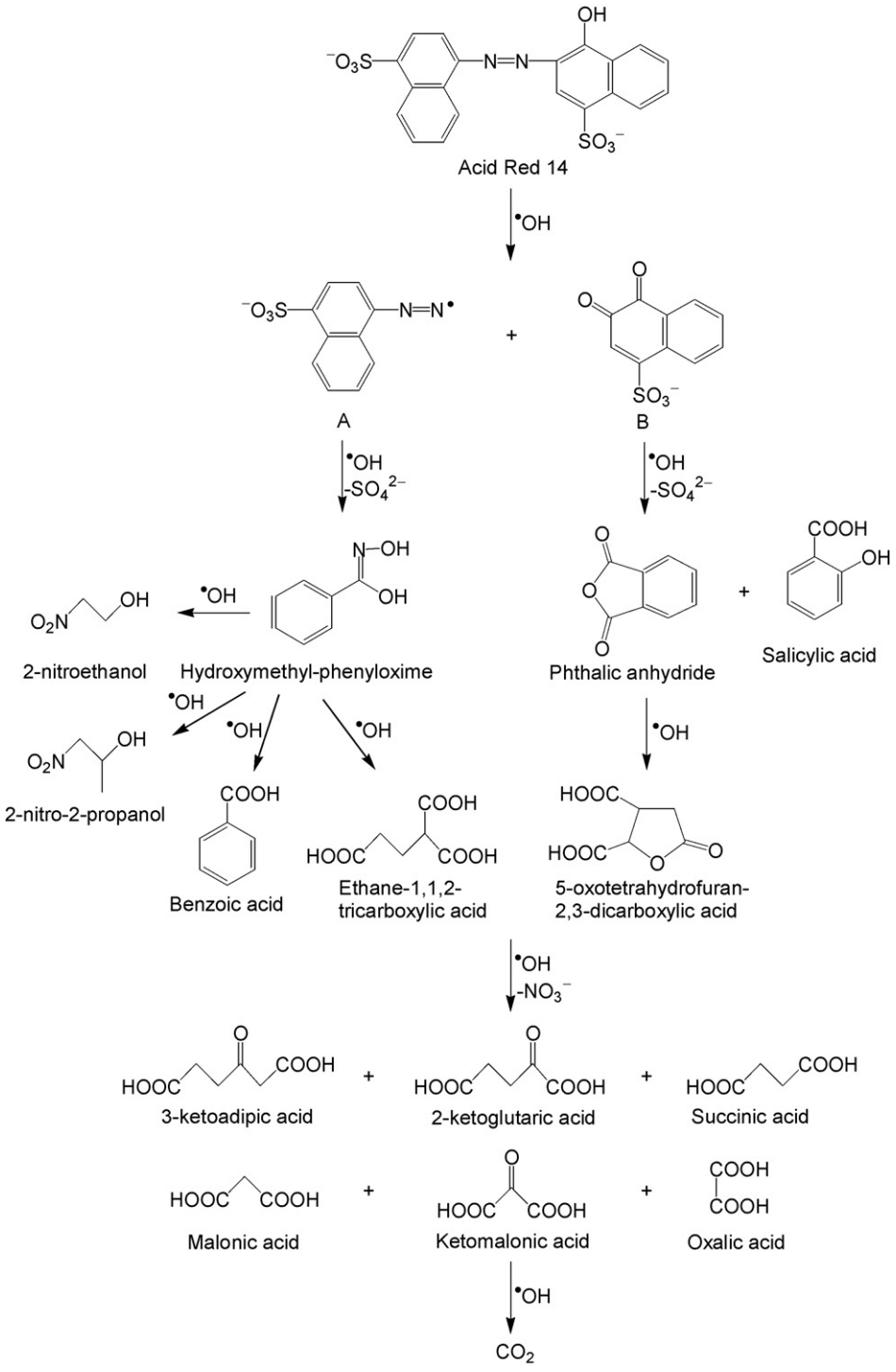

Fig. 27. Proposed reaction sequence for the degradation of the azo dye Acid Red 14 by electro-Fenton. Adapted from Ref. [186].

enhanced by addition of H_2O_2 in acidic medium. The quickest color removal for 300 cm^3 of 0.01 g dm^{-3} of the above dyes in the presence of 0.88 mM H_2O_2 at liquid flow rate of 100 cm^3 min^{-1} was obtained at pH 3.5 and 20 kV of voltage amplitude, leading to 98% decolorization efficiency in 60 min. The main disadvantage of this procedure is the excessive energy requirements for its application at industrial scale. Similar high operational costs have been reported for a dielectric barrier discharge reactor composed of a quartz cylinder and a coaxial steel rod that generates ozone and UV light at high voltage of 20–30 kV [195]. This system can totally decolorize Acid Red 27 wastewaters of pH 3.0 in the presence of H_2O_2.

6. Photoassisted electrochemical methods

Photoassisted AOPs based on the photochemical and/or photocatalytic action of UV irradiation have also received increasing interest for wastewater remediation [39,196]. In these procedures the intensity and wavelength of the incident light play a notable role on the destruction rate of organic pollutants. The use

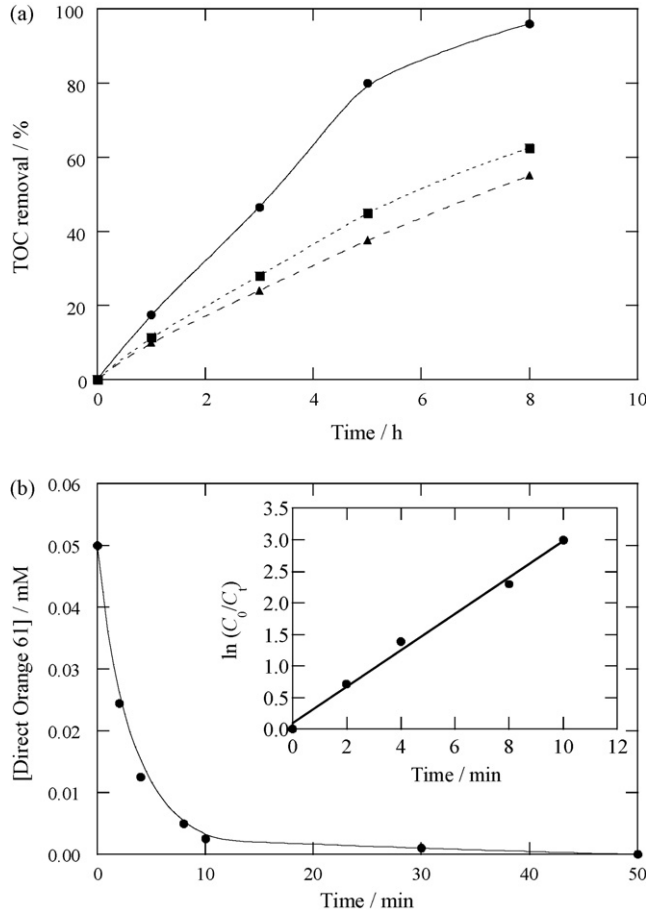

Fig. 28. (a) Influence of Fe^{2+} concentration on TOC removal for 500 cm^3 of 1.0 mM Direct Orange 61 solutions in 0.05 M Na_2SO_4 of pH 3.0 treated by electro-Fenton with the undivided cell of Fig. 25a with a 5.5 cm^2 Pt sheet as anode and a 60 cm^2 carbon felt piece as cathode at 100 mA and room temperature. Initial Fe^{2+} content: (●) 0.1 mM, (■) 0.2 mM and (▲) 0.5 mM. (b) Decay kinetics for a 0.050 mM dye solution with 0.1 mM Fe^{2+} at 60 mA. The inset plot gives the kinetic analysis considering that Direct Orange 61 follows a pseudo-first-order reaction. Adapted from Ref. [177].

of UVA (315–400 nm), UVB (285–315 nm) and UVC (<285 nm) lights as energy sources is commonly distinguished to explain the degradation processes involved in them [107,197]. Photo-Fenton (H_2O_2/Fe^{2+}/UV system) and heterogeneous TiO_2 photocatalysis (TiO_2/UV system) are considered the most promising photoassisted AOPs. From these technologies, two emerging photoassisted electrochemical approaches have been proposed [39,101,196]:

(i) The PEF method, in which the contaminated solution treated under electro-Fenton conditions is exposed to UV illumination favouring the generation of homogeneous •OH and the photodegradation of complexes of Fe(III) with organics.
(ii) The photoelectrocatalytic method, where a TiO_2-based thin film anode is irradiated with an UV light to produce electron excitation and positively charges holes, which can oxidize organics and water giving heterogeneous •OH. The constant current density or bias potential applied to the semiconductor electrode promotes the efficient separation of electron–hole pairs from electron transfer by an external circuit and accelerates the production of holes and heterogeneous •OH as oxidizing species.

The major disadvantage of photoassisted systems is the excessive energy cost of artificial UV light used. This can be solved

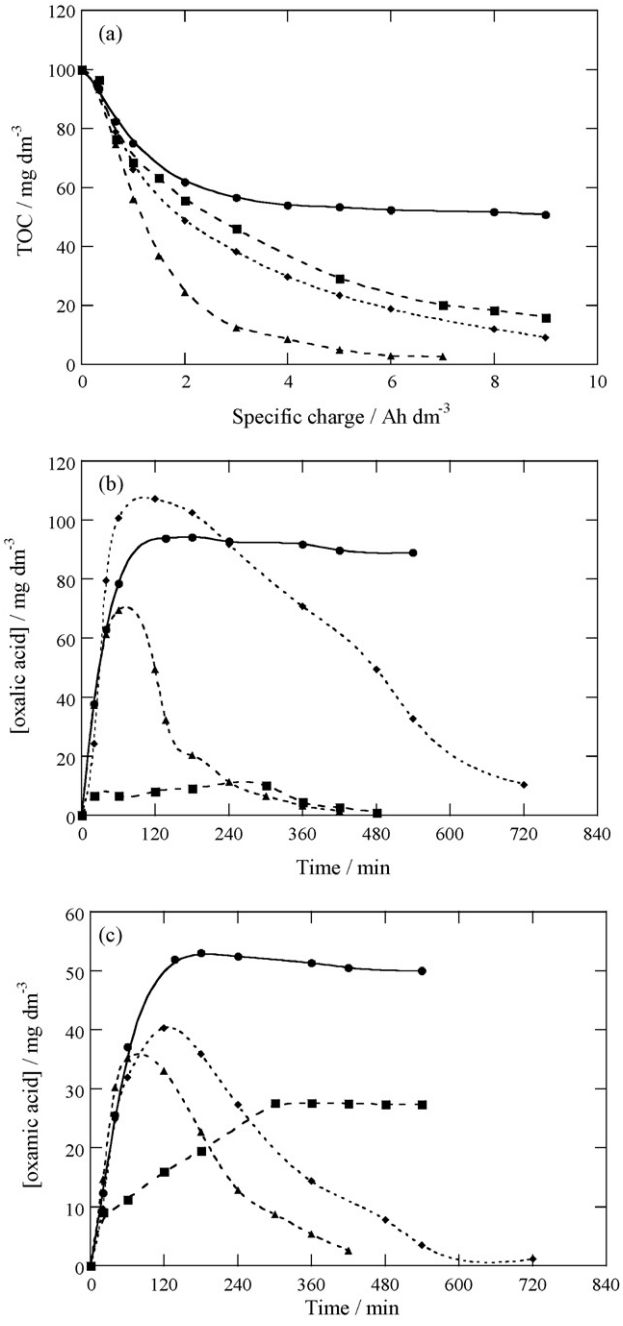

Fig. 29. (a) Dependence of TOC on specific charge and evolution of the concentration of (b) oxalic and (c) oxamic acids during the mineralization of 100 cm^3 of 220 mg dm^{-3} Indigo Carmine solutions in 0.05 M Na_2SO_4 of pH 3.0 at 100 mA and 35 °C using the Pt/O_2 or BDD/O_2 cell of Fig. 25c with electrodes of 3 cm^2 area. (●) Electro-Fenton with Pt and 1.0 mM Fe^{2+}; (■) photoelectro-Fenton with Pt and 1.0 mM Fe^{2+}; (◆) electro-Fenton with BDD and 1.0 mM Fe^{2+}; (▲) photoelectro-Fenton with Pt and 1.0 mM Fe^{2+} + 0.25 mM Cu^{2+}. Adapted from Ref. [187].

by means of alternative and more attractive methods based on sunlight ($\lambda > 300$ nm) as inexpensive energy source, which are expected to be rapidly developed in the next future [198,199].

Recent research on removing dyes by PEF [174,175,183,187,196] and photoelectrocatalysis [101,107,108,112,119,132,197,200–204] has demonstrated their better performance than the corresponding EF and EO treatments, respectively. This can be deduced from comparison of data of Tables 2 and 6 with those of Table 7, which collects selected results for the above photoassisted electrochemical methods. Coupling treatments of

Table 7
Percentage of color removal and TOC decay determined for removing synthetic organic dyes from wastewaters under several photoelectro-Fenton and photoelectrocatalytic conditions.

Dye[a]	C_0/mg dm^{-3}	Experimental conditions	j[b]/mA cm^{-2}	Color removal/%	TOC decay/%	Ref.
Photoelectro-Fenton						
Graphite cloth/graphite cloth cell						
Acid Orange 7 (Orange II)	50	400 cm^3, 0.05 M Na_2SO_4, 0.2 mM Fe^{2+}, pH 3.0, 75 mW cm^{-2} UVA light, 1 h	300	100	80	[183]
Pt/O_2 diffusion cell						
Acid Blue 64 (Indigo Carmine)	220	100 cm^3, 0.05 M Na_2SO_4, 1.0 mM Fe^{2+}, pH 3.0, 35 °C, 6 W UVA light, 9 h	33.3	100	84	[187]
	220	Addition of 0.25 mM Cu^{2+}, 7 h	33.3	100	>97	
Photoelectrocatalysis						
Ti/TiO_2 anode						
Reactive Blue 4	0.05[c]	50 cm^3, 0.01 M Na_2SO_4, pH 12, 450 W UVA light, 1 h	1.0[d]	100	37	[101]
Reactive Orange 16 (Remazol Brilliant Orange 3R)	0.04[c]	50 cm^3, 450 W UVA light, 3 h				[201]
		0.5 M Na_2SO_4, pH 12.0	1.0[e]	100	56	
		0.5 M NaCl, pH 4.0	1.0[e]	100	62	
Acid Orange 52 (Methyl Orange)	10	120 cm^3, 0.1 M NaCl, 40 °C, 2 h				[197]
		100 W UVA light	1.0[d]	93	–[f]	
		300 W tungsten halogen lamp	1.0[d]	94	–[f]	
Ti/$Ru_{0.3}Ti_{0.7}O_2$ anode						
Reactive Red 198	30	0.02 M Na_2SO_4, pH 5.7, 30 °C, 250 W UVC light, 3 h	50	100	63	[132]
Direct Red 81	0.1[c]	60 cm^3, 0.1 M $NaClO_4$, pH 7.0, 60 °C, 18 W UVC light, 3 h	25	100	74	[107]
Direct Black 36	0.1[c]	the same at pH 8.5	25	62	0	
Acid Violet 1	0.1[c]	the same at pH 7.0	25	100	57	[112]

[a] Color index (common) name.
[b] Applied current density.
[c] mM concentration.
[d] Anode potential (V vs. Ag/AgCl).
[e] Anode potential (V vs. SCE).
[f] Not determined.

EF with photoelectrocatalysis [196,204] and TiO_2 photocatalysis with indirect electro-oxidation with active chlorine [205] have also been reported. The main characteristics of photoassisted techniques are described below.

6.1. Photoelectro-Fenton method

This EAOP consists in the simultaneous use of electrogenerated H_2O_2 in the presence of Fe^{2+} (EF conditions) and UV illumination of the solution to mineralize dyes. The degradation action of UVA irradiation can be accounted for by: (i) greater regeneration of Fe^{2+} and production of homogeneous $^{\bullet}OH$ from photoreduction of $Fe(OH)^{2+}$, the predominant Fe^{3+} species in acid medium [167], by photo-Fenton reaction (65) and/or (ii) photodecarboxylation of complexes of Fe(III) with generated carboxylic acids, as shown in reaction (66) for Fe(III)–oxalate complexes ($Fe(C_2O_4)^+$, $Fe(C_2O_4)_2^-$ and $Fe(C_2O_4)_3^{3-}$) [189]:

$$Fe(OH)^{2+} + h\nu \rightarrow Fe^{2+} + {}^{\bullet}OH \quad (65)$$

$$2Fe(C_2O_4)_n^{(3-2n)} + h\nu \rightarrow 2Fe^{2+} + (2n-1)C_2O_4^{2-} + 2CO_2 \quad (66)$$

The effectiveness of photo-Fenton reaction (65) for regenerating Fe^{2+} and thus accelerating H_2O_2 decomposition from Fenton's reaction (55) can be observed in Fig. 26b, since the steady concentration of this species in curve *c* under EF conditions at 300 mA falls to the value of curve *d* when a 6 W UVA light illuminates the 0.05 M Na_2SO_4 solution of pH 3.0 in a Pt/O_2 diffusion cell [190]. In contrast, if the solution is exposed to a more energetic UVC irradiation, direct photochemical degradation of organics, along with much faster photolysis of electrogenerated H_2O_2 to homogeneous $^{\bullet}OH$ via reaction (67), are also feasible [39].

$$H_2O_2 + h\nu \rightarrow 2{}^{\bullet}OH \quad (67)$$

The comparative EF and PEF treatments of Reactive Red 120 and Reactive Black 5 have been reported by Kusvuran et al. [174,175]. Both EAOPs were tested with 250 cm^3 of O_2-saturated solutions containing 20–100 mg dm^{-3} of each azo dye and a threefold mM Fe^{2+} content at pH 3.0 in the cathodic compartment of a three-electrode divided cell equipped with a Pt gauze anode and a 15 cm^2 carbon felt cathode. Hydrogen peroxide was produced at $E_{cat} = -0.55$ V vs. SCE and an UVC lamp of $\lambda_{max} = 254$ nm was used in PEF. The decolorization process in EF followed a pseudo-first kinetics and its rate decreased as dye concentration increased (see Table 5) since the same quantity of oxidant $^{\bullet}OH$ is produced from Fenton's reaction (55) in all cases. After 30 min of this treatment, overall decolorization was found for 20 mg dm^{-3} of both dyes, but only about 80–85% color removal was attained for 100 mg dm^{-3}. The PEF process always provided a quicker decolorization, mainly by the generation of more homogeneous $^{\bullet}OH$ via reactions (65) and (67). However, a very small TOC decay of ca. 20% was obtained for 100 mg dm^{-3} of both dyes in 3 h of EF, which only raised up to ca. 29% using PEF. Toxicity measurements showed that solutions degraded for 90 min by EF and PEF can be disposed safely to environment because of the low toxicity of by-products formed.

A much efficient PEF process has been described for Orange II by Peralta-Hernández et al. [183] when treated 400 cm^3 of a 50 mg dm^{-3} solution of this azo dye containing 0.2 mM Fe^{2+} in

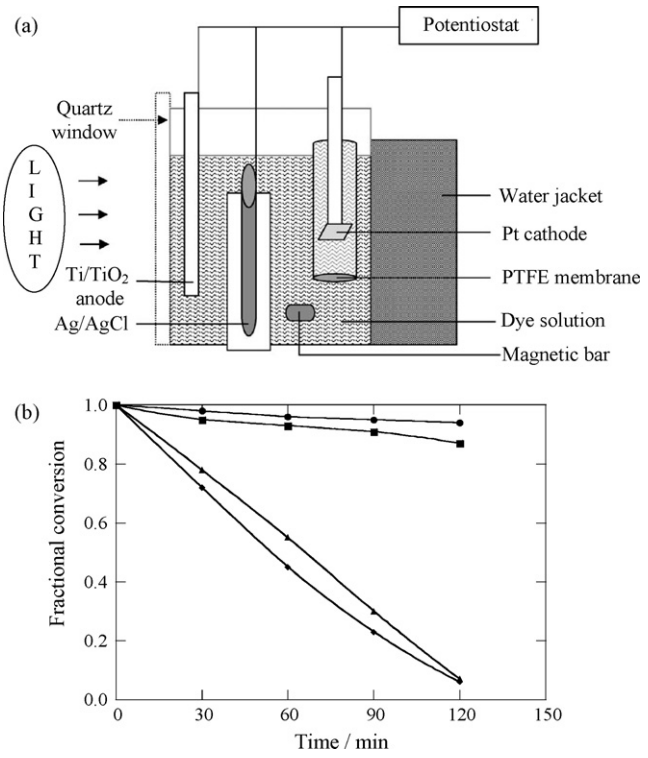

Fig. 30. (a) Sketch of the photoelectrochemical system with a stirred three-electrode two-compartment tank reactor utilized for the photoelectrocatalytic decolorization of Methyl Orange. The anode was a 5 cm × 2 cm plate of Ti coated with TiO_2, the cathode was a 1 cm^2 Pt sheet and the light source was placed 8 cm away from the sample. (b) Fractional conversion for 120 cm^3 of a 10 mg dm^{-3} Methyl Orange solution in 0.1 M NaCl at E_{anod} = 1.0 V vs. Ag/AgCl and 40 °C under illumination with a (●) 50 W tungsten halogen lamp, (■) 30 W fluorescent lamp, (▲) 100 W UVA lamp and (◆) 300 W tungsten halogen lamp. Adapted from Ref. [197].

0.05 M Na_2SO_4 at pH 3.0 using a concentric annular undivided graphite cloth/graphite cloth flow reactor with 164 cm^2 cathode area at 300 mA cm^{-2} and liquid flow rate of 100 cm^3 min^{-1} in batch operation mode. The PEF treatment was performed with a central 75 mW cm^{-2} UVA lamp of λ_{max} = 360 nm under O_2-bubbling for H_2O_2 electrogeneration, leading to complete decolorization in less than 5 min and 80% TOC removal in 1 h due to the great generation of homogeneous $^{\bullet}OH$ from Fenton's reaction (55) and photo-Fenton reaction (65). Similar decolorization rate, but a smaller TOC decay of 63%, was found for the EF system under comparable conditions.

Following the EF degradation of Indigo Carmine in a Pt/O_2 diffusion cell described in Section 5.2.3, Brillas and co-workers [187] considered its PEF treatment by irradiating the 100 cm^3 dyeing solution with a 6 W UVA light of λ_{max} = 360 nm. As illustrated in Fig. 29a for 220 mg dm^{-3} of the dye and 1.0 mM Fe^{2+} at 100 mA, this procedure yielded 84% TOC removal after consumption of 9 Ah dm^{-3} in 9 h, much higher than 49% obtained in EF. HPLC analysis of the ultimate oxalic (see Fig. 29b) and oxamic (see Fig. 29c) acids in PEF showed complete disappearance of the former at 9 h, whereas a steady concentration of the latter remained in solution. The highest mineralization of this EAOP was associated with the quick photolysis of Fe(III)–oxalate complexes by UVA irradiation from reaction (66). However, this method was unable to provide total decontamination because of the large stability of Fe(III)–oxamate complexes formed. A further attempt was made for increasing its oxidation power by adding Cu^{2+} as co-catalyst. The Cu^{2+}/Cu^{+} system is also catalytic involving the reduction of Cu^{2+} to Cu^{+} with $HO_2^{\bullet}$ by reaction (68) and/or with organic radicals $R^{\bullet}$ by reaction (69), followed by regeneration of Cu^{2+} by oxidation of Cu^{+} with H_2O_2 giving homogeneous $^{\bullet}OH$ from the Fenton-like reaction (70) [206]:

$$Cu^{2+} + HO_2^{\bullet} \rightarrow Cu^{+} + H^{+} + O_{2(g)} \quad (68)$$

$$Cu^{2+} + R^{\bullet} \rightarrow Cu^{+} + R^{+} \quad (69)$$

$$Cu^{+} + H_2O_2 \rightarrow Cu^{2+} + {}^{\bullet}OH + OH^{-} \quad (70)$$

Surprisingly, it was found that the PEF treatment with Pt and 1.0 mM Fe^{2+} and 0.25 mM Cu^{2+} as co-catalysts allowed almost total mineralization (>97% TOC removal) at about Q = 7 Ah dm^{-3} (see Fig. 29a) owing to a much faster and complete destruction of both oxalic and oxamic acids (see Fig. 29b and c). This synergistic behaviour of Fe^{2+} and Cu^{2+} was related to the simultaneous photolysis of Fe(III)–oxalate and mineralization of competitively formed Cu(II)–oxalate and Cu(II)–oxamate complexes with homogeneous $^{\bullet}OH$. This work opens the doors to the search of other co-catalysts with ability to enhance the mineralization rate of dyes in PEF.

6.2. Photoelectrocatalysis

The nanocrystalline from anatase of TiO_2 is a semiconductor material extensively utilized in photocatalysis for light-induced oxidation of organic pollutants in wastewaters. It possesses very attractive properties for this application such as low cost, low toxicity and a wide band gap of 3.2 eV, which results in good stability and prevents photo-corrosion [204]. Photocatalysis involves the irradiation of anatase TiO_2 nanoparticles in colloidal suspension or deposited as a thin film on Ti by UV photons of sufficient energy ($\lambda < 380$ nm) to promote an electron from the valence band to the conduction band (e_{CB}^{-}) generating a positively charged vacancy or hole (h_{VB}^{+}) as follows [196,204,207]:

$$TiO_2 + h\nu \rightarrow e_{CB}^{-} + h_{VB}^{+} \quad (71)$$

Organics can then be directly oxidized by the hole or by heterogeneous hydroxyl radical formed from the following reaction between the photogenerated vacancy and adsorbed water:

$$h_{VB}^{+} + H_2O \rightarrow {}^{\bullet}OH + H^{+} \quad (72)$$

In addition, other weaker ROS (superoxide radical ion $O_2^{\bullet -}$, $HO_2^{\bullet}$ and H_2O_2) and more $^{\bullet}OH$ can be produced from the photoinjected electron by the following reactions [196]:

$$e_{CB}^{-} + O_2 \rightarrow O_2^{\bullet -} \quad (73)$$

$$O_2^{\bullet -} + H^{+} \rightarrow HO_2^{\bullet} \quad (74)$$

$$2HO_2^{\bullet} \rightarrow H_2O_2 + O_2 \quad (75)$$

$$H_2O_2 + O_2^{\bullet -} \rightarrow {}^{\bullet}OH + OH^{-} + O_2 \quad (76)$$

The major loss in efficiency of photocatalysis is due to the recombination of electrons promoted to the valence band either with unreacted holes or with adsorbed hydroxyl radicals [204]:

$$e_{CB}^{-} + h_{VB}^{+} \rightarrow TiO_2 + \text{heat} \quad (77)$$

$$e_{CB}^{-} + {}^{\bullet}OH \rightarrow OH^{-} \quad (78)$$

The electrochemical technology can provide much higher efficiency for wastewater remediation by means of photoelectrocatalysis. This photoassisted method consists in the application of either a constant j or a constant bias anodic potential (E_{anod}) to a

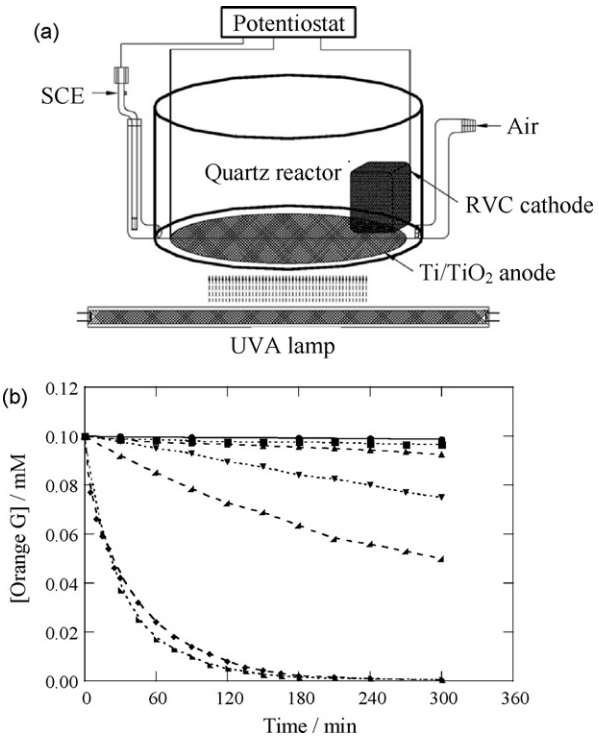

Fig. 31. (a) Experimental set-up of the aerated three-electrode undivided quartz cell with 5 cm^2 electrodes used for the photoassisted electrochemical oxidation of 30 cm^3 of a 0.1 mM Orange G solution in 0.01 M Na_2SO_4 of pH 6.2 with a 8 W UVA lamp of λ_{max} = 365 nm. In photoelectrocatalysis the bias potential applied to the Ti/TiO_2 anode was 0.71 V vs. SCE, while an E_{cat} of −0.54 or −0.71 V vs. SCE was applied to the reticulated vitreous carbon (RVC) for H_2O_2 electrogeneration. (b) Dye concentration decay from (●) direct photolysis, (■) electro-oxidation with a TiO_2/Pt cell, (▲) TiO_2 photocatalysis, (▼) photoelectrocatalysis with a TiO_2/Pt cell, (◢) photoelectrocatalysis with a TiO_2/RVC cell, (◆) photoelectro-Fenton with 17.6 mg dm^{-3} Fe^{2+} at pH 3.0 with a Fe/RVC cell and (◣) electro-Fenton coupled to photoelectrocatalysis with 17.2 mg dm^{-3} Fe^{2+} at pH 3.0 using a TiO_2/RVC cell. Adapted from Ref. [196].

TiO_2-based thin film anode subjected to UV illumination. In this scenario, the photoinduced electrons are continuously extracted from the anode by an external electrical circuit. This causes the inhibition of reactions (73)–(78) and favours the production of higher amount of holes from reaction (71) and heterogeneous •OH from reaction (72), thus largely enhancing organics oxidation in comparison to photocatalysis [196,200,204].

The electrochemical cells used in photoelectrocatalysis are tank or flow reactors that permit the pass of UV light through a quartz glass to reach the exposed surface of the TiO_2-based anode with the minimum loss of incident irradiation. Examples of systems and cells for treating synthetic organic dyes can be seen in Figs. 10a, 30a and 31a. The most typical photoanodes are Ti meshes or plates coated with TiO_2 [101,197,200,201] or Ti/$Ru_{0.3}Ti_{0.7}O_2$ [107,108,112,119,132]. The former is utilized in a three-electrode cell under potentiostatic conditions since it is stable at low current density, whereas the latter is a DSA-type material and its large stability at high j permits its use in two-electrode reactors. The decolorization efficiency and percentages of COD and/or TOC removals in this technique are also determined by means of Eqs. (9)–(11).

Carneiro et al. [101] evidenced the generation of strong oxidants in the photoelectrocatalysis of 50 cm^3 of a 0.05 mM Reactive Blue 4 solution in 0.01 M Na_2SO_4 of pH 12.0 filling the anodic compartment of a three-electrode divided cell containing a 10 cm^2 Ti/TiO_2 anode biased at E_{anod} = 1.0 V vs. Ag/AgCl. After 1 h of treatment, 20% decolorization efficiency was attained by EO, whereas 100% color removal was found when the anode was illuminated by a 450 W UVA light (incident irradiation of 50 mW cm^{-2}). Although the oxidation of organics was strongly enhanced under the latter conditions, TOC was only reduced by 37% as expected by the formation of intermediates that are hardly oxidized by holes and heterogeneous •OH. The same group reported an interesting influence of the supporting electrolyte on the photoelectrocatalysis of the azo dye Reactive Orange 16 as a function of solution pH [200,201]. These experiments were carried with 0.04–0.05 mM solutions of this dye in 0.025–0.5 M NaCl or Na_2SO_4 in the pH range 2.0–12.0 using the above photoelectrochemical cell at E_{anod} = 1.0 V vs. SCE. In all cases overall decolorization was obtained in approximately 20 min. However, faster degradation was determined at pH < 6.0 for chloride media and at pH > 10.0 for sulphate effluents. The superiority of NaCl in acidic media was ascribed to the large ability of the holes formed at the photoanode from reaction (71) to oxidize Cl^- to active chlorine species (Cl_2, HClO and ClO^-) and probably other radicals such as $Cl^•$ and $Cl_2^•$, which oxidize organics more quickly than heterogeneous •OH produced in Na_2SO_4 via reaction (72). The opposite trend in alkaline solutions was related to the strong inhibition of the generation of chlorinated oxidants from Cl^- decelerating the destruction of pollutants. After 3 h of photoelectrocatalysis of 0.04 mM Methyl Orange, 62 and 56% mineralization was achieved in 0.5 M NaCl at pH 4.0 and 0.5 M Na_2SO_4 at pH 12.0, respectively.

The effect of the light source and its intensity on the decolorization efficiency of Methyl Orange has been studied by Zainal et al. [197] using the photoelectrochemical reactor of Fig. 30a. Solutions of 120 cm^3 with 10 mg dm^{-3} of this azo dye in 0.1 M NaCl at 40 °C were treated under illumination of the 10 cm^2 Ti/TiO_2 anode by several UVA and visible lamps at an anodic bias potential of 1.0 V vs. SCE. Fig. 30b shows that at 2 h of photoelectrocatalysis only 6 and 13% fractional conversion was found for 50 W tungsten halogen and 30 W fluorescent lamps, respectively, whereas the increase in potency of the tungsten halogen lamp to 300 W leads to 94% color removal, slightly higher than 93% obtained for the 100 W UVA lamp. These findings evidence the production of more photons with suitable energy for electron excitation in TiO_2 by the UVA lamp, although they are generated in larger extent by the fluorescent lamp than the tungsten halogen one at similar intensity. An enhancement of dye decolorization is then expected at higher intensity since more significant amount of electron–hole pairs should be formed, as found when the potency of the tungsten halogen lamp rises from 50 to 300 W. The fractional conversion of the Methyl Orange solution only underwent a slight decrease after 20 runs of 2 h using the 300 W tungsten halogen lamp that induced a photocurrent of ca. 0.5 mA. This indicates that TiO_2 is a good anode material for removing dyes with a long lifetime at low E_{anod} and current values.

When a Ti/$Ru_{0.3}Ti_{0.7}O_2$ photoanode is employed, greater dyes concentrations can be treated because it permits the pass of higher current density with larger stability. For this electrode, comparative treatments by EO (see Section 4.3.2 and Table 2) and by photoelectrocatalysis (see Table 7) have been reported. Thus, Pelegrini et al. [119] found 15% color and 7.2% TOC decays after 2 h of direct exposition of 30 mg dm^{-3} Reactive Blue 19 solutions of pH 11.0 to a 500 W UVC irradiation in a quartz three-electrode cell. Photoelectrocatalysis with a 5 cm^2 Ti/$Ru_{0.3}Ti_{0.7}O_2$ anode at E_{anod} = 1.8 V vs. Ag/AgCl under the same irradiation gave 95% color removal and 52% TOC reduction at 2 h, much higher than 35% decolorization efficiency and 9.6% TOC removal obtained by EO under comparable conditions. The synergistic effect found in photoelectrocatalysis was related to the simultaneous formation of heterogeneous •OH on RuO_2 from water discharge by reaction (25) and on TiO_2 via reaction (72) owing to photogenerated holes by

reaction (71). A similar behaviour has been reported by Catanho et al. [132] when treating 30 mg dm^{-3} Reactive Red 198 solutions in 0.02 M Na_2SO_4 at pH 5.4 by photocatalysis, EO and photoelectrocatalysis using the two-electrode photoelectrochemical flow cell of Fig. 10a and a 250 W UVC light source at flow rate of 18 dm^3 h^{-1}. No significant effect of temperature between 20 and 45 °C on the three methods was found. In the j range 5–30 mA cm^{-2} the color and TOC removal rates in photoelectrocatalysis was simply the sum of the photocatalytic and electrochemical rates, but at higher j until 89 mA cm^{-2} they became much greater. The energy cost was thus reduced from 95×10^6 kWh (kg dye)$^{-1}$ for EO to 15×10^6 kWh (kg dye)$^{-1}$ for photoelectrocatalysis after 3 h of electrolysis at 50 mA cm^{-2}.

The influence of the light source on a Ti/$Ru_{0.3}Ti_{0.7}O_2$ photoanode has been clarified by Socha et al. [107,112] by comparing the EO and photoelectrocatalysis of azo dyes Direct Red 81, Direct Black 36 and Acid Violet 1. These trials were made with 60 cm^3 of 0.1 mM dyes solutions in 0.1 M $NaClO_4$ at pH 7.0–8.5 using a conventional divided cell with electrodes of 20 cm^2 area at 25 mA cm^{-2} and 60 °C for 3 h. Direct exposition of all solutions to 18 W UVC, UVB and UVA lamps during this time gave poor color (<12%) and TOC (<10%) decays. Complete decolorization of Direct Red 81 and Acid Violet 1 solutions under electrolysis was always found and their corresponding TOC was reduced by 74 and 57% in photoelectrocatalysis with UVC light, values higher than 61–65 and 32–36% determined for this method with UVB and UVA lights and for EO, respectively. In contrast, the Direct Black 5 effluent was not degraded, undergoing a weak decolorization of 62% by photoelectrocatalysis with UVC light and about 40% for the other treatments. These results evidence that coupled production of heterogeneous $^{\bullet}OH$ on RuO_2 and TiO_2 in a Ti/$Ru_{0.3}Ti_{0.7}O_2$ anode only takes place in large extent when it is irradiated with an UVC light, since smaller energetically photons supplied by UVB and UVA lights do not promote efficiently the formation of electron–hole pairs in the mixed oxide.

6.3. Coupled photoassisted treatments

An interesting study made by Xie and Li [196] has shown the superiority of coupling electro-Fenton with photoelectrocatalysis for removing the azo dye Orange G with respect to EO and other single photoassisted methods. Comparative experiments were performed with the quartz reactor of Fig. 31a for 5 h. The cell was filled with 30 cm^3 of 0.1 mM solution of the dye containing 0.01 M Na_2SO_4 at pH 6.2 and an 8 W UVA lamp was used as light source. Fig. 31b shows that Orange G is not directly photolyzed under UVA irradiation, being slightly destroyed in about 3% by EO with a TiO_2/Pt cell at E_{anod} = 0.71 V vs. SCE and in 8% by TiO_2 photocatalysis, as expected if small amounts of oxidizing species ($^{\bullet}OH$ and/or holes) are formed at the TiO_2 surface. Photoelectrocatalysis using the TiO_2/Pt cell enhances dye removal to 25% owing to the photogeneration of more amounts of oxidant holes by the pass of current. The oxidation power of this technique can be improved to yield 50% dye destruction if the Pt cathode is replaced by a RVC electrode at E_{cat} = −0.54 V vs. SCE since it is also oxidized with H_2O_2 produced from O_2 reduction via reaction (50). In contrast, Orange G disappears completely when applying photoelectro-Fenton with a Fe/RVC cell using ca. 17 mg dm^{-3} Fe^{2+}, pH 3.0 and E_{cat} = −0.71 V vs. SCE and its decolorization rate even slightly increases if electro-Fenton under the same conditions is coupled to photoelectrocatalysis with a TiO_2/RVC cell, as a result of the additional formation of large amounts of homogeneous $^{\bullet}OH$ from Fenton's reaction (55) and/or photo-Fenton reaction (65). The latter method also provided the greatest mineralization of 74% in 5 h. Peralta-Hernández et al. [204] also described a strong improvement of the decolorization efficiency and TOC removal of 250 cm^3 of O_2-saturated solutions with 2 mg dm^{-3} of the azo dye Direct Yellow 52 in 0.05 M Na_2SO_4 and 0.25 or 0.50 mM Fe^{2+} at pH 2.0 when treated by EF coupled to photoelectrocatalysis in comparison to single EF using a concentric annular undivided TiO_2/graphite cloth flow cell with a central 75 mW cm^{-2} UVA lamp in batch operation mode.

On the other hand, Neelavannan et al. [205] considered the treatment of 20 mg dm^{-3} of the azo dye Procion Blue in a flow plant composed of an electrochemical reactor with a Ti/RuO_2 anode and a stainless steel cathode, both of 40 cm^2 area, connected to a Ti thin film photoreactor of 5 cm diameter × 27 cm height irradiated by a 6 W UVA lamp. After 7 h of batch operation at flow rate of 20 cm^3 min^{-1}, the TOC of 1 dm^3 of an effluent with 3 g dm^{-3} NaCl at pH 2.0 was reduced by 20% from direct photolysis and by 84% from indirect electro-oxidation with active chlorine at 20 mA cm^{-2}. However, a greater increase to 96% mineralization was found when 40 mg dm^{-3} of anatase TiO_2 was suspended in the effluent and photocatalysis coupled to indirect electro-oxidation was applied under the same conditions. The former technique then produces high concentration of oxidants on the TiO_2 surface that accelerates the destruction of pollutants in competition with homogeneous active chlorine species formed in the latter.

7. Conclusions

Efficient methods for destroying synthetic organic dyes from wastewaters at lab and pilot plant scale have been recently developed from the electrochemical technology. The most suitable electrode materials and optimized experimental conditions have been established in most electrochemical techniques for different cell configurations. However, much more research efforts are needed to clarify the decolorization efficiency and degradation attained for a larger variety of dyestuffs to apply these methods to industrial level. EC has demonstrated to be an effective and economical technology for almost total decolorization of chloride dyes wastewaters either using Fe or Al anodes, although it yields poor decontamination owing to partial oxidation of pollutants with Fe^{2+} and/or active chlorine and desorption of by-products from the sludge formed. In the case of electrochemical reduction, cathode materials with higher degradation power are required before its acceptance as alternative for dyes treatment. In contrast, EO provides a simple, viable and promising EAOP for the remediation of chloride-free effluents of these pollutants. Highly stable anode materials such as PbO_2 and mainly BDD electrodes can yield total decolorization and mineralization of dyeing solutions because of the efficient mediated oxidation mainly with heterogeneous $^{\bullet}OH$ formed at water discharge potentials. Indirect electro-oxidation mediated by electrogenerated active chlorine allows overall color removal and high degradation degree for chloride dyes effluents, but its application can be limited by the production of undesirable toxic chlorinated by-products. EF is an attractive emerging EAOP yielding almost complete mineralization of these compounds by the action of additional homogeneous $^{\bullet}OH$ formed from Fenton's reaction between catalytic Fe^{2+} and H_2O_2 electrogenerated at a carbonaceous cathode. The enhancement of the degradation rate of this process when the solution is irradiated by UVA light in the PEF method is well recognized, although the possible synergistic role of other co-catalysts should be clarified. Photoelectrocatalysis with generation of holes and heterogeneous $^{\bullet}OH$ as oxidants at the surface of a TiO_2-based thin film photoanode under UV irradiation has lower ability for dyes destruction. While decolorization of these pollutants is fast in EO, indirect electro-oxidation with strong oxidants and photoassisted methods, their much slower degradation strongly increases the energy consump-

tion required for total mineralization. Research focused to the application of these methods to color removal and production of more biodegradable compounds as pre-treatment stage for biological post-treatment should be performed to propose more economical coupled methods. The alternative use of inexpensive and renewable sunlight in PEF and photoelectrocatalysis should also be investigated to make much more attractive photoassisted processes in practice.

References

[1] E. Guivarch, S. Trevin, C. Lahitte, M.A. Oturan, Environ. Chem. Lett. 1 (2003) 38–44.
[2] G.M. Walker, L.R. Weatherley, Sep. Sci. Technol. 35 (2000) 1329–1341.
[3] S. Raghu, C. Ahmed Basha, J. Hazard. Mater. 149 (2007) 324–330.
[4] O. Tünay, I. Kabdasli, D. Ohron, G. Cansever, Water Sci. Technol. 40 (1999) 237–244.
[5] R.A. Masoud, A.A. Haroun, N.H. El-Sayed, J. Appl. Polym. Sci. 101 (2006) 174–179.
[6] J. Liu, Paper Technol. 46 (2005) 31–36.
[7] A. Slampova, D. Smela, A. Vondrackova, I. Jancarova, V. Kuban, Chem. Listy 95 (2001) 163–168.
[8] S. Chaudhuri, K. Ray, U.R. Chaudhuri, R. Chakraborty, J. Food Sci. Technol. 41 (2004) 1–8.
[9] V.K. Gupta, R. Jain, S. Varshney, J. Hazard. Mater. 142 (2007) 443–448.
[10] R. Malik, D.S. Ramteke, S.R. Wate, Waste Manage. 27 (2007) 1129–1138.
[11] G.M. Hasselman, D.F. Watson, J.R. Stromberg, D.F. Bocian, D. Holten, J.S. Lindsey, G.J. Meyer, J. Phys. Chem. B 110 (2006) 25430–25440.
[12] D. Wrobel, A. Bogut, R.M. Ion, J. Photochem. Photobiol. A: Chem. 138 (2001) 7–22.
[13] R.J. Turesky, J.P. Freeman, R.D. Holland, D.M. Nestorick, D.W. Miller, D.L. Ratnasinghe, F.F. Kadlubar, Chem. Res. Toxicol. 16 (2003) 1162–1173.
[14] D. Orhon, S. Sözen, E. Görgün, E. Cokgör, N. Artan, Water Sci. Technol. 39 (1999) 177–184.
[15] N.M.H. El Defrawy, Int. J. Environ. Stud. 59 (2002) 573–587.
[16] M. Malaiyandi, N. Nehrukumar, Pollut. Res. 25 (2006) 339–342.
[17] M.S. Field, R.G. Wilhelm, J.F. Quinlan, T.J. Aley, Environ. Monit. Assess. 38 (1995) 75–97.
[18] D. Sabaliunas, S.F. Webb, A. Hauk, M. Jacob, W.S. Eckhoff, Water Res. 37 (2003) 3145–3154.
[19] E. Forgacs, T. Cserhati, G. Oros, Environ. Int. 30 (2004) 953–971.
[20] T. Robinson, G. McMullan, R. Marchant, P. Nigam, Bioresour. Technol. 77 (2001) 247–255.
[21] S.D. Desphande, Ind. J. Fibre Text. Res. 26 (2001) 136–142.
[22] G.A. Montero, C.B. Smith, W.A. Hendrix, D.L. Butcher, Ind. Eng. Chem. Res. 39 (2000) 4806–4812.
[23] S.S. Kumar, K. Joseph, J. Ind. Pollut. Control 22 (2006) 345–352.
[24] T. Platzek, C. Lang, G. Grohmann, U.S. Gi, W. Baltes, Human Exp. Toxicol. 18 (1999) 552–559.
[25] G. Oros, T. Cserhati, E. Forgacs, Fresen. Environ. Bull. 10 (2001) 319–322.
[26] S. Tsuda, M. Murakami, N. Matsusaka, K. Kano, K. Taniguchi, Y.F. Sasaki, Toxicol. Sci. 61 (2001) 92–99.
[27] A. Ahmad, M. Alam, Chem. Environ. Res. 12 (2003) 5–13.
[28] R. Mala, S.S. Babu, J. Ind. Pollut. Control 21 (2005) 315–320.
[29] K.P. Sharma, S. Sharma, S. Sharma, P.K. Singh, S. Kumar, R. Grover, P.K. Sharma, Chemosphere 69 (2007) 48–54.
[30] S.M.A.G. Ulson de Souza, E. Forgiarini, A.A. Ulson de Souza, J. Hazard. Mater. 147 (2007) 1073–1078.
[31] M.C. Gutierrez, M. Crespi, J. Soc. Dyes Col. 115 (1999) 342–345.
[32] O.J. Hao, H. Kim, P.C. Chiang, Crit. Rev. Environ. Sci. Technol. 30 (2000) 449–502.
[33] M.M. Naim, Y.M. El Abd, Sep. Purif. Methods 31 (2002) 171–228.
[34] A.B. dos Santos, F.J. Cervantes, J.B. van Lier, Bioresour. Technol. 98 (2007) 2369–2385.
[35] K. Rajeshwar, J.G. Ibanez, Fundamentals and Application in Pollution Abatement, Academic Press, San Diego, CA, 1997.
[36] D. Genders, N. Weinberg (Eds.), Electrochemistry for a Cleaner Environment, The Electrosynthesis Company Inc., New York, 1992.
[37] D. Pletcher, F.C. Walsh, Industrial Electrochemistry, 2nd ed., Blackie Academic & Professional, London, 1993.
[38] D. Simonson, Chem. Soc. Rev. 26 (1997) 181–189.
[39] E. Brillas, P.L. Cabot, J. Casado, in: M. Tarr (Ed.), Chemical Degradation Methods for Wastes and Pollutants Environmental and Industrial Applications, Marcel Dekker, New York, 2003, pp. 235–304.
[40] G. Chen, Sep. Purif. Technol. 38 (2004) 11–41.
[41] M. Panizza, G. Cerisola, Electrochim. Acta 51 (2005) 191–199.
[42] C.A. Martínez-Huitle, S. Ferro, Chem. Soc. Rev. 35 (2006) 1324–1340.
[43] A. Kraft, Int. J. Electrochem. Sci. 2 (2007) 355–385.
[44] C. Barrera-Díaz, F. Ureña-Nuñez, E. Campos, M. Palomar-Pardavé, M. Romero-Romo, Radiat. Phys. Chem. 67 (2003) 657–663.
[45] J. Gregory, J. Duan, Pure Appl. Chem. 73 (2001) 2017–2026.
[46] J.G. Ibanez, M.M. Singh, Z. Szafran, J. Chem. Educ. 75 (1998) 1040–1041.
[47] O.T. Can, M. Bayramoglu, M. Kobya, Ind. Eng. Chem. Res. 42 (2003) 3391–3396.
[48] N. Modirshahla, M.A. Behnajady, S. Kooshaiian, Dyes Pigments 74 (2007) 249–257.
[49] M.Y.A. Mollah, P. Morkovsky, J.A.G. Gomes, M. Kesmez, J. Parga, D.L. Cocke, J. Hazard. Mater. B114 (2004) 199–210.
[50] S.H. Lin, C.-F. Peng, Water Res. 28 (1994) 277–282.
[51] N. Daneshvar, A. Oladegaragoze, N. Djafarzadeh, J. Hazard. Mater. B129 (2006) 116–122.
[52] N. Daneshvar, A.R. Khataee, A.R. Amani Ghadim, M.H. Rasoulifard, J. Hazard. Mater. 148 (2007) 566–572.
[53] P. Cañizares, C. Jimenez, F. Martinez, C. Saez, M.A. Rodrigo, Ind. Eng. Chem. Res. 46 (2007) 6189–6195.
[54] A. Gurses, M. Yalcin, C. Dogar, Waste Manage. 22 (2002) 491–499.
[55] S.H. Lin, C.-F. Peng, Water Res. 30 (1996) 587–592.
[56] S.H. Lin, M.L. Chen, Water Res. 31 (1997) 868–876.
[57] K. Muthukumar, A. Arunagiri, N. Anantharaman, P. Shumugha, A.A. Sundaram Basha, J. Ind. Pollut. Control 19 (2003) 281–288.
[58] B. Griggs, Contaminant removal apparatus installation method, PCT WO Patent 2003/086981 A1 (2003).
[59] N. Daneshvar, H. Ashassi-Sorkhabi, M.B. Kasiri, J. Hazard. Mater. B112 (2004) 55–62.
[60] L. Szpyrkowicz, Ind. Eng. Chem. Res. 44 (2005) 7844–7853.
[61] P. Cañizares, F. Martinez, J. Lobato, M.A. Rodrigo, Ind. Eng. Chem. Res. 45 (2006) 3474–3480.
[62] E.-E. Chang, H.-J. Hsing, C.-S. Ko, P.-C. Chiang, J. Chem. Technol. Biotechnol. 82 (2007) 488–495.
[63] M.Y.A. Mollah, S.R. Pathak, P.K. Patil, M. Vayuvegula, T.S. Agrawal, J.A.G. Gomes, M. Kesmez, D.L. Cocke, J. Hazard. Mater. B109 (2004) 165–171.
[64] M. Kashefialasl, M. Khosravi, R. Marandi, K. Seyyedi, Int. J. Environ. Sci. Technol. 2 (2006) 365–371.
[65] I.A. Sengil, M. Oezacar, B. Oemuerlue, Chem. Biochem. Eng. Q. 18 (2004) 391–401.
[66] N. Daneshvar, H. Ashassi-Sorkhabi, A. Tizpar, Sep. Purif. Technol. 31 (2003) 153–162.
[67] A. Lopes, S. Martins, A. Morao, M. Magrinho, I. Goncalves, Port. Electrochim. Acta 22 (2004) 279–294.
[68] A.K. Golder, N. Hridaya, A.N. Samanta, S. Ray, J. Hazard. Mater. B127 (2005) 134–140.
[69] B.K. Körbahti, J. Hazard. Mater. 145 (2007) 277–286.
[70] P. Fongsatitkul, P. Elefsiniotis, B. Boonyanitchakul, J. Environ. Sci. Health A 41 (2006) 1183–1195.
[71] M. Muthukumar, M.T. Karuppiah, G.B. Raju, Sep. Purif. Technol. 55 (2007) 198–205.
[72] H.-J. Hsing, P.-C. Chiang, E.-E. Chang, M.-Y. Chen, J. Hazard. Mater. 141 (2007) 8–16.
[73] Y. Xiong, P.J. Strunk, H. Xia, X. Zhu, H.T. Karlsson, Water Res. 35 (2001) 4226–4230.
[74] S. Song, Z. He, J. Qiu, L. Xu, J. Chen, Sep. Purif. Technol. 55 (2007) 238–245.
[75] Q. Zhuo, H. Ma, B. Wang, L. Gu, J. Hazard. Mater. 142 (2007) 81–87.
[76] C.-H. Wu, C.-L. Chang, C.-Y. Kuo, Dyes Pigments 76 (2008) 187–194.
[77] A. Alinsafi, M. Khemis, M.N. Pons, J.P. Leclerc, A. Yaacoubi, A. Benhammou, A. Nejmeddine, Chem. Eng. Process. 44 (2005) 461–470.
[78] M. Kobya, E. Demirbas, O.T. Can, M. Bayramoglu, J. Hazard. Mater. B132 (2006) 183–188.
[79] T. Picard, G. Cathalifaud-Feuillade, M. Mazet, C. Vandensteendam, J. Environ. Monit. 2 (2000) 77–80.
[80] P. Cañizares, F. Martinez, C. Jimenez, J. Lobato, M.A. Rodrigo, Environ. Sci. Technol. 40 (2006) 6418–6424.
[81] L. Szpyrkowicz, Ann. Chim. -Rome 92 (2002) 1025–1034.
[82] G. Duca, M. Gonta, V. Matveevici, D. Porubin, O. Nistor, Environ. Eng. Manage. J. 3 (2004) 621–627.
[83] J.-S. Do, M.-L. Chen, J. Appl. Electrochem. 24 (1994) 785–790.
[84] T.-K. Kim, C. Park, E.-B. Shin, S. Kim, Desalination 150 (2002) 165–175.
[85] M. Bayramoglu, M. Kobya, O.T. Can, M. Sozbir, Sep. Purif. Technol. 37 (2004) 117–125.
[86] C.-L. Yang, J. McGarrahan, J. Hazard. Mater. B127 (2005) 40–47.
[87] R.Y. Amaresh, M. Arivazhagan, Chem. Eng. World 42 (2007) 86–90.
[88] R.Y. Amaresh, M. Arivazhagan, P. Sivashanmugham, Indian J. Environ. Protect. 27 (2007) 516–526.
[89] I. Kabdasli, I. Arslan-Alaton, B. Vardar, O. Tunay, Water Sci. Technol. 55 (2007) 125–134.
[90] L. Fan, Y. Zhou, W. Yang, G. Chen, F. Yang, J. Hazard. Mater. B137 (2006) 1182–1188.
[91] L. Fan, Y. Zhou, W. Yang, G. Chen, F. Yang, Dyes Pigments 76 (2008) 440–446.
[92] R. Jain, M. Bhargava, N. Sharma, Ind. Eng. Chem. Res. 42 (2003) 243–247.
[93] R. Jain, S. Varshney, S. Sikarwar, J. Colloid Interf. Sci. 313 (2007) 248–253.
[94] P.A. Carneiro, C.S. Fugivara, R.F.P. Nogueira, N. Boralle, M.V.B. Zanoni, Port. Electrochim. Acta 21 (2003) 49–67.
[95] P.A. Carneiro, N. Boralle, N.R. Stradiotto, M. Furlan, M.V.B. Zanoni, J. Braz. Chem. Soc. 15 (2004) 587–594.
[96] Ch. Comninellis, Electrochim. Acta 39 (1994) 1857–1862.
[97] B. Marselli, J. Garcia-Gomez, P.A. Michaud, M.A. Rodrigo, Ch. Comninellis, J. Electrochem. Soc. 150 (2003) D79–D83.
[98] Z. Shen, W. Wang, J. Jia, J. Ye, X. Feng, A. Peng, J. Hazard. Mater. B84 (2001) 107–116.

[99] M.J. Pacheco, M.L.F. Ciríaco, A. Lopes, I.C. Gonçalves, M.R. Nunes, M.I. Pereira, Port. Electrochim. Acta 24 (2006) 273–282.
[100] Z.M. Shen, D. Wu, J. Yang, T. Yuan, W.H. Wang, J.P. Jia, J. Hazard. Mater. B131 (2006) 90–97.
[101] P.A. Carneiro, M.E. Osugi, C.S. Fugivara, N. Boralle, M. Furlan, M.V.B. Zanoni, Chemosphere 59 (2005) 431–439.
[102] C. Cameselle, M. Pazos, M.A. Sanromán, Chemosphere 60 (2005) 1080–1086.
[103] Y. Lei, Z. Shen, X. Chen, J. Jia, W. Wang, Water SA 32 (2006) 205–210.
[104] M. Cerón-Rivera, M.M. Dávila-Jiménez, M.P. Elizalde-González, Chemosphere 55 (2004) 1–10.
[105] H.S. Awad, N. Abo Galwa, Chemosphere 61 (2005) 1327–1335.
[106] A. Sakalis, K. Fytianos, U. Nickel, A. Voulgaropoulos, Chem. Eng. J. 119 (2006) 127–133.
[107] A. Socha, E. Sochocka, R. Podsiadły, J. Sokołowska, Color. Technol. 122 (2006) 207–212.
[108] A. Socha, E. Chrzescijanska, E. Kusmierek, Dyes Pigments 67 (2005) 71–75.
[109] S. Hattori, M. Doi, E. Takahashi, T. Kurosu, M. Nara, S. Nakamatsu, Y. Nishiki, T. Furuta, M. Iida, J. Appl. Electrochem. 33 (2003) 85–91.
[110] M.M. Dávila-Jiménez, M.P. Elizalde-González, A. Gutiérrez-González, A.A. Peláez-Cid, J. Chromatogr. A 889 (2000) 253–259.
[111] V. López-Grimau, M.C. Gutiérrez, Chemosphere 62 (2006) 106–112.
[112] A. Socha, E. Sochocka, R. Podsiadły, J. Sokołowska, Dyes Pigments 73 (2007) 390–393.
[113] A. Kraft, M. Stadelmann, M. Blaschke, J. Hazard. Mater. B103 (2003) 247–261.
[114] A.M. Faouzi, B. Nasr, G. Abdellatif, Dyes Pigments 73 (2007) 86–89.
[115] S. Ammar, R. Abdelhedi, C. Flox, C. Arias, E. Brillas, Environ. Chem. Lett. 4 (2006) 229–233.
[116] A. Fernandes, A. Morão, M. Magrinho, A. Lopes, I. Gonçalves, Dyes Pigments 61 (2004) 287–296.
[117] M.A. Sanromán, M. Pazos, M.T. Ricart, C. Cameselle, Chemosphere 57 (2004) 233–239.
[118] J. Hastie, D. Bejan, M. Teutli-León, N.J. Bunce, Ind. Eng. Chem. Res. 45 (2006) 4898–4904.
[119] R. Pelegrini, P. Peralta-Zamora, A.R. de Andrade, J. Reyes, N. Durán, Appl. Catal. B: Environ. 22 (1999) 83–90.
[120] L.S. Andrade, L.M.M. Ruotolo, R.C. Rocha-Filho, N. Bocchi, S.R. Biaggio, J. Iniesta, V. García-García, V. Montiel, Chemosphere 66 (2007) 2035–2043.
[121] X. Chen, G. Chen, P.L. Yue, Chem. Eng. Sci. 58 (2003) 995–1001.
[122] X. Chen, G. Chen, F. Gao, P.L. Yue, Environ. Sci. Technol. 37 (2003) 5021–5026.
[123] X. Chen, F. Gao, G. Chen, J. Appl. Electrochem. 35 (2005) 185–191.
[124] X. Chen, G. Chen, Sep. Purif. Technol. 48 (2006) 45–49.
[125] M. Panizza, G. Cerisola, Appl. Catal. B: Environ. 75 (2007) 95–101.
[126] T. Bechtold, A. Turcanu, W. Schrott, Diamond Rel. Mater. 15 (2006) 1513–1519.
[127] P. Cañizares, A. Gadri, J. Lobato, B. Nasr, R. Paz, M.A. Rodrigo, C. Saez, Ind. Eng. Chem. Res. 45 (2006) 3468–3473.
[128] C. Saez, M. Panizza, M.A. Rodrigo, G. Cerisola, J. Chem. Technol. Biotechnol. 82 (2007) 575–581.
[129] M. Faouzi, P. Cañizares, A. Gadri, J. Lobato, B. Nasr, R. Paz, M.A. Rodrigo, C. Saez, Electrochim. Acta 52 (2006) 325–331.
[130] P. Cañizares, B. Louhichi, A. Gadri, B. Nasr, R. Paz, M.A. Rodrigo, C. Saez, J. Hazard. Mater. 146 (2007) 552–557.
[131] E. Butrón, M.E. Juárez, M. Solis, M. Teutli, I. Gonzalez, J.L. Nava, Electrochim. Acta 52 (2007) 6888–6894.
[132] M. Catanho, G.R.P. Malpass, A.J. Motheo, Appl. Catal. B: Environ. 62 (2006) 193–200.
[133] A. Savaş Koparal, Y. Yavuz, C. Gürel, Ü. Bakir Öğütveren, J. Hazard. Mater. 145 (2007) 100–108.
[134] C. Carvalho, A. Fernandes, A. Lopes, H. Pinheiro, I. Gonçalves, Chemosphere 67 (2007) 1316–1324.
[135] M. Panizza, A. Barbucci, R. Ricotti, G. Cerisola, Sep. Purif. Technol. 54 (2007) 382–387.
[136] M. Panizza, G. Cerisola, J. Hazard. Mater. 153 (2007) 83–88.
[137] C.A. Martínez-Huitle, E. Brillas, Angew. Chem. Int. Ed. 47 (2008) 1998–2005.
[138] L.V. Venczel, C.A. Likirdopulos, C.E. Robinson, M.D. Sobsey, Water Sci. Technol. 50 (2004) 141–146.
[139] H. Bergmann, T. Iourtchouk, K. Schops, K. Bouzek, Chem. Eng. J. 85 (2002) 111–117.
[140] M.E.H. Bergmann, J. Rollin, Catal. Today 124 (2007) 198–203.
[141] L. Szpyrkowicz, C. Juzzolino, S.N. Kaul, S. Daniele, M.D. De Faveri, Ind. Eng. Chem. Res. 39 (2000) 3241–3248.
[142] L. Szpyrkowicz, R. Cherbanski, G.H. Kelsall, Ind. Eng. Chem. Res. 44 (2005) 2058–2068.
[143] D. Rajkumar, J.G. Kim, J. Hazard. Mater. B136 (2006) 203–212.
[144] D. Rajkumar, B.J. Song, J.G. Kim, Dyes Pigments 72 (2007) 1–7.
[145] C. Boxall, G.H. Kelsall, Inst. Chem. Eng. Symp. Ser. 127 (1992) 59–70.
[146] S. Raghu, C. Ahmed Basha, J. Hazard. Mater. B139 (2007) 381–390.
[147] N.M. Abu Ghalwa, F.R. Zaggout, J. Environ. Sci. Health A 41 (2006) 2271–2282.
[148] C.-H. Yang, Can. J. Chem. Eng. 77 (1999) 1161.
[149] C.-H. Yang, C.-C. Lee, T.-C. Wen, J. Appl. Electrochem. 30 (2000) 1043–1051.
[150] N. Mohan, N. Balasubramanian, V. Subramanian, Chem. Eng. Technol. 24 (2001) 749–753.
[151] J.D. Donaldson, S.M. Grimes, N.G. Yasri, B. Wheals, J. Parrick, W.E. Errington, J. Chem. Technol. Biotechnol. 77 (2002) 756–760.
[152] K. Muthukumar, P.S. Sundaram, N. Anantharaman, C.A. Basha, J. Chem. Technol. Biotechnol. 79 (2004) 1135–1141.
[153] S.S. Vaghela, A.D. Jethva, B.B. Metha, S.P. Dave, S. Adimurthy, G. Ramachandraiah, Environ. Sci. Technol. 39 (2005) 2848–2855.
[154] N. Mohan, N. Balasubramanian, J. Hazard. Mater. B136 (2006) 239–243.
[155] N. Mohan, N. Balasubramanian, C. Ahmed Basha, J. Hazard. Mater. 147 (2007) 644–651.
[156] J. Bandara, P.T. Wansapura, S.P.B. Jayathilaka, Electrochim. Acta 52 (2007) 4161–4166.
[157] A.G. Vlyssides, M. Loizidou, P.K. Karlis, A.A. Zorpas, D. Papaioannou, J. Hazard. Mater. B70 (1999) 41–52.
[158] D. Doğan, H. Türkdemir, J. Chem. Technol. Biotechnol. 80 (2005) 916–923.
[159] E. Chatzisymeon, N.P. Xekoukoulotakis, A. Coz, N. Kalogerakis, D. Mantzavinos, J. Hazard. Mater. B137 (2006) 998–1007.
[160] L. Szpyrkowicz, M. Radaelli, J. Appl. Electrochem. 36 (2006) 1151–1156.
[161] L. Szpyrkowicz, M. Radaelli, S. Daniele, A. Baldacci, S. Kau, Ind. Eng. Chem. Res. 46 (2007) 6732–6736.
[162] C.-T. Wang, J. Environ. Sci. Health A 38 (2003) 399–413.
[163] M.A. Sanromán, M. Pazos, C. Cameselle, J. Chem. Technol. Biotechnol. 79 (2004) 1349–1353.
[164] M.J. Kupferle, A. Galal, P.L. Bishop, J. Environ. Eng. 132 (2006) 514–518.
[165] L. Plant, M. Jeff, Chem. Eng. 101 (1994) 16–20.
[166] D. Pletcher, Acta Chem. Scand. 53 (1999) 745–750.
[167] Y. Sun, J.J. Pignatello, Environ. Sci. Technol. 27 (1993) 304–310.
[168] M.A. Oturan, J.J. Aaron, N. Oturan, J. Pinson, Pestic. Sci. 55 (1999) 558–562.
[169] M.A. Oturan, J. Appl. Electrochem. 30 (2000) 477–478.
[170] C. Flox, P.L. Cabot, F. Centellas, J.A. Garrido, R.M. Rodríguez, C. Arias, E. Brillas, Appl. Catal. B: Environ. 75 (2007) 17–28.
[171] P.C. Foller, R.T. Bombard, J. Appl. Electrochem. 25 (1995) 613–627.
[172] A. Alvarez Gallegos, Y. Vergara García, A. Zamudio, Sol. Energy Mater. Sol. Cells 88 (2005) 157–167.
[173] E. Brillas, R.M. Bastida, E. Llosa, J. Casado, J. Electrochem. Soc. 142 (1995) 1733–1741.
[174] E. Kusvuran, O. Gulnaz, S. Irmak, O.M. Atanur, H.I. Yavuz, O. Erbatur, J. Hazard. Mater. B109 (2004) 85–93.
[175] E. Kusvuran, S. Irmak, H.I. Yavuz, A. Samil, O. Erbatur, J. Hazard. Mater. B119 (2005) 109–116.
[176] A. Lahkimi, M.A. Oturan, N. Oturan, M. Chaouch, Environ. Chem. Lett. 5 (2007) 35–39.
[177] S. Hammami, N. Oturan, N. Bellakhal, M. Dachraoui, M.A. Oturan, J. Electroanal. Chem. 610 (2007) 75–84.
[178] M.A. Oturan, E. Guivarch, N. Oturan, I. Sirés, Appl. Catal. B: Environ. 82 (2008) 244–254.
[179] N. Daneshvar, S. Aber, V. Vatanpour, M.H. Rasoulifard, J. Electroanal. Chem. 615 (2008) 165–175.
[180] A. Wang, J. Qu, J. Ru, H. Liu, J. Ge, Dyes Pigments 65 (2005) 227–233.
[181] L. Xu, H. Zhao, S. Shi, G. Zhang, J. Ni, Dyes Pigments 77 (2008) 158–164.
[182] C.-T. Wang, J.-L. Hu, W.-L. Chou, Y.-M. Kuo, J. Hazard. Mater. 152 (2008) 601–606.
[183] J.M. Peralta-Hernández, Y. Meas-Vong, F.J. Rodríguez, T.W. Chapman, M.I. Maldonado, L.A. Godínez, Dyes Pigments 76 (2008) 656–662.
[184] M. Zhou, Q. Yu, L. Lei, G. Barton, Sep. Purif. Technol. 57 (2007) 380–387.
[185] M. Zhou, Q. Yu, L. Lei, Dyes Pigments 77 (2008) 129–136.
[186] Z. Shen, J. Yang, X. Hu, Y. Lei, X. Ji, J. Jia, W. Wang, Environ. Sci. Technol. 39 (2005) 1819–1826.
[187] C. Flox, S. Ammar, C. Arias, E. Brillas, A.V. Vargas-Zavala, R. Abdelhedi, Appl. Catal. B: Environ. 67 (2006) 93–104.
[188] H. Gallard, J. De Laat, B. Legube, New J. Chem. 22 (1998) 263–268.
[189] Y. Zuo, J. Hoigné, Environ. Sci. Technol. 26 (1992) 1014–1022.
[190] E. Brillas, J.C. Calpe, J. Casado, Water Res. 34 (2000) 2253–2262.
[191] S. Leonard, P.M. Gannett, Y. Rojanasakul, D. Schwegler-Berry, V. Castranova, V. Vallvathan, X.L. Shi, J. Inorg. Biochem. 70 (1998) 239–244.
[192] J. Chen, M. Liu, J. Zhang, Y. Xian, L. Jin, Chemosphere 53 (2003) 1131–1136.
[193] M. Pimentel, N. Oturan, M. Dezotti, M.A. Oturan, Appl. Catal. B: Environ. 83 (2008) 140–149.
[194] A.T. Sugiarto, T. Ohshima, M. Sato, Thin Solid Films 407 (2002) 174–178.
[195] Y.S. Mok, J.O. Jo, IEEE Trans. Plasma Sci. 34 (2006) 2624–2629.
[196] Y.B. Xie, X.Z. Li, Mater. Chem. Phys. 95 (2006) 39–50.
[197] Z. Zainal, C.Y. Lee, M.Z. Hussein, A. Kassim, N.A. Yusof, J. Hazard. Mater. B118 (2005) 197–203.
[198] W. Gernjak, M. Fuerhacker, P. Fernández-Ibañez, J. Blanco, S. Malato, Appl. Catal. B: Environ. 64 (2006) 121–130.
[199] A. Durán, J.M. Monteagudo, E. Amores, Appl. Catal. B: Environ. 80 (2008) 42–50.
[200] M.V.B. Zanoni, J.J. Sene, M.A. Anderson, J. Photochem. Photobiol. A 157 (2003) 55–63.
[201] P.A. Carneiro, M.E. Osugi, J.J. Sene, M.A. Anderson, M.V.B. Zanoni, Electrochim. Acta 49 (2004) 3807–3820.
[202] M.H. Habibi, N. Talebian, J.-H. Choi, Thin Solid Films 515 (2006) 1461–1469.
[203] G. Li, J. Qua, X. Zhang, H. Liu, H. Liu, J. Mol. Catal. A: Chem. 259 (2006) 238–244.
[204] J.M. Peralta-Hernández, Y. Meas-Vong, F.J. Rodríguez, T.W. Chapman, M.I. Maldonado, L.A. Godínez, Water Res. 40 (2006) 1754–1762.
[205] M.G. Neelavannan, M. Revathi, C. Ahmed Basha, J. Hazard. Mater. 149 (2007) 371–378.
[206] H. Gallard, J. De Laat, B. Legube, Rev. Sci. Eau 12 (1999) 715–728.
[207] D. Robert, S. Malato, Sci. Total Environ. 291 (2002) 85–97.